# ERRATA

| Page | |
|---|---|
| Notices | The statement: "DDC release to OTS is authorized", should be deleted. |
| DD 1473 | The statement: "DDC release to OTS is authorized", should be deleted from block 10. |

# DEVELOPMENT OF SUBSONIC BASE PRESSURE PREDICTION METHODS,

TECHNICAL REPORT AFFDL-TR-65-157

VOLUME II

AUGUST 1965

AF FLIGHT DYNAMICS LABORATORY
RESEARCH AND TECHNOLOGY DIVISION
AIR FORCE SYSTEMS COMMAND
WRIGHT PATTERSON AIR FORCE BASE, OHIO

PROJECT NO. 1366, TASK NO. 136613

(PREPARED UNDER CONTRACT NO. AF 33(615)-1615 BY THE AERODYNAMICS GROUP, CONVAIR DIVISION, GENERAL DYNAMICS CORPORATION IN SAN DIEGO, CALIFORNIA. J. E. BUTSKO, W. V. CARTER AND W. HERMAN, AUTHORS).

## NOTICES

When Government drawings, specifications, or other data are used for any purpose other than in connection with a definitely related Government procurement operation, the United States Government thereby incurs no responsibility nor any obligation whatsoever; and the fact that the Government may have formulated, furnished, or in any way supplied the said drawings, specifications, or other data, is not to be regarded by implication or otherwise as in any manner licensing the holder or any other person or corporation, or conveying any rights or permission to manufacture, use, or sell any patented invention that may in any way be related thereto.

Qualified users may obtain copies of this report from DDC. Foreign announcement and dissemination of this report is not authorized. ~~DDC release to OTS is~~ [redacted]

Copies of this report should not be returned to the Research and Technology Division unless return is required by security considerations, contractual obligations, or notice on a specific document.

AF-WP-O-FEB 65 1500

# FOREWORD

Volume II contains the results of the wind tunnel test data for the development of subsonic base pressure prediction methods conducted by the Convair Division of General Dynamics Corporation, San Diego, California. This work was supported under contract AF33(615)-1615 Project No. 1366, Air Force Task 136613 under the direction of Mr. G. M. Gilbert and Lt. L. W. Rogers, USAF of the Air Force Flight Dynamics Laboratory, Research and Technology Division, located at Wright-Patterson Air Force Base, Ohio.

This report was released by the authors 28 October 1965 for publication as an RTD Technical Report.

This technical report has been reviewed and is approved.

Alfred C. Draper

TABLE OF CONTENTS

ILLUSTRATIONS

Illustrations (cont'd)

Illustrations (cont'd)

# LIST OF TABLES

# 1/ INTRODUCTION

Wind tunnel tests were conducted in the San Diego State College smoke wind tunnel, in the Convair 8' x 12' low speed wind tunnel and the California Institute of Technology (Cal. Tech.) Merrill 32" x 45" wind tunnel at subsonic speeds, on a series of two-dimensional and three-dimensional models. These tests were funded as part of Air Force Contract AF33(613)-1615 on "Development of Subsonic Base Pressure Prediction Methods", sponsored by the Air Force Flight Dynamics Laboratory, Wright-Patterson Air Force Base, Ohio.

The purpose of the San Diego State smoke wind tunnel tests was to collect base pressure data from different configurations which would be used, along with data from the literature survey, to define two-dimensional and three-dimensional configurations for the later more extensive wind tunnel tests that were conducted at the Convair and Cal Tech wind tunnels. The visual wake data was used as a guide in determining probe positions for the wake survey tests to be conducted in these later tests. The comparisons between configurations has been made on a qualitative basis rather than on a quantitative basis. Still photographs were made with all configurations, and base pressures were recorded for all configurations.

The purpose of the Convair and Cal Tech tests was to acquire data from blunt based models that could be used to test the theory for two-dimensional shapes and to provide new data for developing a subsonic base pressure prediction technique. The test program employed several two-dimensional and three-dimensional models selected to furnish data on flow angularity, Reynolds number, base pressures and wake flow characteristics.

Data collected during the tests included 3-component force and moment data, base pressure data, visual flow data, wake surveys with pressure probe, wake surveys with hot-wire probe and forebody pressure data.

This report (Volume II) is presented for the purpose of documenting the data obtained, as required for this program, and includes the methods and scope of testing as well as tabulated, plotted and photographic data.

A discussion of these results is presented in Volume I, Section 6.

## 2/ NOMENCLATURE

| | |
|---|---|
| A | Model reference area (sq ft) |
| b | Model reference span (ft) |
| $\bar{c}$ | Model reference chord (ft) |
| c | Model semi span as used on pressure plots |
| $C_Z$ | Normal force coefficient $\frac{\text{normal force}}{qS}$ referred to body axes |
| ℄ | Center line |
| $C_X$ | Axial force coefficient $\frac{\text{axial force}}{qS}$ referred to body axes |
| $C_m$ | Pitching moment coefficient $\frac{\text{pitching moment}}{qS\bar{c}}$ referred to body axes |
| Cp | Pressure coefficient, $\Delta P/q$ |
| D | Measured drag (lbs) |
| d | X distance from model reference moment center to balance moment center (ft) |
| e | Vertical distance from model moment center to balance moment center (ft) |
| H | Total pressure (psf) |
| h | Distance from model centerline to top of model (ft) |
| L | Measured lift (lbs) |
| l | Model length (ft) |
| M | Measured moment (ft-lb) |
| $M_{ST}$ | Static moment (ft-lb) |
| P | Static pressure (psf) |
| q | Corrected dynamic pressure (lbs/sq ft) |
| $q_m$ | Uncorrected dynamic pressure (lbs/sq ft) |

| | |
|---|---|
| $S_t$ | Strouhal Number $\left(\frac{nd}{U}\right)$ |
| S | Model reference area (sq ft) |
| V | Average tunnel velocity (ft/sec) |
| x | Distance measured from base of model - positive aft (ft) |
| y | Vertical distance measured from model centerline (ft) |
| z | Spanwise distance measured from model centerline (ft) |
| $\alpha$ | Corrected geometric angle-of-attack (degrees) |
| $\alpha_g$ | Geometric angle-of-attack of model and reference plane relative to tunnel centerline (degrees) |
| $\psi$ | Geometric angle-of-yaw of the model reference plane relative to tunnel centerline $\psi = 0$ for these tests |
| $\rho$ | Mass density of air |
| $\infty$ | Free stream conditions |
| $\Lambda$ | Trailing edge sweep (degrees) |
| $u^2$ | Square of instaneous velocity in X-direction $(fps)^2$ |

## 3/ TEST FACILITIES

The wind tunnel facilities used in this program were San Diego State College smoke wind tunnel, the Convair 8' x 12' wind tunnel and the Cal Tech 32" x 45" Merrill wind tunnel. The smoke tunnel, Figure 1, was used to test a series of two-dimensional models. This tunnel has a test section 2.5" x 30" x 36" long, and tests were conducted at Reynolds numbers of approximately $1.8 \times 10^5$ and $0.6 \times 10^6$ per foot. The Convair tunnel was used for both two-dimensional and three-dimensional tests while the Cal Tech tunnel was used for only three-dimensional tests. Both tunnels are of the closed, single return, atmospheric type. Tests were conducted at Reynolds numbers of $.7 \times 10^6$ to $2.2 \times 10^6$ per foot.

A two-dimensional test section was installed in the Convair tunnel for the two-dimensional tests. This test section was formed by installing two walls approximately 12-1/2 feet long, 36 inches apart, from the floor to the ceiling in the test section, see Figure 2. The maximum dynamic pressure that could be attained with this arrangement was 60 lbs/square foot.

The Convair three-dimensional tests were made in the 8' x 12' test section using a single support for the 6-inch diameter body and a tandem two-support for the 3-inch wing. The external balance system was used to measure the forces and moments.

## 4/ DESCRIPTION OF MODELS

### 4.1 SMOKE TUNNEL MODELS

An array of two-dimensional models were fabricated and tested. These models were divided into three series, each with different fineness ratios as shown in Figure 3. The series of configurations were designated as, $T_1$ with a fineness ratio of 6:1, $T_2$ with a 3:1 ratio, and $T_3$ with a 2:1 ratio. The variations tested with these models are as follows:

A. Different nose bluntness with constant base area, thickness, and wetted area. ($T_2$, $T_{2R}$).

B. Different flow angles at the base and nose fineness ratio, with constant base area and wetted area.

($T_1 + F_{10°}$, $T_2$, and $T_3 + B_{10}$)

($T_1$ and $T_2 + B_{10°}$)

($T_3$ and $T_2 + F_{10°}$)

C. Different base area and nose fineness ratio with constant wetted area and constant flow angle.

($T_1 + B_{10°}$, $T_2 + B_{10°}$ and $T_3 + B_{10°}$)

($T_1 + B_{5°}$, $T_2 + B_{5°}$ and $T_3 + B_{5°}$)

($T_1$, $T_2$ and $T_3$)

($T_1 + F_{5°}$ and $T_2 + F_{5°}$)

($T_1 + F_{10°}$, $T_2 + F_{10°}$ and $T_3 + F_{10°}$)

The models with constant thickness at the base ($T_1$, $T_2$ and $T_3$) were 10 inches long, with a surface length of 10.50. The other models had a length of approximately 10 inches but with a surface length equal to the above models. The models were 2.5 inches wide, the width of the tunnel.

The models were fabricated from sugar pine with plastic foam and felt glued to the view side and felt only on the opposite side. A bracket was made which matched the tunnel support and was interchangeable with each model. This bracket allowed the models to be pitched through a range of 0° to 15° using the tunnel pitch mechanism.

A 1/8" O.D. copper tube for measuring base pressures was attached in the center of the base of the models and routed within the model and out the side through the center of the attachment bracket.

4.2 GD/CONVAIR MODELS

A series of two-dimensional models along with the 6-inch body and 3-inch wing were tested in the GD/Convair wind tunnel. These models are described below.

4.2.1 TWO-DIMENSIONAL MODELS. Each of the two-dimensional models had a 36-inch span and 32-inch chord, with a constant section and a blunt base as shown in Figure 4. The basic models were 8, 10, and 12 inches thick. The 8-inch model was tested with a 10° flared trailing edge; the 12-inch model was tested with and without a 10° boattailed trailing edge. The flared and boattailed trailing edge configurations formed a base height and area equal to that of the 10-inch model.

The models were constructed of wood attached to an aluminum spar, and were painted and rubbed to a smooth finish. Transition strips, consisting of a band of No. 180 Carborundum grit, were applied as shown in Figure 5. The models were mounted on the Convair two-dimensional panel support system with the balance center of moments at the 50% chord station. The relationship of the balance center of moments and the model moment reference center is shown in Figure 4.

During runs 7, 9, and 11, a .25-inch thick splitter plate, 36-inch wide, was installed on the model chord plane, extending 60 inches aft of the model base as shown in Figure 5. During runs 4, 8, and 12, a vertical plate was installed on the model center line, extending aft of the model, to permit the recording of flow visualization data, see Figure 6. During these runs with the vertical and splitter plates installed, data were recorded only at 0° angle of attack.

During run 1, no model was installed in the test section. For this run wake survey data pressure rake and hot-wire were recorded on the tunnel centerline 24 and 54-inches aft of the trunnion center.

All two-dimensional models were instrumented with surface and base pressure orifices as shown in Figure 7. Wake survey equipment, consisting of a 48 tube total head pressure rake, 3 static pressure probes, and 2 hot-wire probes, was suspended from the tunnel ceiling, see Figure 8. The location of this equipment relative to the model base and centerlines was varied as indicated in the run index.

Force data were recorded utilizing the low speed wind tunnel external balance system. Pressure data were recorded by photographing a manometer board on which the pressures were displayed as inches of fluid columns. Hot-wire data were recorded utilizing a Shapiro-Edwards hot-wire anemometer in conjunction with a Magnechord tape recorder and a CEC oscillograph. Hot-wire probe data were also visibly displayed on an oscilloscope.

Flow visualization was accomplished by means of the French-Chalk technique. Visual photographs are presented in Figures 9 and 10.

4.2.2. THREE-DIMENSIONAL MODELS TESTED IN CONVAIR WIND TUNNEL. A delta planform wing with a constant thickness of 3.0 inches, a 1.5 inch leading edge radius, and a blunt trailing edge was tested. This wing had a leading edge sweepback of 75° with a maximum wing span at the trailing edge of 19.55 inches. The wing upper and lower surfaces were constructed of a .50 inch aluminum plate, with a birch leading edge and afterbody. Transition grit was applied to the wing as shown in Figure 11.

The wing was mounted in the center of the test section on the two-strut support system with the balance center of moments 19.500 inches forward of the trailing edge. The relationship of the balance center of moments and the model moment reference center is shown in Figure 12. Except for runs 19 and 20, all runs were pitch runs made in the vertical plane of the tunnel. During runs 19 and 20, when the image system bayonets were installed, data were recorded only at 0° angle-of-attack.

A base 6-inch diameter body, 30.55 inches long, with a blunted ogive nose and a constant diameter afterbody was tested. This body was constructed of laminated birch, and was painted and rubbed to a smooth finish, transition grit was applied as shown in Figure 13.

The body was mounted on a single support strut, utilizing a "T" bayonet, with the balance center of moments 16.05 inches forward of the model base. The relationship of the balance center of moments and the model moment reference center if shown in Figure 13. Runs 23 and 24 were pitch runs made in the horizontal plane of the tunnel. During runs 25 and 26, when the image system bayonet was installed, data were recorded only at 0° angle-of-attack.

The three-dimensional models were also instrumented with surface and base pressure orifices as shown in Figures 14 and 15. The same wake survey rake as described for the two-dimensional models were used for the three dimensional tests. The force and pressure data was recorded in the same manner as for the two-dimensional models.

4.3 CAL TECH MODELS

An array of three-dimensional models were tested in the Cal Tech tunnel. The various geometries included a 3-inch thick wing, swept trailing edges, wing with body, wing with cambered upper surface, body with different afterbody shapes and fins and body with a hemispherical nose.

The 3-inch wing was the same as that described in 4.2. This wing was also tested with other model parts to form other configurations. These configurations included testing this wing with 30° and 45° swept trailing edges, Figures 16 and 17, and one-half of the 6-inch diameter body mounted on its surfaces, Figures 18a and 18b.

A 4-inch thick wing, with 75° leading edge sweep back, 15.02 inch span and a 2-inch leading edge radius was tested on the tandem two-support system, as shown in Figures 19a and 19b. The relationship of the balance center of moments and the model moment reference center is shown in Figure 20. Two alternate upper surface camber configurations were also tested, one with a 5° slope and the other 10°, Figures 21a and 21b.

The wing was fabricated from 1/2" aluminum plate on the upper and lower surface and with a birch plywood leading edge and afterbody. The wood afterbody was removable for the alternate camber configurations.

Pressure orifices were installed in the base and on the upper surface at the trailing edge. The locations of these orifices along with their corresponding identification number is shown in Figures 16, 17 and 22.

The 6-inch diameter body with constant diameter afterbody is as described in Section 4.1.2, except a tandem two-support system was used in the Cal Tech tunnel. In addition to the constant diameter afterbody, alternate configurations were tested and are described below.

1. 10° boattail, Figure 23.

2. 10° flare, Figure 23.

3. Constant diameter afterbody with 2 rectangular fins (horizontal), Figure 24.

4. Same as (3) except with 4 rectangular fins, Figures 24 and 25a.

5. Constant diameter afterbody with 2 delta fins (horizontal), Figures 24 and 25b.

6. Same as (5) except with 4 delta fins, Figure 24.

7. 3-D body and a modification consisting of basic constant diameter afterbody with a hemispherical nose, Figures 26a and 26 b.

## 5/ DATA REDUCTION

### 5.1 SAN DIEGO STATE COLLEGE SMOKE TUNNEL TESTS

Base pressure measurements were made from one .065" orifice located in the center of the model base, a 1/8" O.D. pressure tube was connected to a micromanometer for readout, in inches of water.

The velocity used to determine the dynamic pressure (q) was taken at the ℄ of tunnel. The base pressure coefficient was determined from the equation

$$C_{p_b} = \frac{P_b - P_\infty}{q}$$

q = dynamic pressure based on velocity at ℄ of tunnel

The tunnel did not have instrumentation for measuring the tunnel static pressure ($P_\infty$) with a model in the tunnel. A separate tunnel calibration was made to determine this value.

### 5.2 GD/CONVAIR TEST

5.2.1 PRESSURE DATA. Pressures were measured from orifices located on the surface of the model, the base region, and from a wake survey rake. These pressures were connected to a manometer bank and photographs were taken. Pressurelevels were then determined by reading the manometer photographs. Pressure coefficients were calculated as follows:

$$C_p = \frac{P_m - P_\infty}{q}$$

where

$P_m$ - Measured pressure

$P_\infty$ - Free stream

q - Tunnel dynamic pressure

To obtain the average base pressure of each configuration, it was necessary to integrate the pressures, as read from the manometer photographs, over the base area of the model. This was accomplished by determining the area that each orifice acted on and assuming that the pressure acted as a step function between the orifices. Average base pressure was then manually calculated as follows:

$$C_{p_{bavg}} = \frac{\sum_{i=1}^{i=n} C_{p_i} A_i}{\sum_{i=1}^{i=n} A_i}$$

where

$C_{p_i}$ = Pressure at each orifice (i)

$A_i$ = Area (i) each orifice acts over

Average base pressures were corrected for tares by using the average base pressure of the configuration with the image support system and the base pressure without the image system. The difference was then applied as the correction. For configurations that were tested that did not have an image system run, the tare correction was based on the percentage of correction for a similar configuration.

5.2.2 FORCE AND MOMENT DATA. Force and moment were made in the pitch plane only, using the CVAL standard external balance. Three component data, lift, drag, and pitching moment, were recorded. Moment was reduced about the balance center and then transferred to the model moment reference center. The model reference point is presented in Figures 12 and 13. Lift and drag data were reduced to body axis data in the form of normal and axial force coefficients. Data reduction constants are presented in Table 6.

The following equations were used for force and moment data reduction:

$$C_z = \frac{K_1}{qS} (L \cos\alpha + D \sin\alpha)$$

$$C_x = \frac{K_2}{qS} (D \cos\alpha - L \sin\alpha)$$

$$C_m = \frac{K_3}{qS_c} (M + \frac{e}{c} C_z + \frac{a}{c} C_x) + K_4 \frac{L}{qS}$$

$$\alpha = \alpha_g + K_5 \frac{L}{qS}$$

$$q = q_{ct} (1 + K_6 + K_7 \frac{D}{q_{ct} C})$$

where

$K_1$ through $K_7$ are blockage and wall correction factors, reference CVAL Report TR-782.

5.3 CAL TECH TEST

5.3.1 PRESSURE DATA. Pressures were measured and recorded the same as discussed in Section 5.2.1. Pressure levels were determined from photographs of the manometers and pressure coefficients were calculated as follows:

$$C_p = \frac{P_m - P_\infty}{q_\infty} = \frac{P_m - P_4}{P_9 - P_4} \times \frac{P_9 - P_4}{q_\infty} + \frac{P_4 - P_\infty}{q_\infty}$$

where

$P_m$ = Measured pressure

$P_\infty$ = Free stream static pressure

$P_9$ and $P_4$ = Tunnel reference pressures used to set tunnel q

The average base pressures for the Cal Tech Configurations were obtained in the same manner as discussed in Section 5.1.1.

5.3.2 FORCE AND MOMENT DATA. Three component force and moment data were measured using the external balance at the Cal Tech tunnel. Data were taken only in the pitch plane. Moments were taken about the balance reference center and then transferred to the model moment reference center. Lift and drag data were reduced to body axis data. Table 7 presents the constants used for data reduction.

The following are the equations used for the force and moment data reduction:

$$C_L = \frac{L}{qA}$$

$$C_D = \frac{D}{qA}$$

$$C_z = -(C_L \cos\alpha + C_D \sin\alpha)$$

$$C_x = -(C_D \cos\alpha - C_L \sin\alpha)$$

$$C_{m_{MR}} = \frac{M - M_{ST}}{q\ AC} + C_L\left(\frac{d}{c} \cos\alpha - \frac{e}{c} \sin\alpha\right) + C_D\left(\frac{d}{c} \sin\alpha + \frac{e}{c} \cos\alpha\right)$$

No wall corrections were applied to the force and moment data; however, a tunnel blockage correction was applied.

5.4 TARES

Aerodynamic tare runs were made for the 3-inch wing, 4-inch wing and 6-inch diameter body. The tares from these runs were interpolated for the other three dimensional configurations. The tares included corrections for model and tunnel flow dissymmetry as well as tare interference effects of the support system.

# 6/ PRESENTATION OF DATA

Low speed wind tunnel tests have been made to determine the aerodynamic force, surface pressure, base pressure and wake flow characteristics. The data from these tests are presented in photographic, tabulated and graphic form. The run index, in Section 7.0 lists the order in which the runs were made for the San Diego State smoke tunnel, the Convair and the Cal Tech tests. These tests were made to furnish the experimental data for the theoretical portion of this program. Photographs and sketches of the model configurations are shown in Figure 1 through 29. The effect of Reynolds Number was investigated during both the Convair and the Cal Tech tests in the range from .7 x $10^6$ to 2.2 x $10^6$ per foot. The data are only presented in this section and the results are discussed in Section 6 of Volume 1.

## 6.1 SMOKE TUNNEL TEST

Photographs of the flow field for configuration $T_2$ are presented in Figures 27, 28 and 29. The photographs, as well as others presented in reference 3, were used as a guide in determining probe positions for the wake survey conducted in the later tests. Tabulated base pressure coefficient data for all configurations tested are presented in Tables 8, 9 and 10.

## 6.2 CONVAIR AND CAL TECH TESTS

6.2.1 PRESSURE DATA. The results for the two-dimensional tests are presented on Figures 30 through 45. Figures 30 through 33 are average base pressures whereas the data shown on these plots include the effects of base angle, Reynolds number, angle-of-attack, transition strip, and splitter plate on the base pressure coefficient. In addition, contour plots of the base pressure coefficient are presented, as well as surface pressures for the forebody.

The average base pressure data for the three-dimensional tests are shown on Figures 46 through 54. Figures 55 and 56 show surface pressures. These data show the effects of base angle, nose bluntness, fin configurations, trailing-edge sweep, body with 3-inch wing, wing camber, angle-of-attack and Reynolds Number on base pressure coefficient. In addition, a comparison of surface pressures on the 3-D Body is also presented.

Average values of base pressure coefficient measured for the different models and their configurations are presented in Tables 11 and 12.

6.2.2 FORCE AND MOMENT DATA. Figures 57 through 61 present the force and moment data from both the GD/Convair test and the Cal Tech wind tunnel test. The data is presented as $C_Z$, $C_X$, and $C_m$ with a variation of angle-of-attack. It should be noted that the base area of the 3-D body configurations was used as the reference area and the planform area of the wing configurations is used for reference area for the respective configurations. The pitching moments for the body configurations are destabilizing due to the choice of the model reference moment center located at the model base.

6.2.3 AIRFLOW VISUALIZATION. Figures 9 and 10 present photographs of the flow patterns set up on french-chalked vertical splitter plates which were used for wake flow visualization on the two-dimensional configurations $T_{10}$, $T_8 + F_{10}$ and $T_{12} + B_{10}$.

6.2.4 PRESSURE WAKE SURVEY. Figures 62 through 69 present plots of total and static pressure surveys obtained in the Convair tunnel using the wake survey rake. Wake surveys were obtained for configurations $T_{10}$, $T_8 + F_{10}$, $T_{12} + B_{10}$, $M_1$ and $W_3$. Data are also presented for the two-dimensional models with the splitter plate.

Figures 62 through 65 present the distribution of static pressure in the wake region. In general the static pressure is lower along the centerline, corresponding to the loss in total head shown by the total pressure distributions.

Figures 66 through 69 present plots of lines of constant value of the parameter $\frac{H - P_\infty}{q_\infty}$, a measure of the total head loss in the wake region. The plots were obtained by crossplotting the original data obtained from the wake total pressure survey, which yielded plots of total pressure versus vertical station at each longitudinal survey station.

6.2.5 HOT-WIRE ANEMOMETER WAKE SURVEY. The hot-wire anemometer data obtained by surveying the wake of selected configurations were recorded on oscillograph and magnetic tape. Figure 70 through 79 show typical oscillograph traces of velocity fluctuations measured in the wake of configurations $T_{10}$, $T_{10}$ + P and $M_1$, $W_3$ and $W_4$.

Figures 75 through 79 present data that has been used for correlation of wake flow properties as presented in section 2.3 of Volume I.

# 7/ RUN INDEX

A complete list of tests accomplished during the wind tunnel program for the San Diego State College Smoke Wind Tunnel, the Convair 8' x 12' tunnel and the Cal Tech Merrill Wind Tunnel are presented in Tables 1, 3 and 4. Table 2 describes the models tested in the smoke tunnel and Table 5 is a description of Model Components tested in the Convair and Cal Tech Tunnels.

## 7.1 SAN DIEGO STATE COLLEGE SMOKE WIND TUNNEL TEST

Table 1 lists the run index for the test program conducted in this tunnel in June 1964. Table 2 lists the description of smoke tunnel model configurations.

## 7.2 CONVAIR 8' x 12' WIND TUNNEL TEST

Table 3 lists the run index for the experimental program conducted in this tunnel during the period of 27 November 1964 through 4 December 1964.

## 7.3 CAL TECH MERRILL WIND TUNNEL TEST

Table 4 lists the run index for this phase of the experimental program conducted in the Cal Tech Merrill 32" x 45" tunnel during the period of 9 December 1964 through 17 December 1964. Table 5 lists the model components tested in both the Convair and the Cal Tech Tunnels.

## 8/ REFERENCES

1. Reynolds, H. A., "Convair Low Speed Wind Tunnel Handbook Vol. I, Facilities," General Dynamics/Report ZT-043, April 1961.

2. Reynolds, H. A., "Low Speed Wind Tunnel Test of Several General Dynamics/Astronautics Models Selected for an Investigation of Base Flow Phenomena at Subsonic Speeds", General Dynamics/Preliminary Report CVAL 393, January 1965.

3. Carter, W. V., Butsko, J. E., "An Investigation of Subsonic Two Dimensional Base Pressures and Flow Field Visualization Conducted Dynamics/Astronautics Report GDA-DDE-64-074, September 1964.

9/ FIGURES

The following figures consist of sketches, photographs, and plotted data. It should be noted that all dimensions on the following sketches are in inches, model scale.

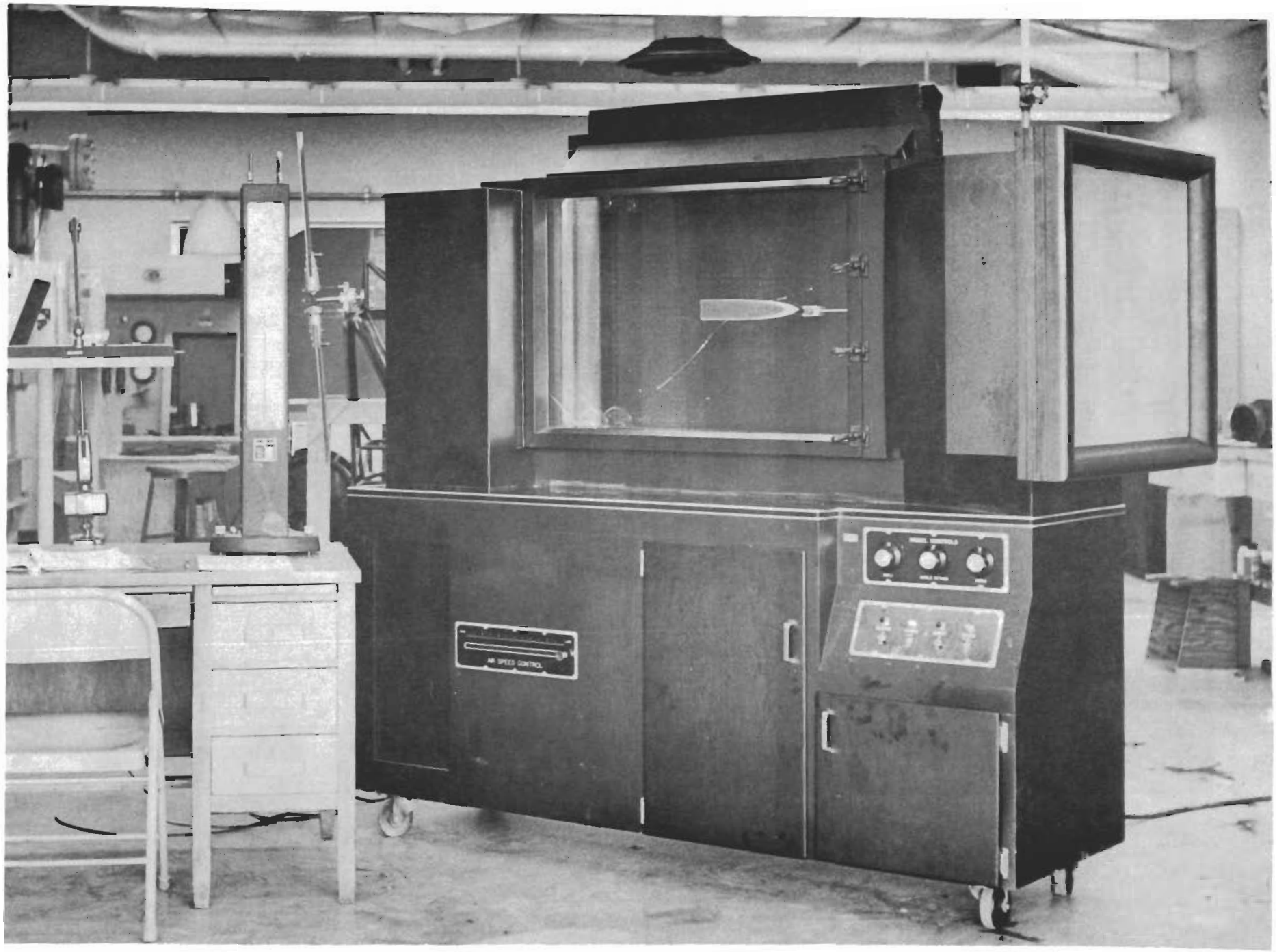


FIGURE 1 San Diego State College Smoke Wind Tunnel

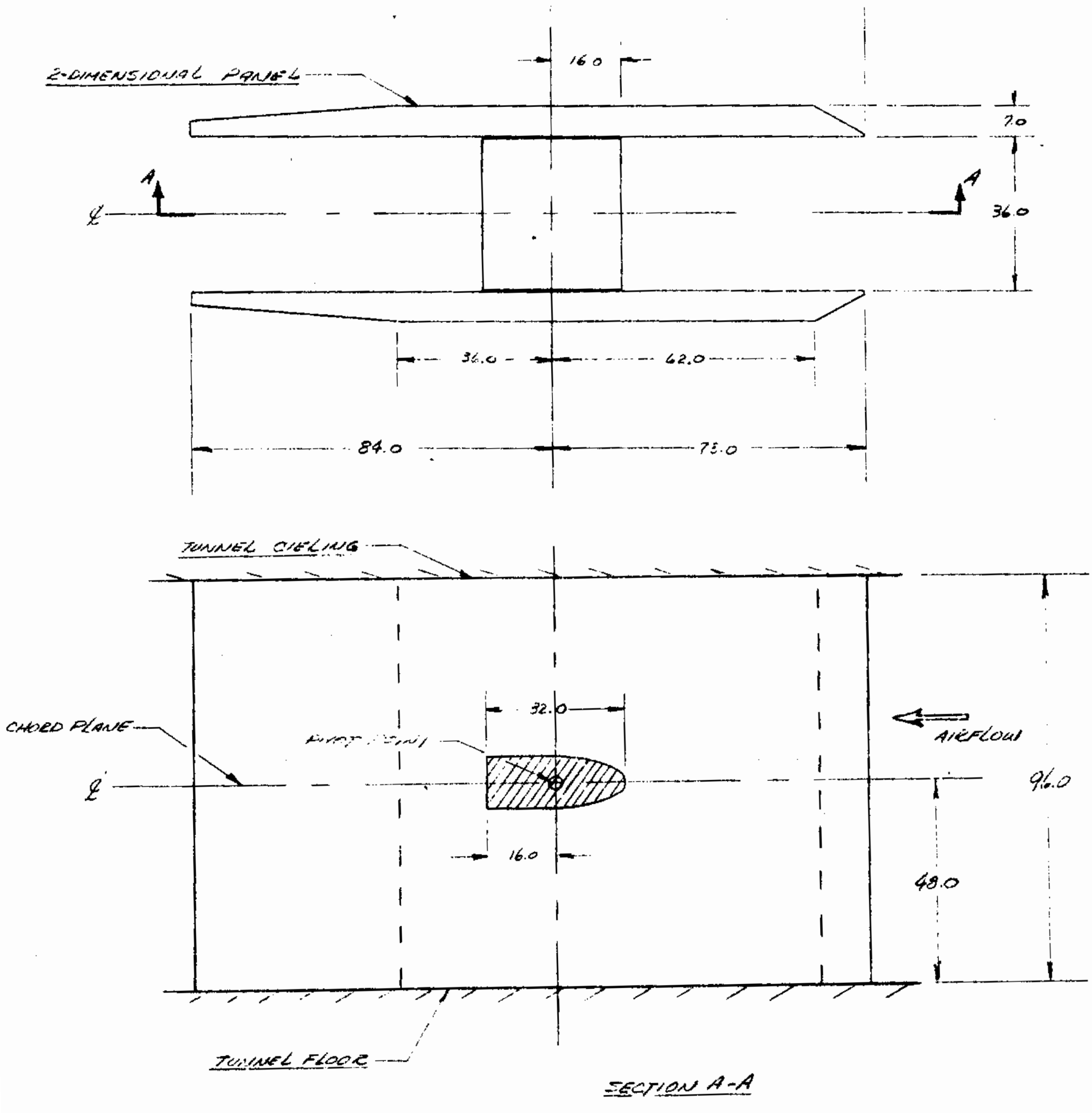


FIGURE 2 Two Dimensional Model Installation

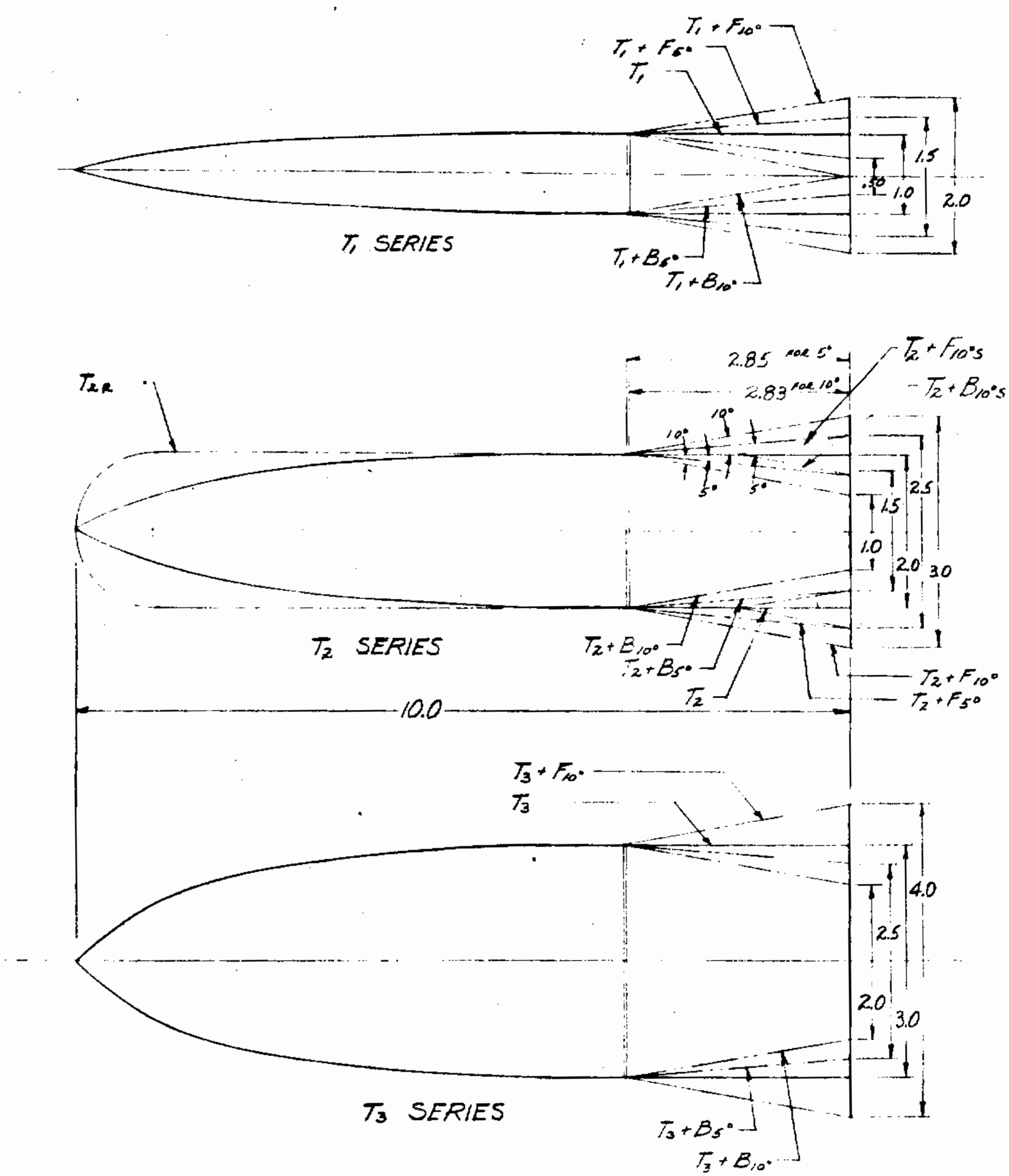


FIGURE 3 Smoke Tunnel Model Geometry

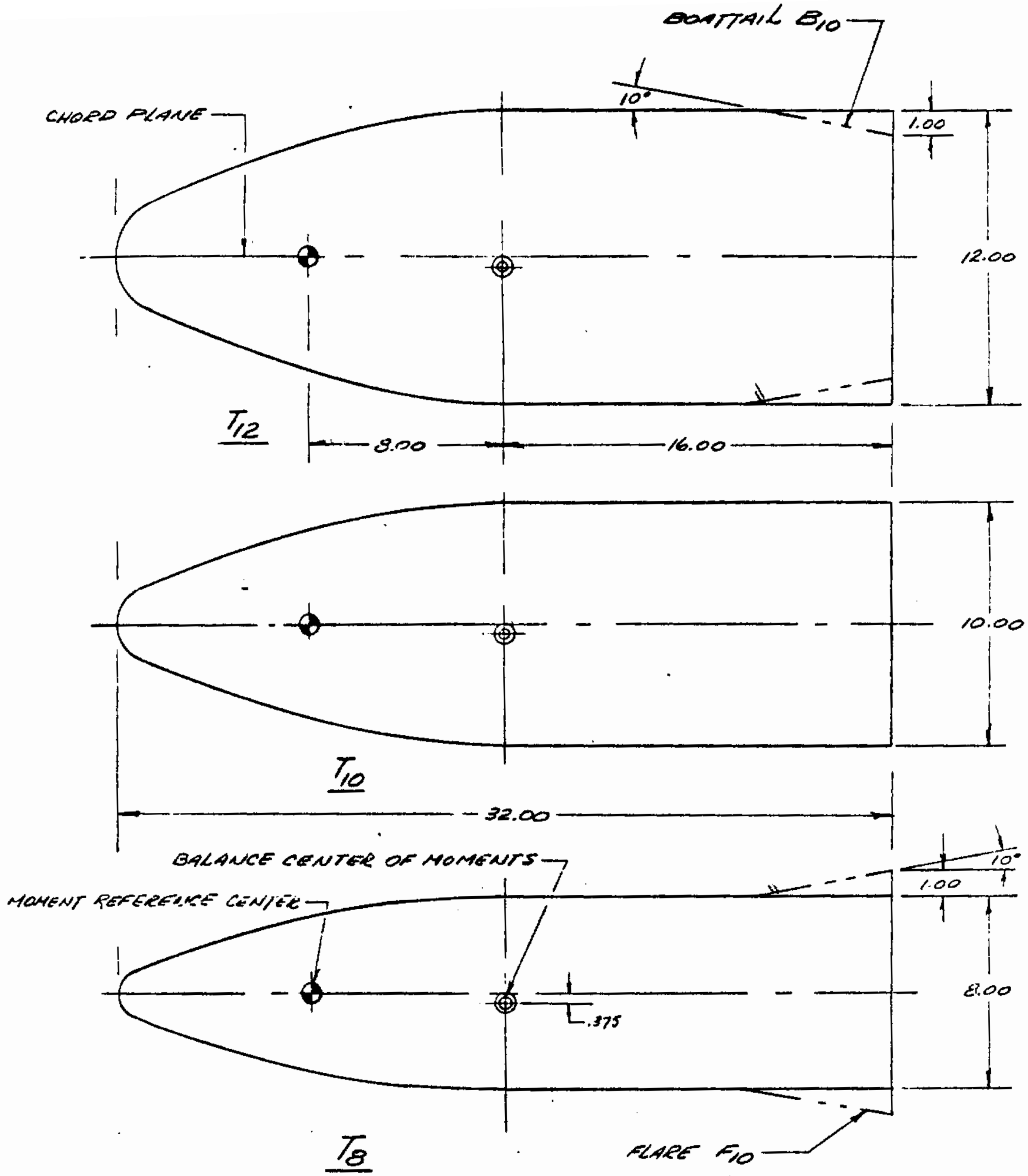


2. MODEL SPAN = 36.00 INCHES.
1. MODELS ARE SYMMETRICAL ABOUT CHORD PLANE.

FIGURE 4 Two Dimensional Models

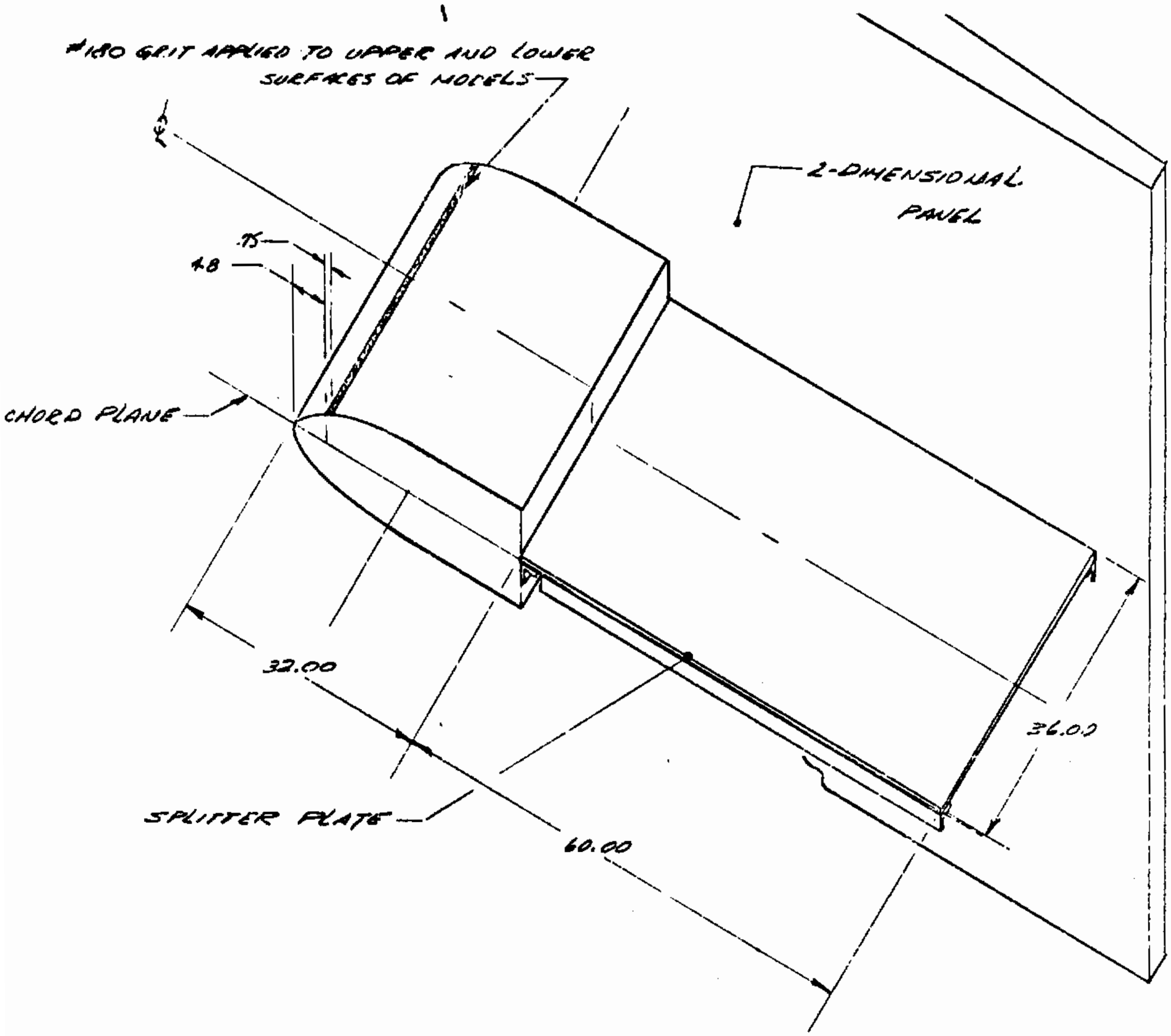


FIGURE 5 Transition Grit Application and Splitter Plate

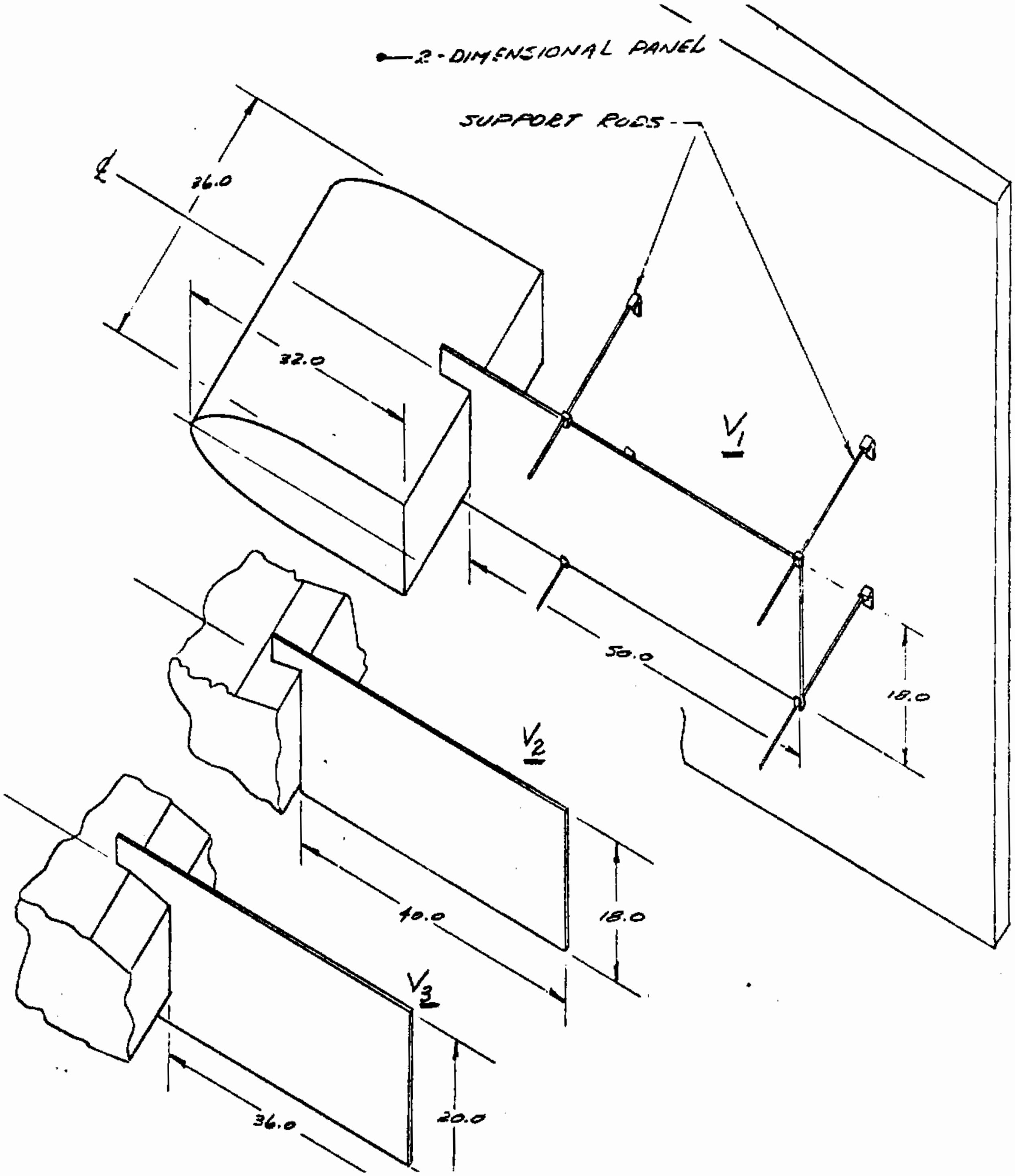


FIGURE 6 Vertical Plate Installation

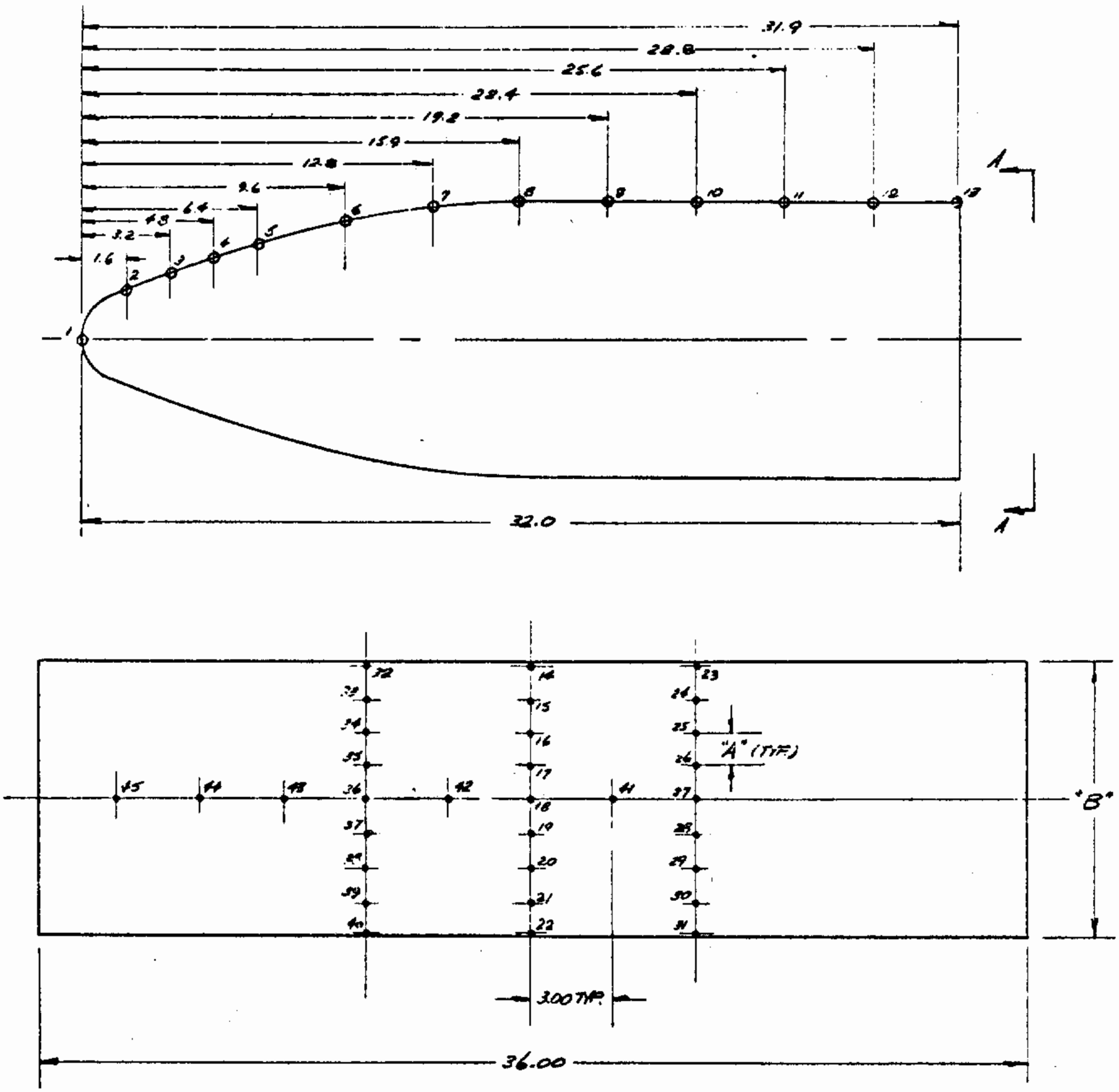


| MODEL | "A" | "B" |
|---|---|---|
| $T_8F_{10}$, $T_{10}$, $T_{12}B_{10}$ | 1.225 | 10.00 |
| $T_{12}$ | 1.475 | 12.00 |

VIEW A-A
(LOOKING FORWARD)

FIGURE 7 Pressure Orifice Locations 2-D Models

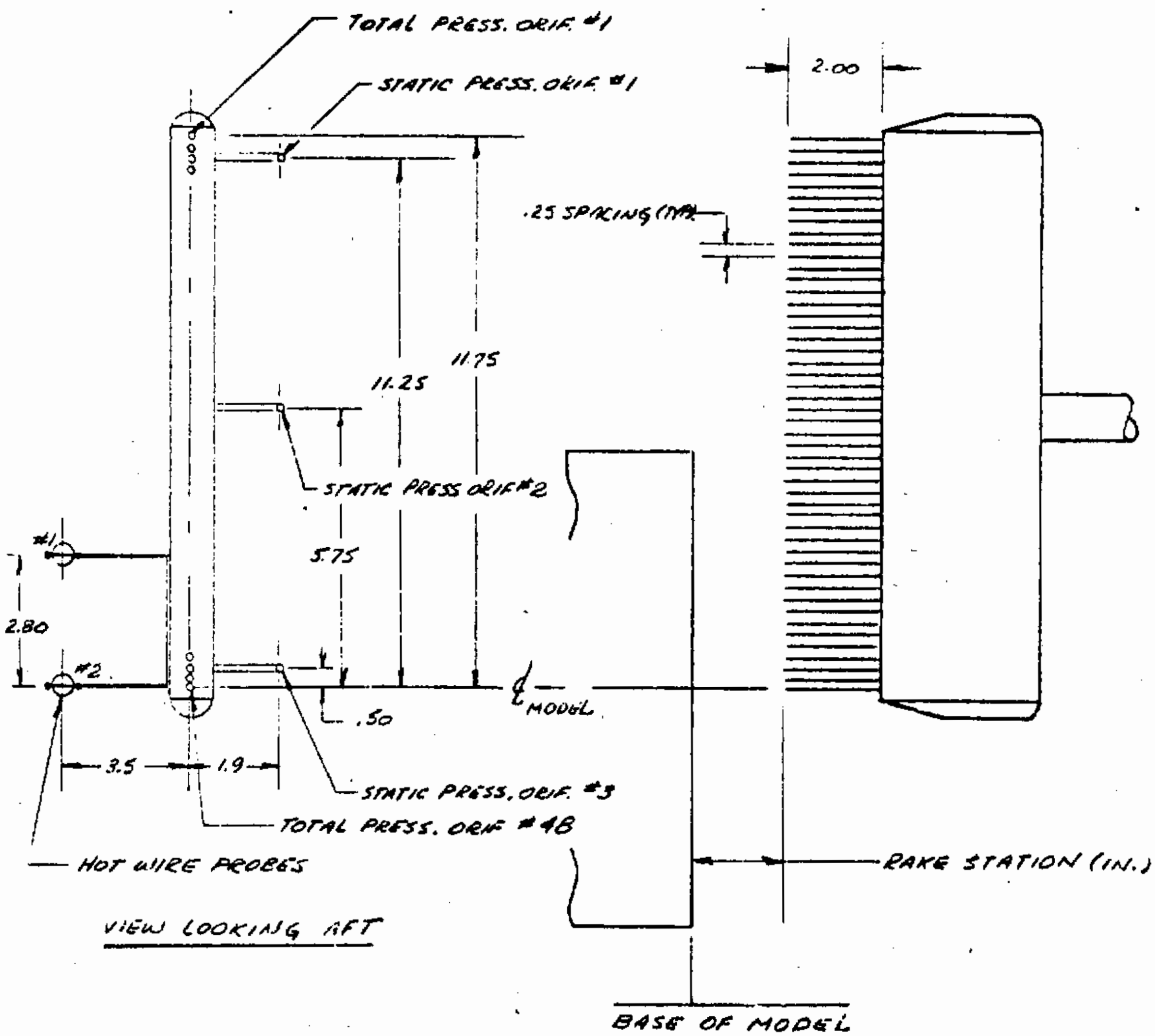


Notes:

1. With the 2-dimensional models, the lower total-head orifice (#48) was in line with the model chord plane at the model centerline.
2. With the 3-dimensional wing, $W_3$, the lower total-head orifice (#48) was in line with the wing chord plane at various butt line locations.
3. With the 3-dimensional body, $B_1$, the lower total-head orifice (#48) was in line with the model vertical centerline, with either the total-head or static pressure tubes in line with the model horizontal centerline as indicated by the word total or static in the pressure data tabulations.
4. The hot wire probes extended .6 inches forward of the total-head pressure probes. When used with Body $B_1$, the probes were located on the opposite side of the rake than shown above.

FIGURE 8 Wake Survey Rake Installation

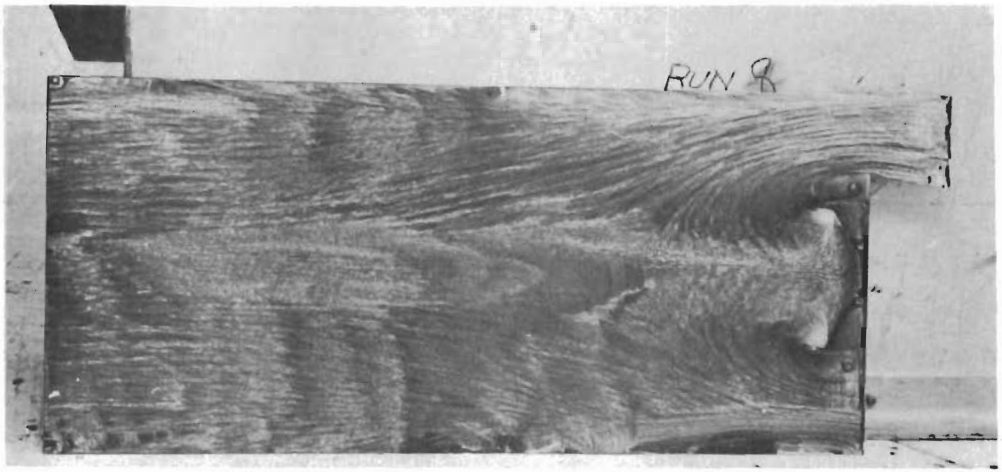


$T_8 + F_{10}$

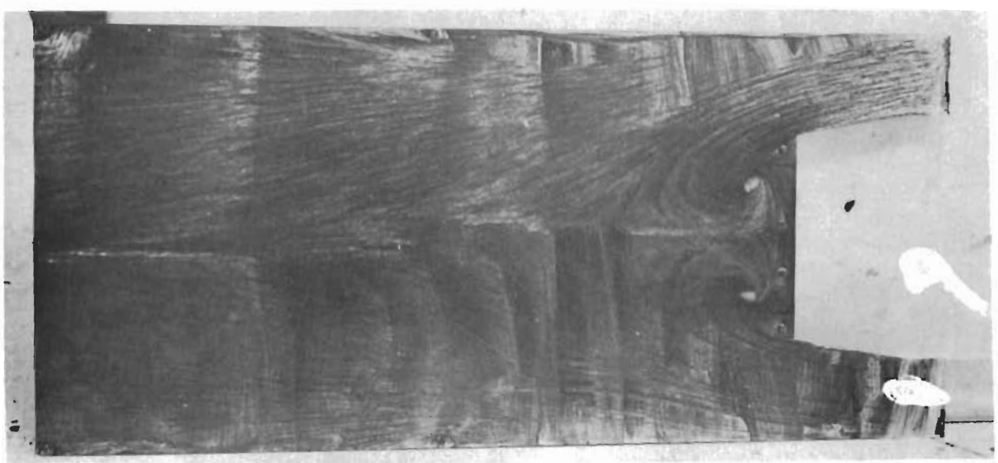

$T_{12} + B_{10}$

FIGURE 10- Flow Visualization of 2-D Model with Flare and Boattail

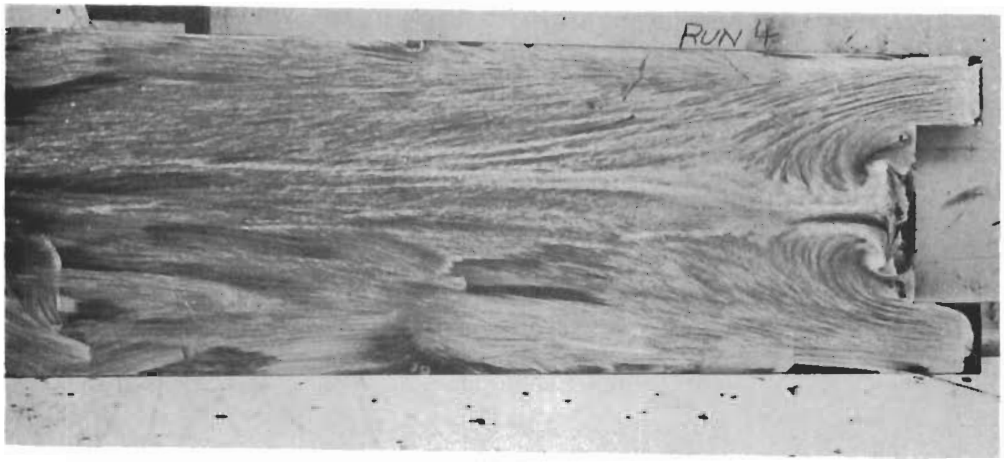


$T_{10}$

$T_{10}$

FIGURE 9 - Flow Visualization of 2-D Model with 10-Inch Base

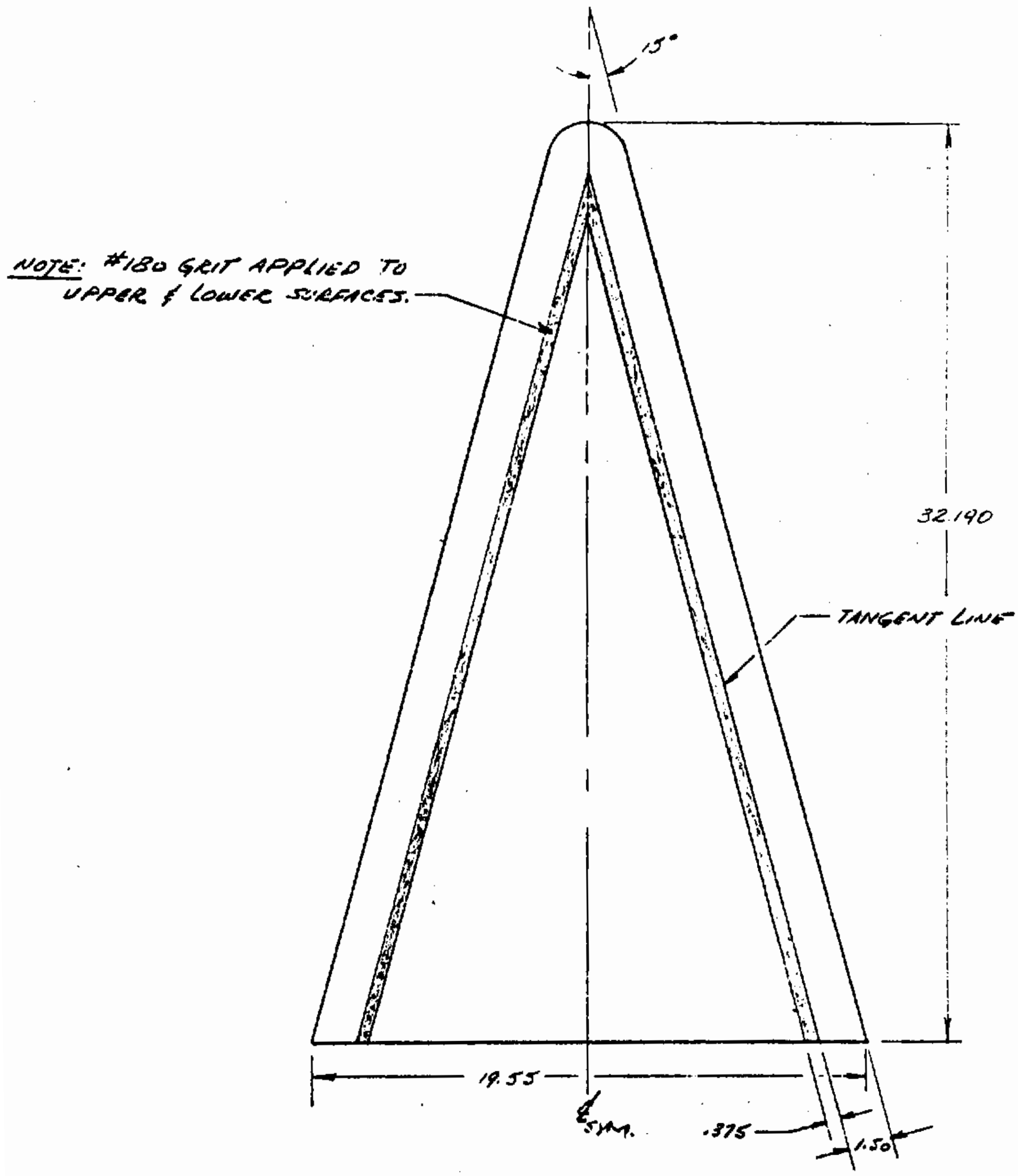


FIGURE 11 Transition Grit Application - Wing W3

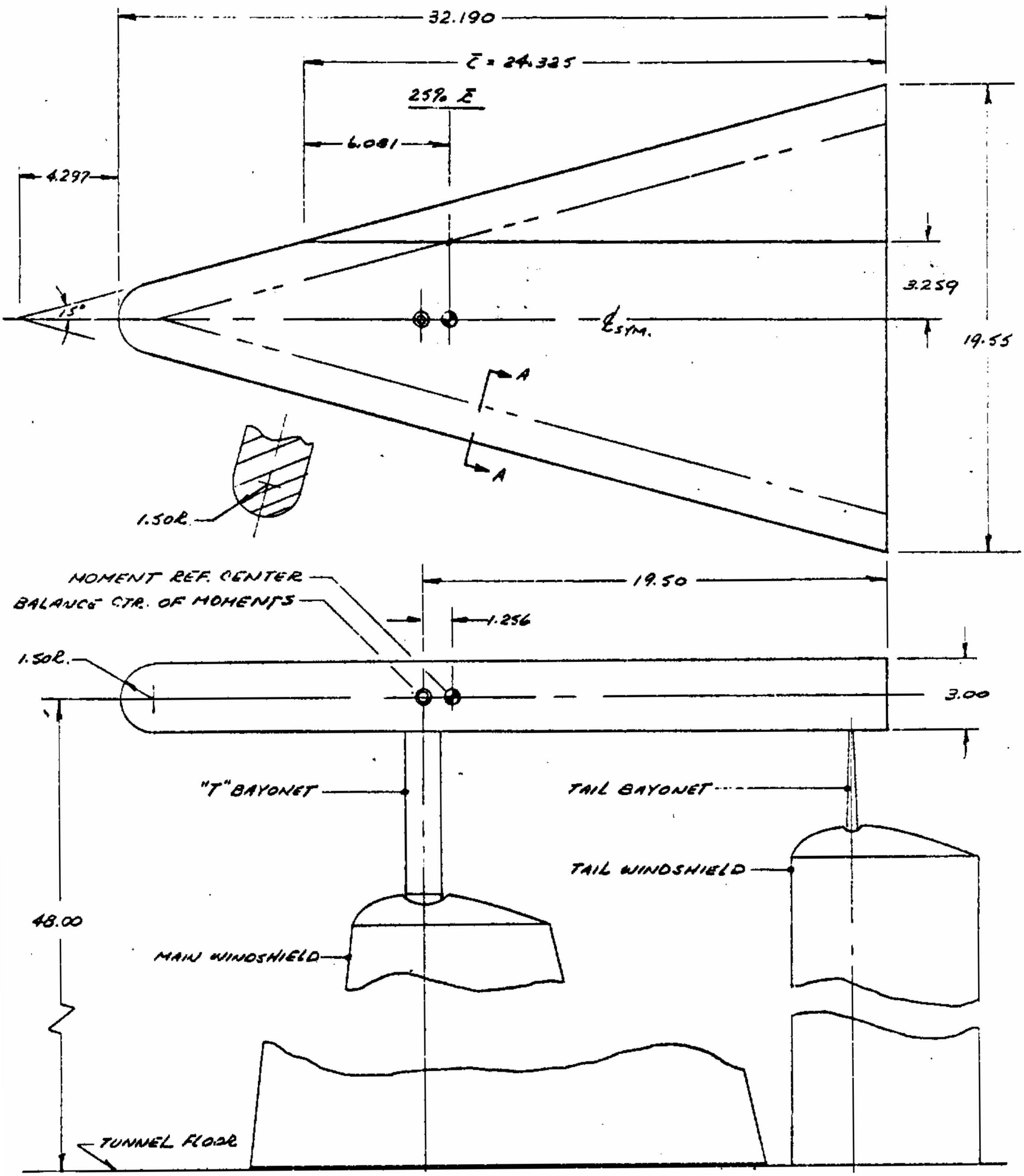


FIGURE 12 Three Dimensional Wing - $W_3$

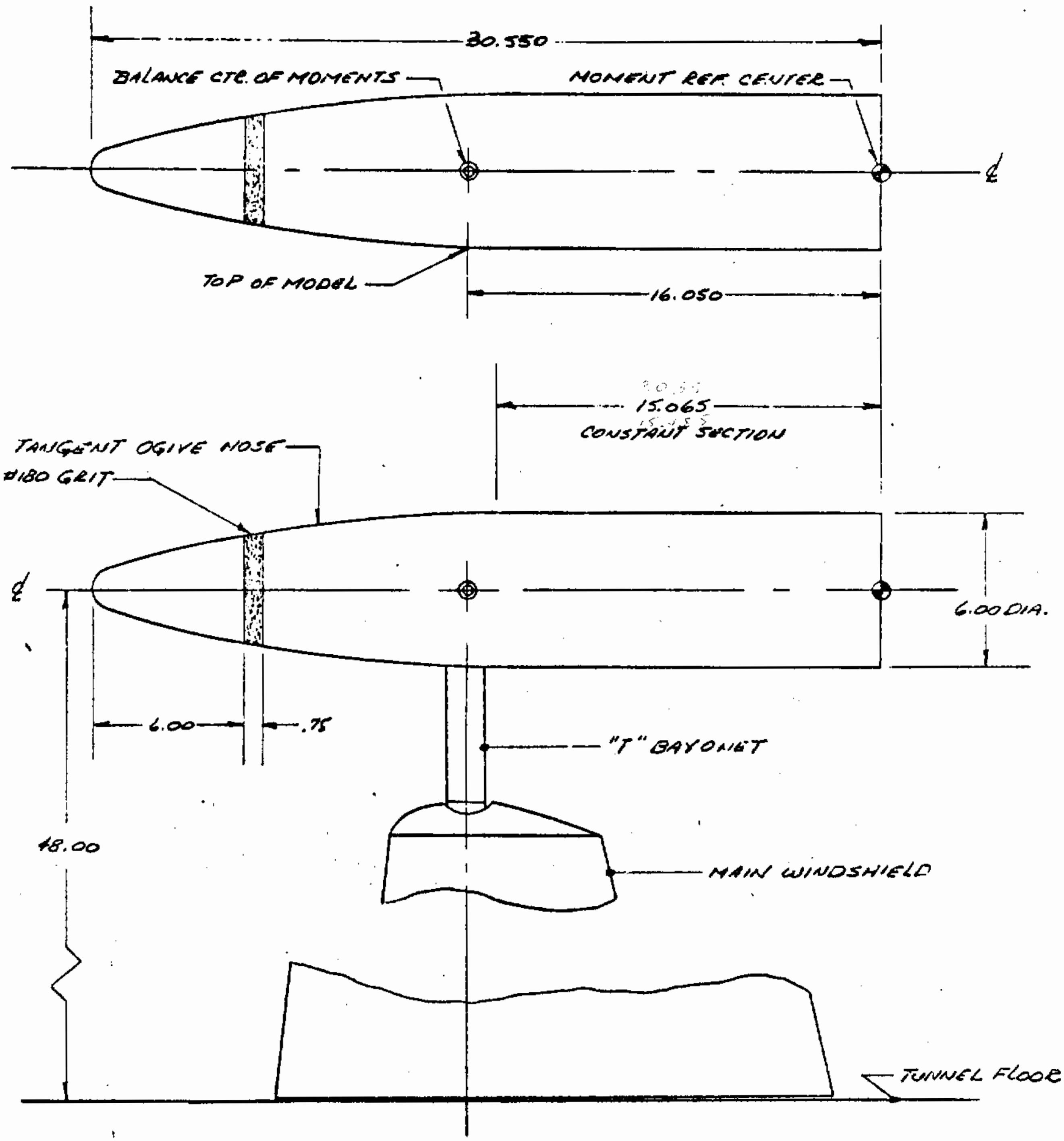


FIGURE 13 Three-Dimensional Body - $M_1$

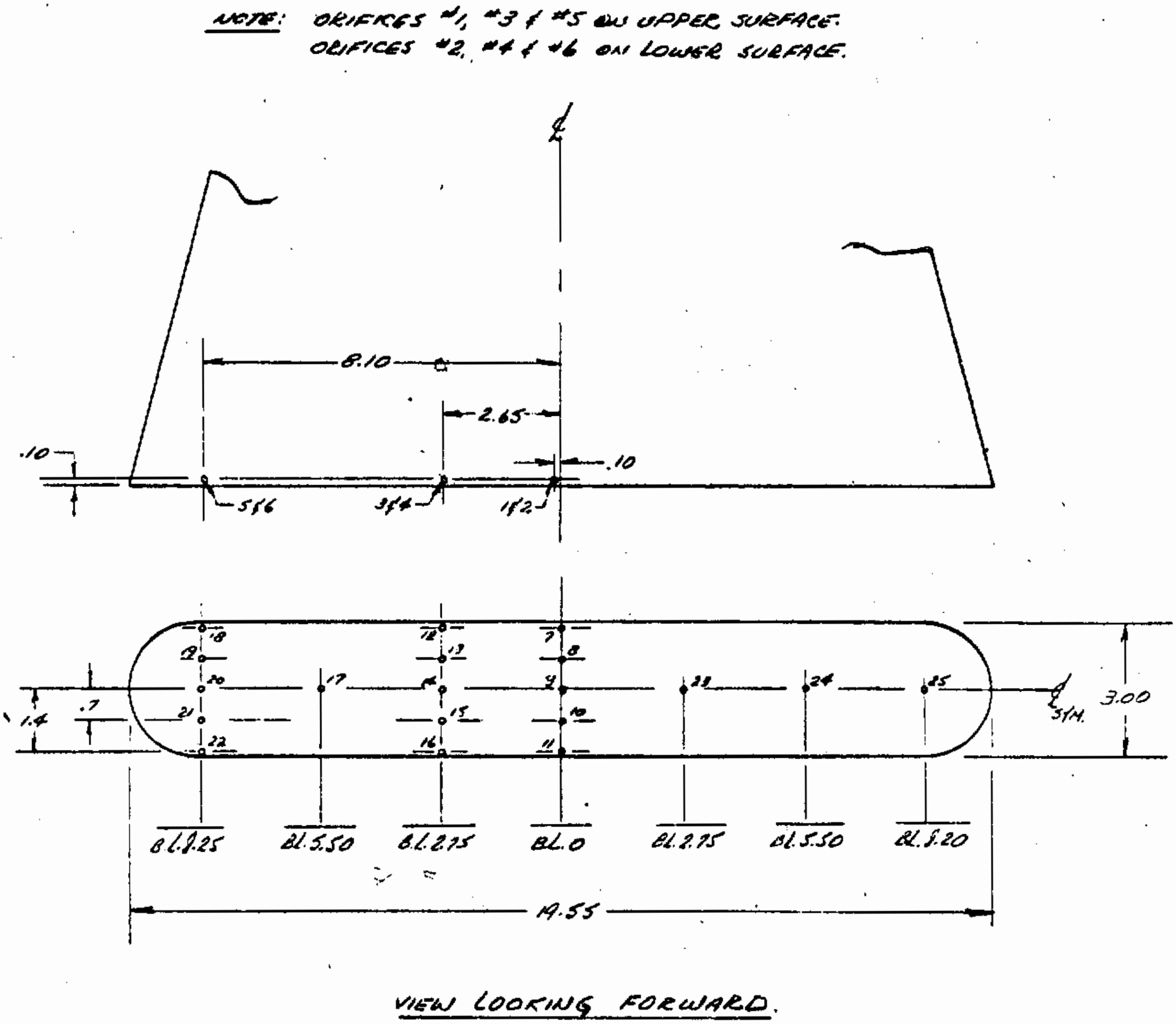


FIGURE 14 Pressure Orifice Location - $W_3$

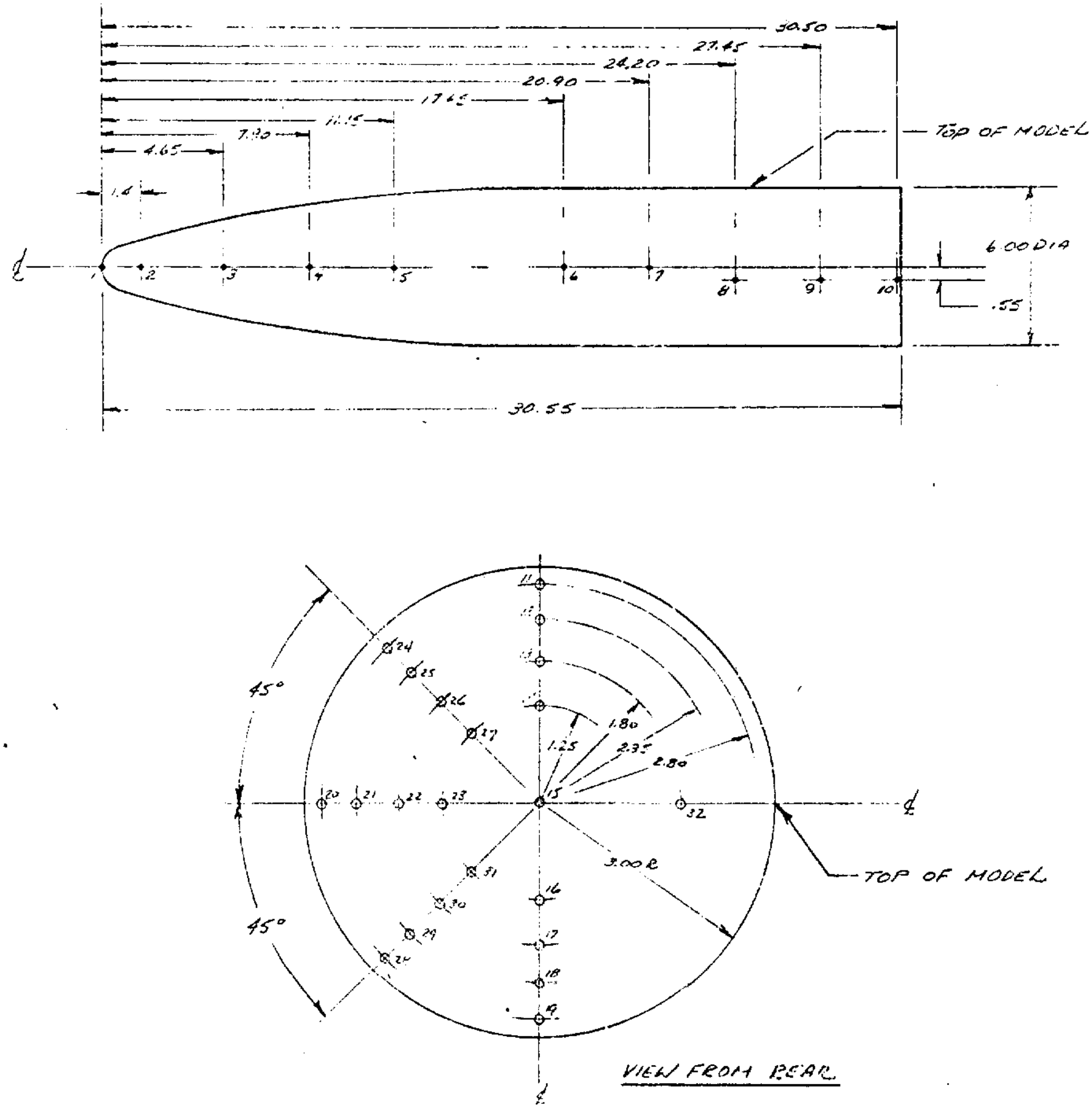


FIGURE 15 Pressure Orifice Location - $M_1$

NOTE:
ORIFICE #17, #19 & #21 ON TOP SURFACE
ORIFICE #18, #20 & #22 ON BOTTOM SURFACE

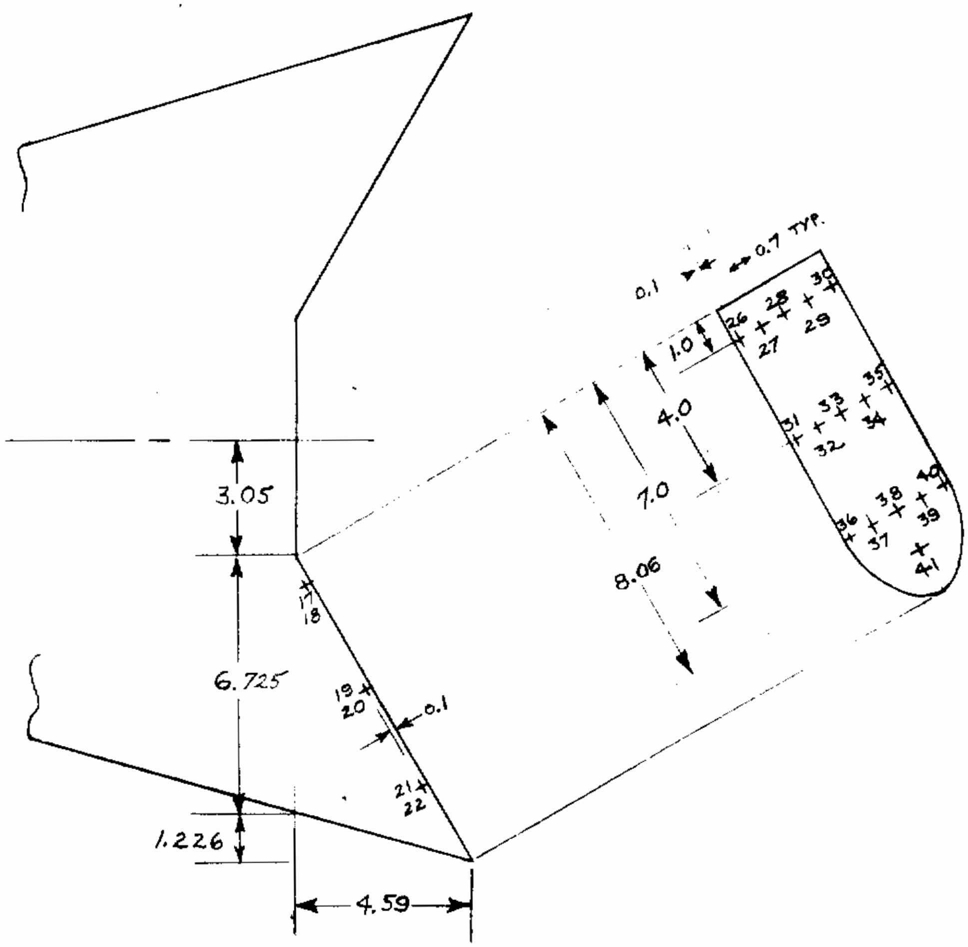


FIGURE 16 3-inch Wing with 30 Degree Trailing Edge Sweep

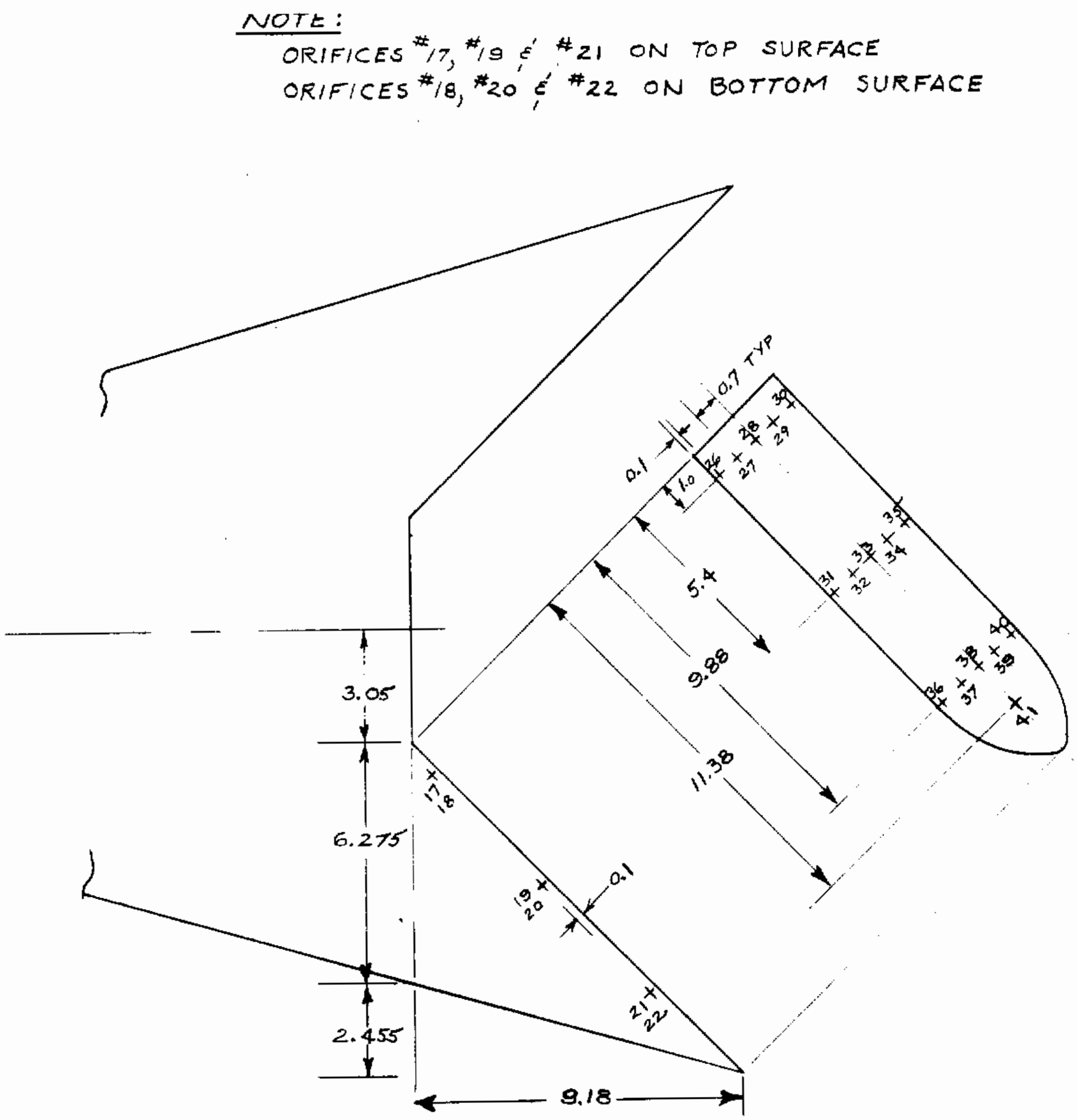


FIGURE 17 3-Inch Wing with 45 Degree Trailing Edge Sweep

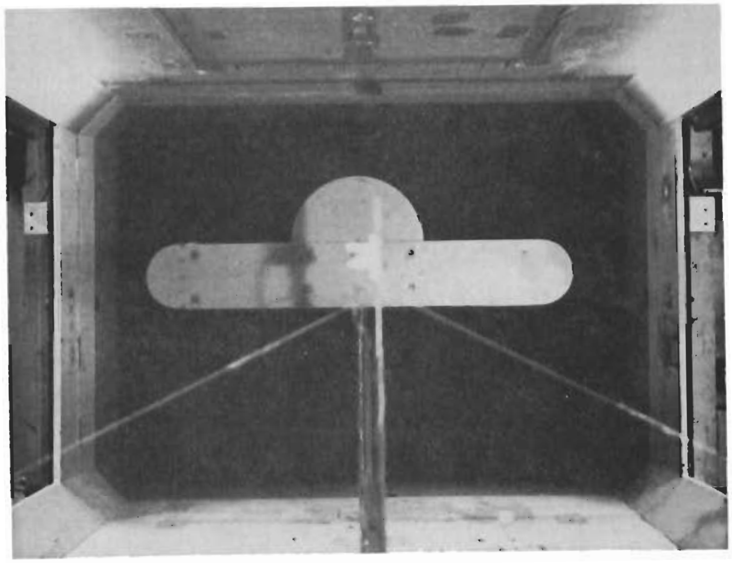

FIGURE 18a End View - 6 Inch Body on Three Inch Wing

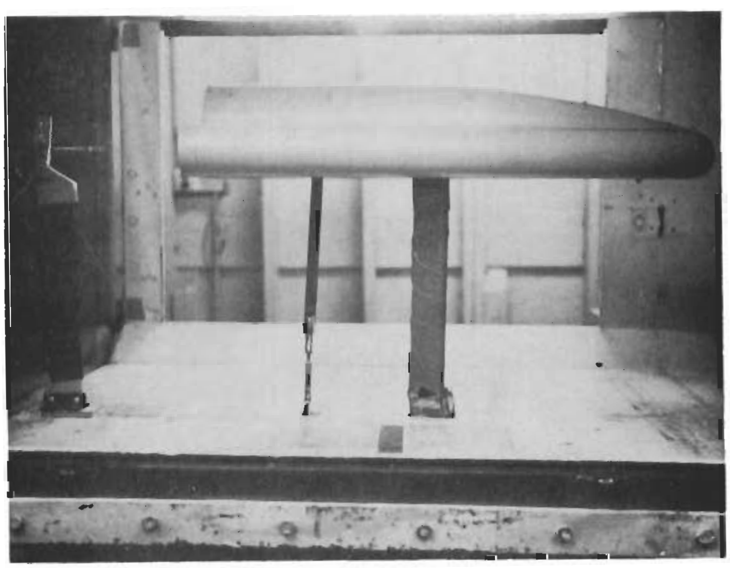

FIGURE 18b Side View 6-Inch Body on 3 Inch Wing

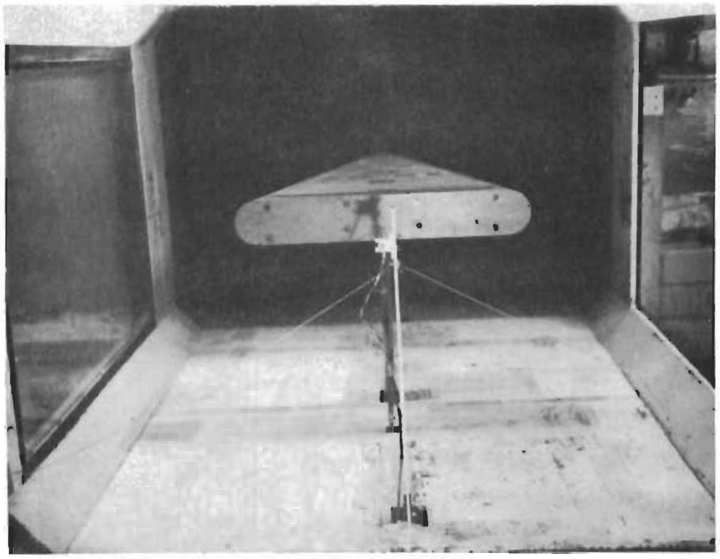

FIGURE 19a End View - 4 Inch Wing

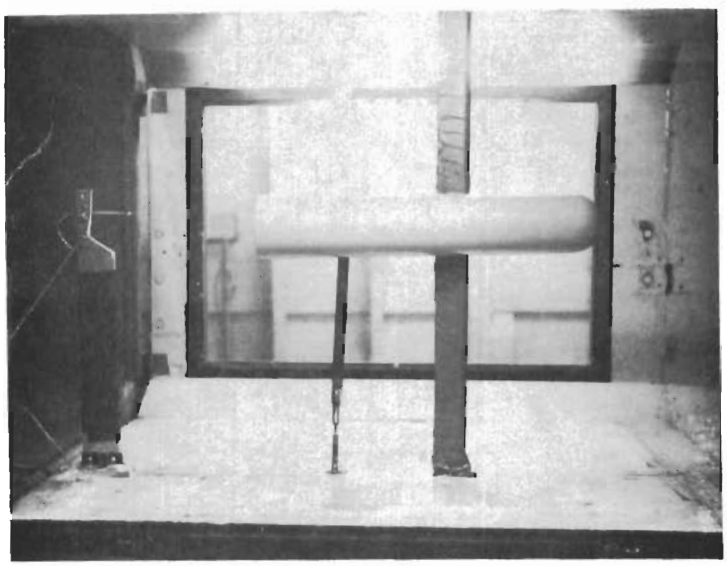

FIGURE 19b Side View - 4 Inch Wing

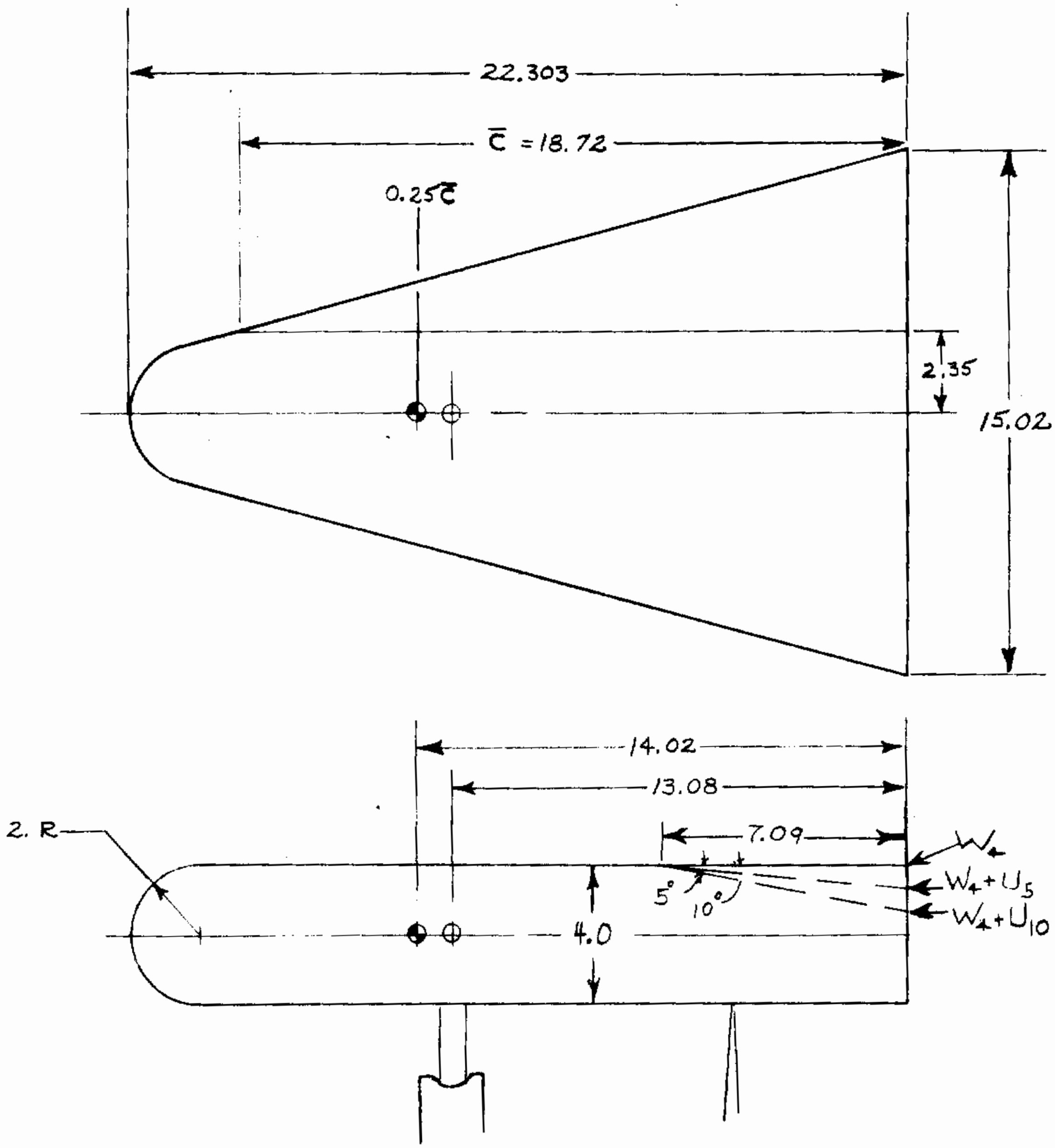


FIGURE 20 Three-Dimensional 4 Inch Wing

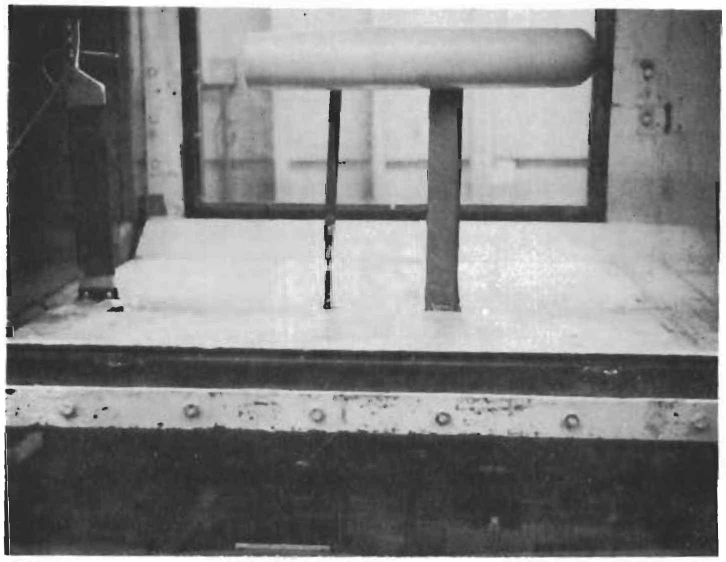

FIGURE 21a - 4-Inch Wing with 5° Cambered Upper Surface

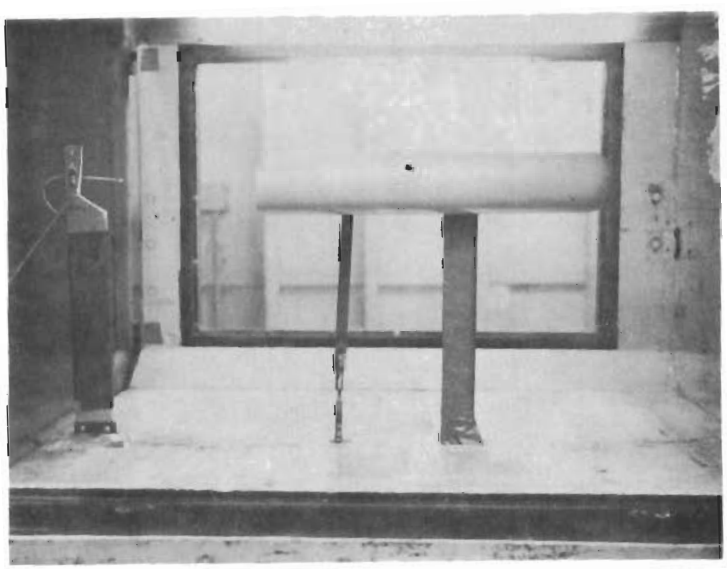

FIGURE 21b- 4-Inch Wing with 10° Cambered Upper Surface

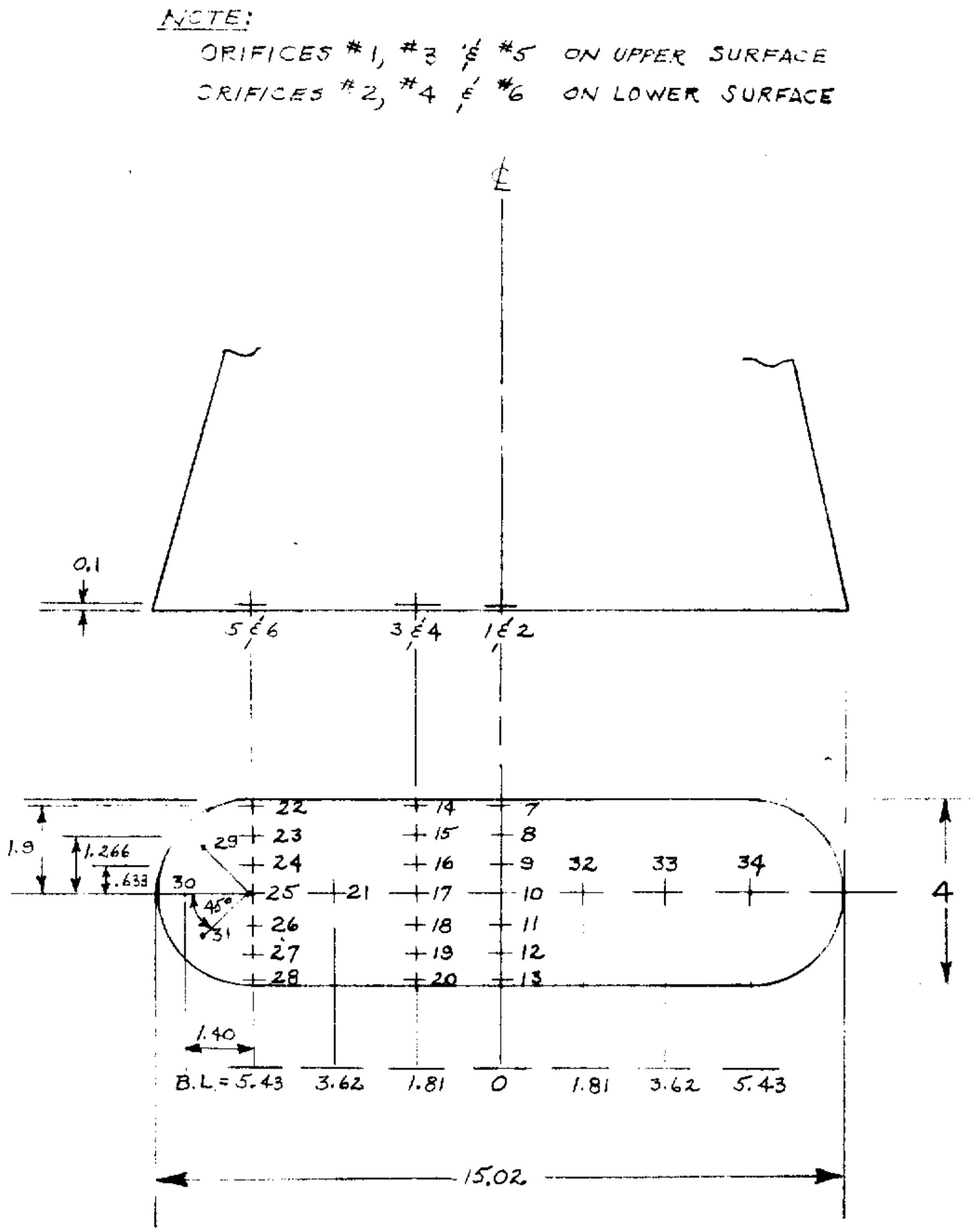


FIGURE 22 Pressure Orifice Location - Wing $W_4$

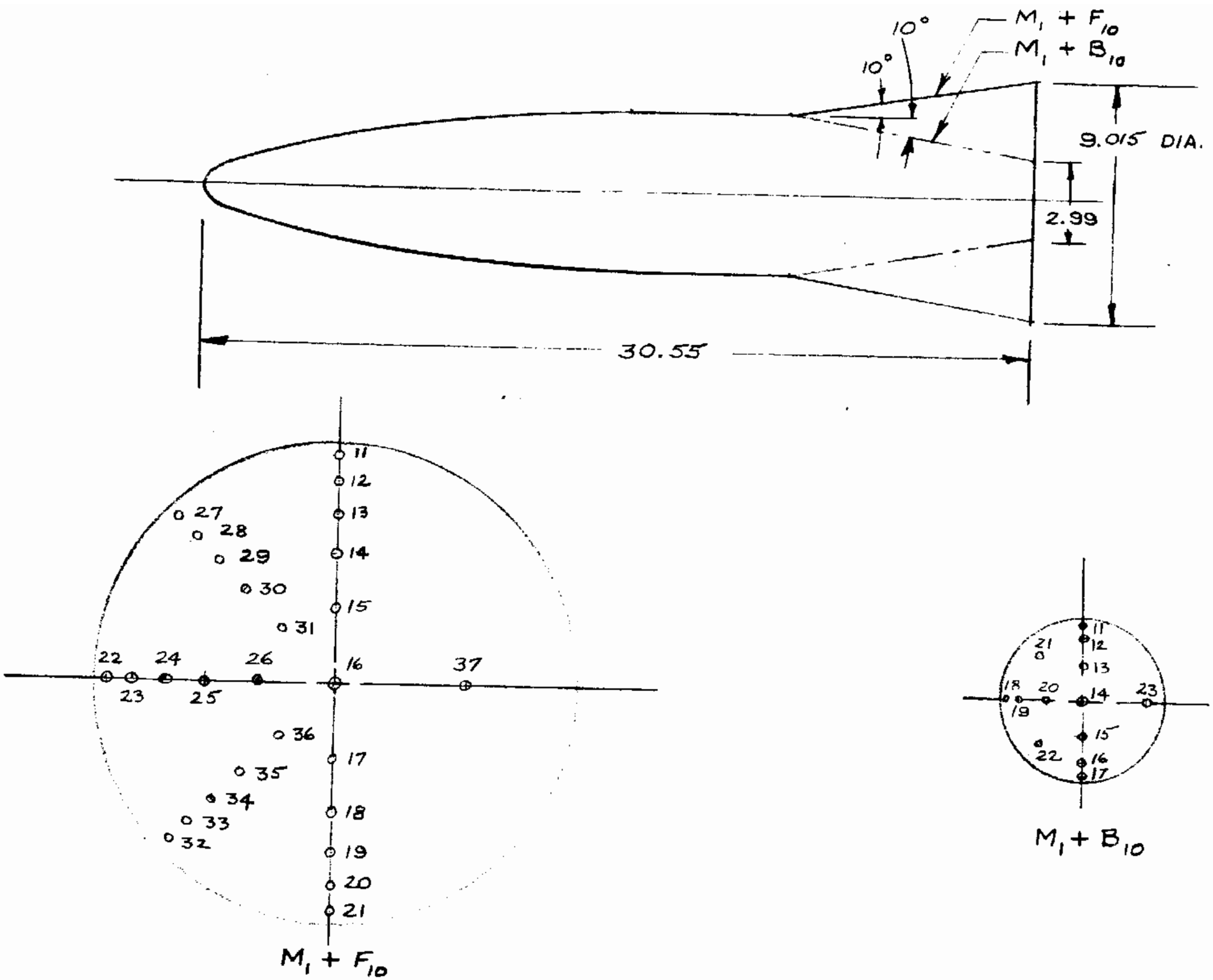


FIGURE 23 Location and Pressure Orifices for 3-D Body with Boattail and Flare.

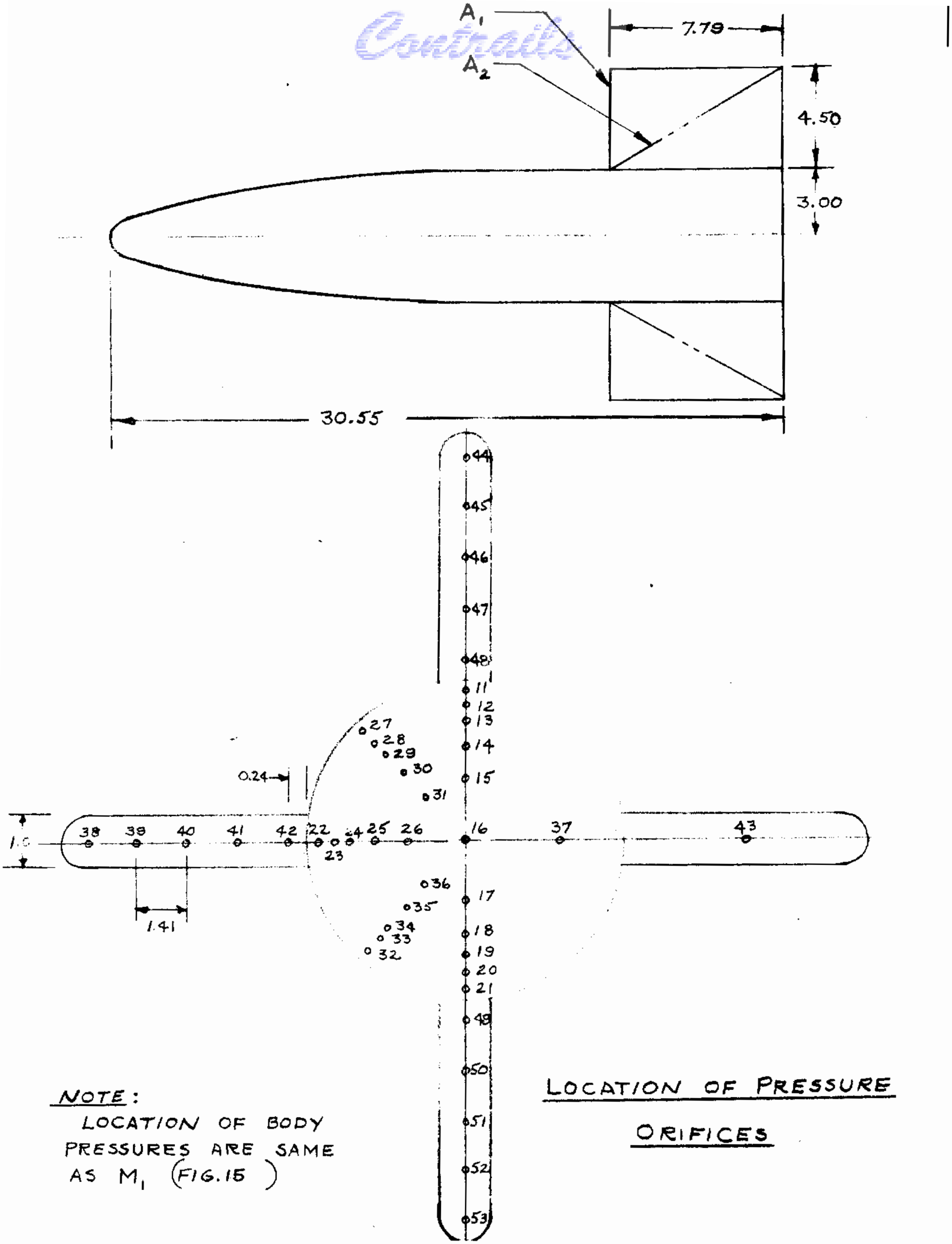


FIGURE 24 3-D Body with Rectangular and Delta Fins

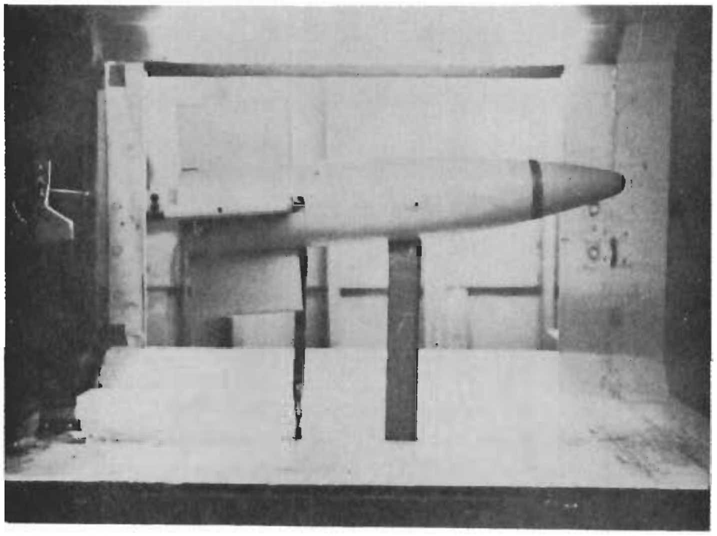

FIGURE 25a - 3-D Body With Rectangular Fins - $M_1 + A_1$

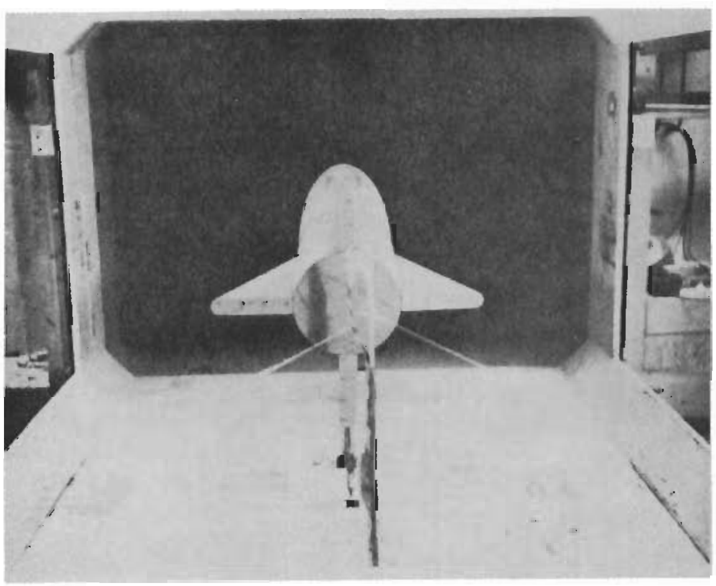

FIGURE 25b - 3-D Body with Delta Fin -- $M_1 + 1/2\ A_2$

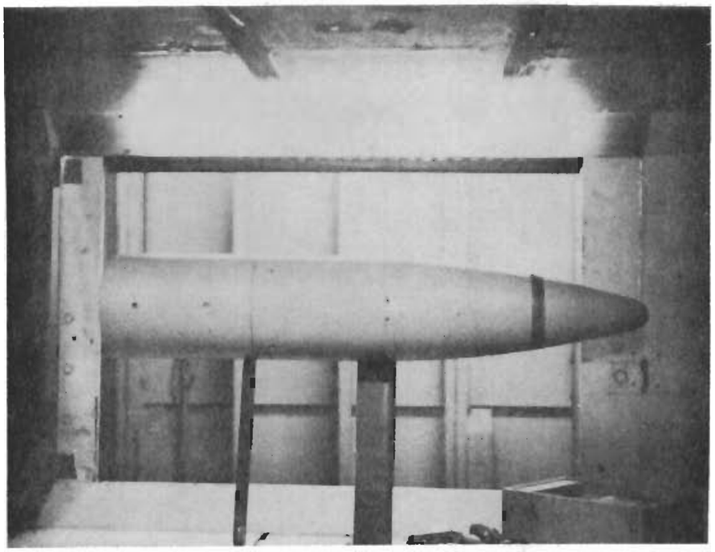

FIGURE 26a - 3-D Body - $M_1$

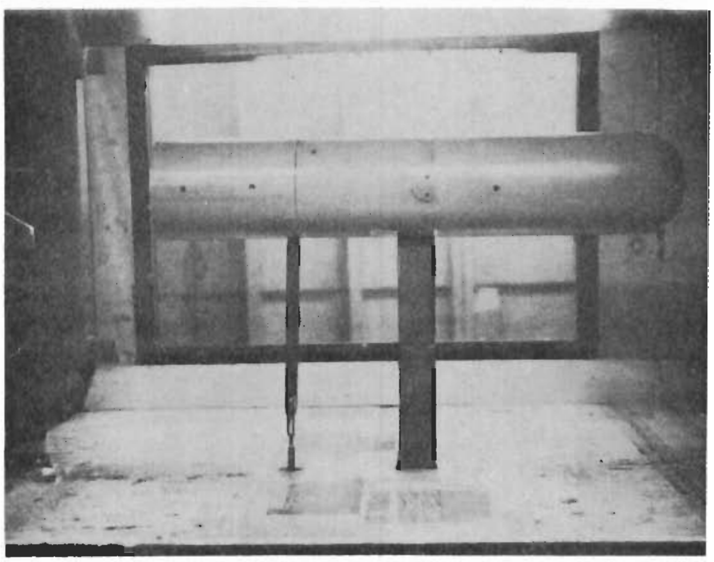

FIGURE 26b - 3-D Body with Blunt Nose - $M_1 + R$

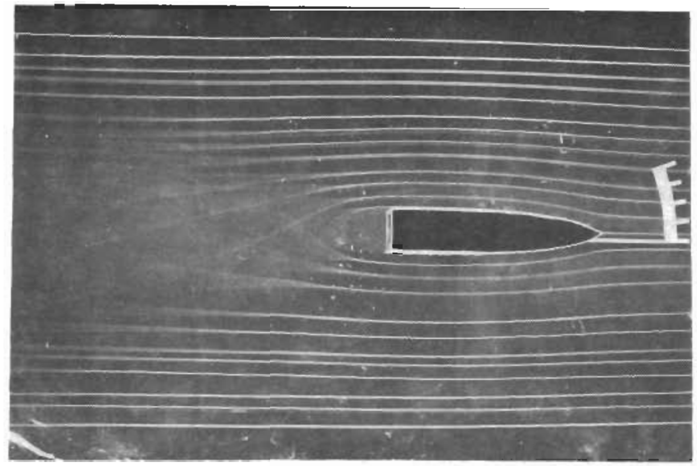

$\alpha = 0°$

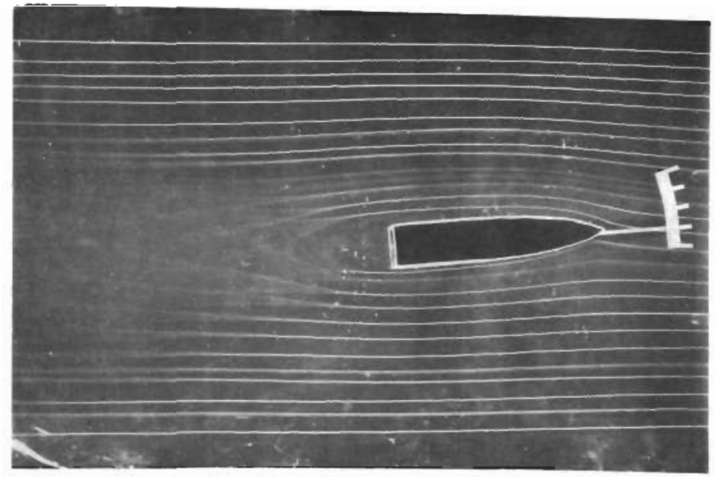

$\alpha = 5°$

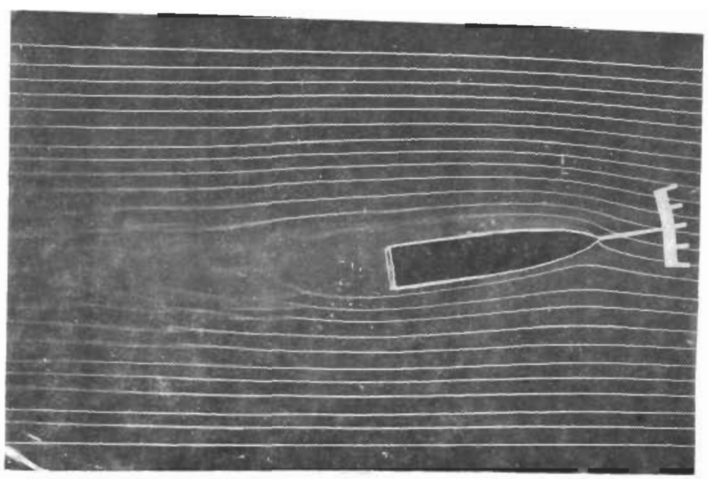

$\alpha = 10°$

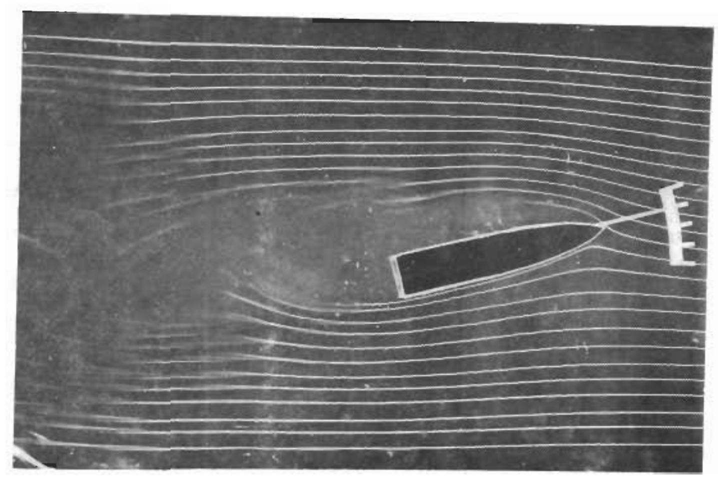

$\alpha = 15°$

FIGURE 27 Configuration $T_2$ Flow Field

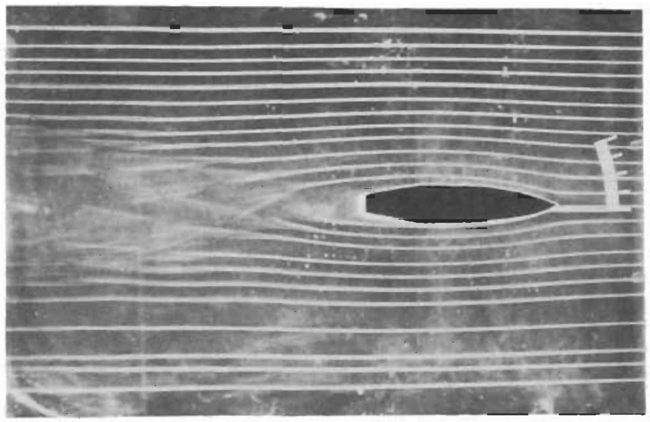

$\alpha = 0°$

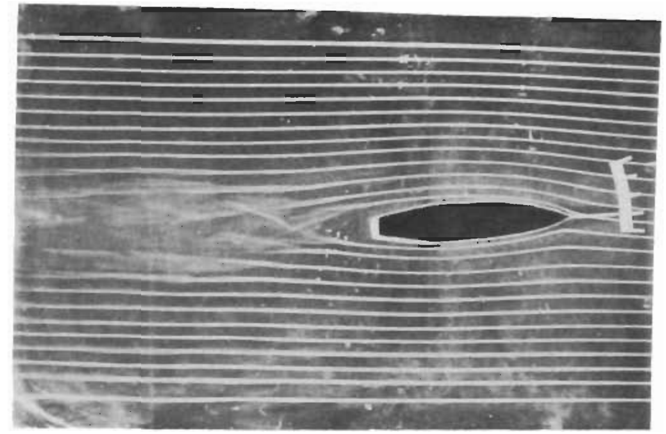

$\alpha = 5°$

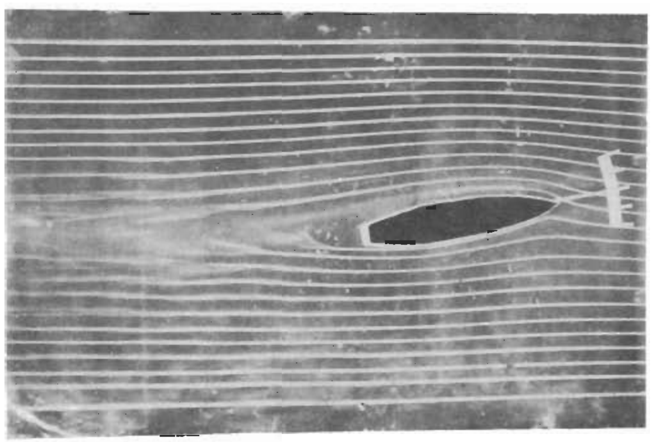

$\alpha = 10°$

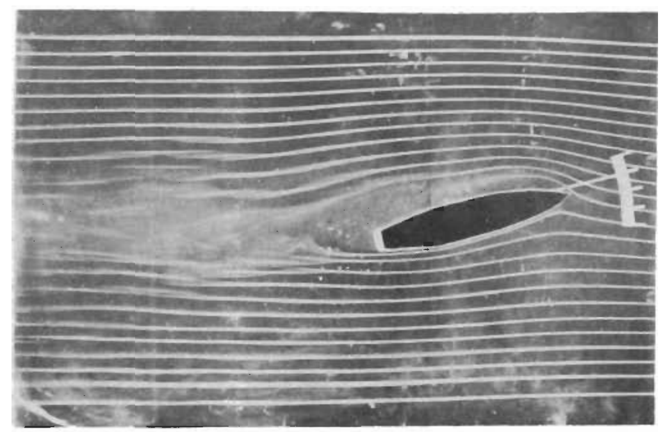

$\alpha = 15°$

**FIGURE 28** **Configuration $T_2 + B_{10}$ Flow Field**

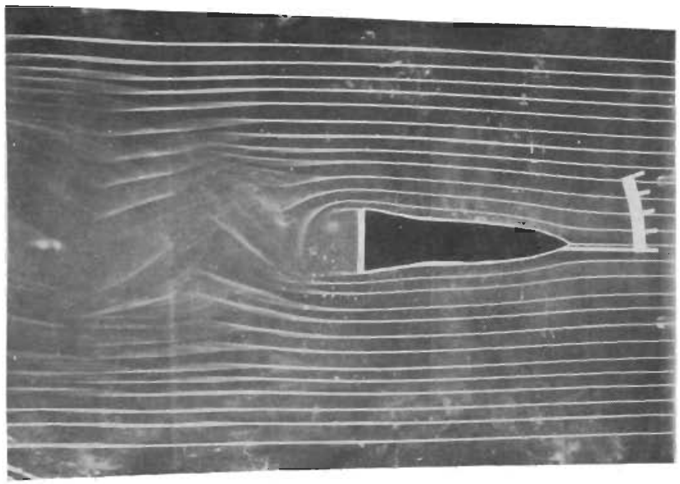

$\alpha = 0°$

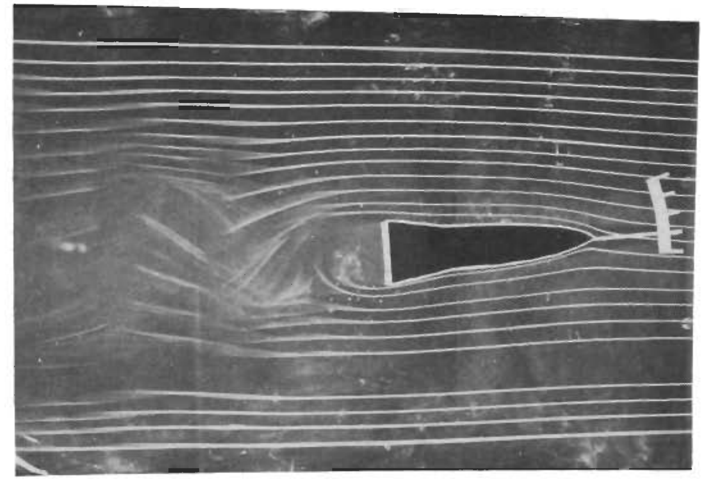

$\alpha = 5°$

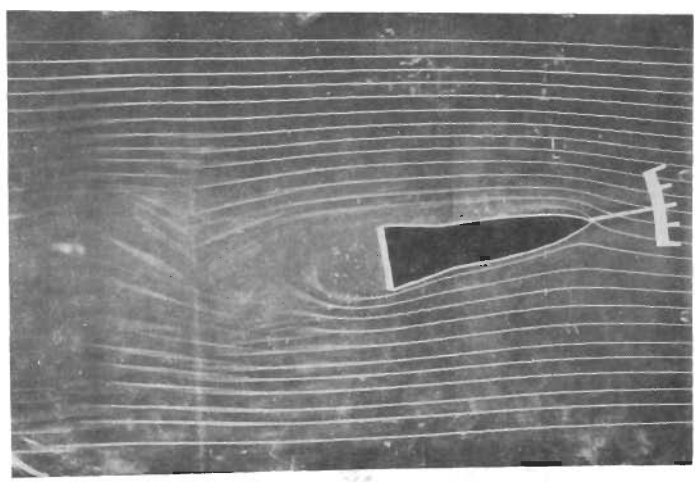

$\alpha = 10°$

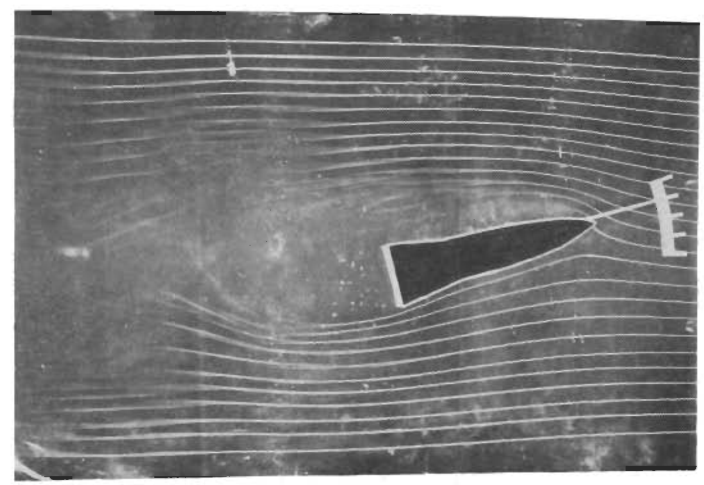

$\alpha = 15°$

FIGURE 29 Configuration $T_2 + F_{10}$ Flow Field

| Sym. | Run | Config. | q |
|---|---|---|---|
| O | 5 | $T_{10}$ | 60 |
| Δ | 6 | $T_{10}$ | 30 |
| O | 13 | $T_{12}+B_{10}$ | 60 |
| Δ | 14 | $T_{12}+B_{10}$ | 30 |
| O | 10 | $T_8+F_{10}$ | 60 |

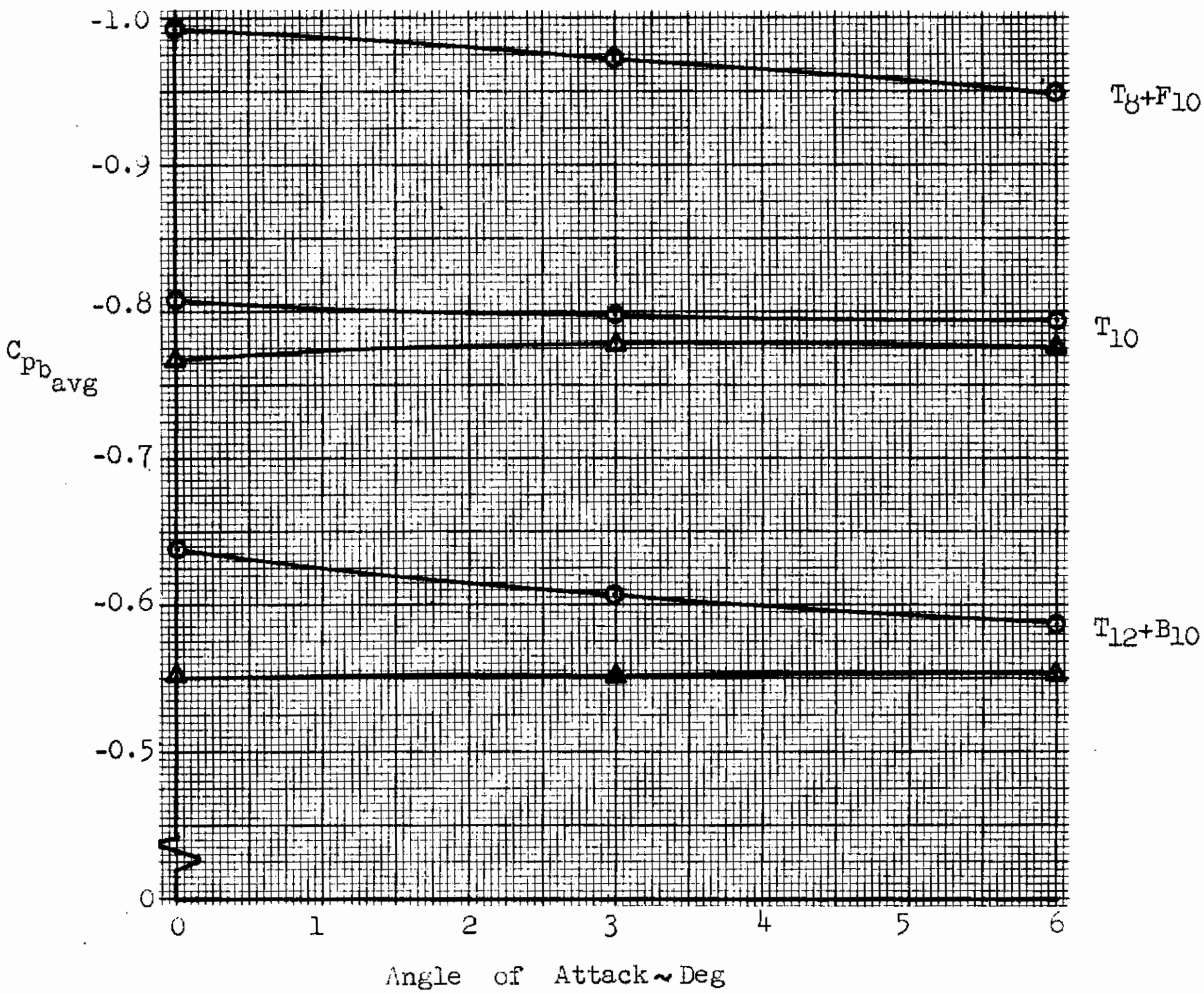


FIGURE 30 **Effect of Angle of Attack & Reynolds Number on Average Base Pressure Coefficient - 2-D Configurations**

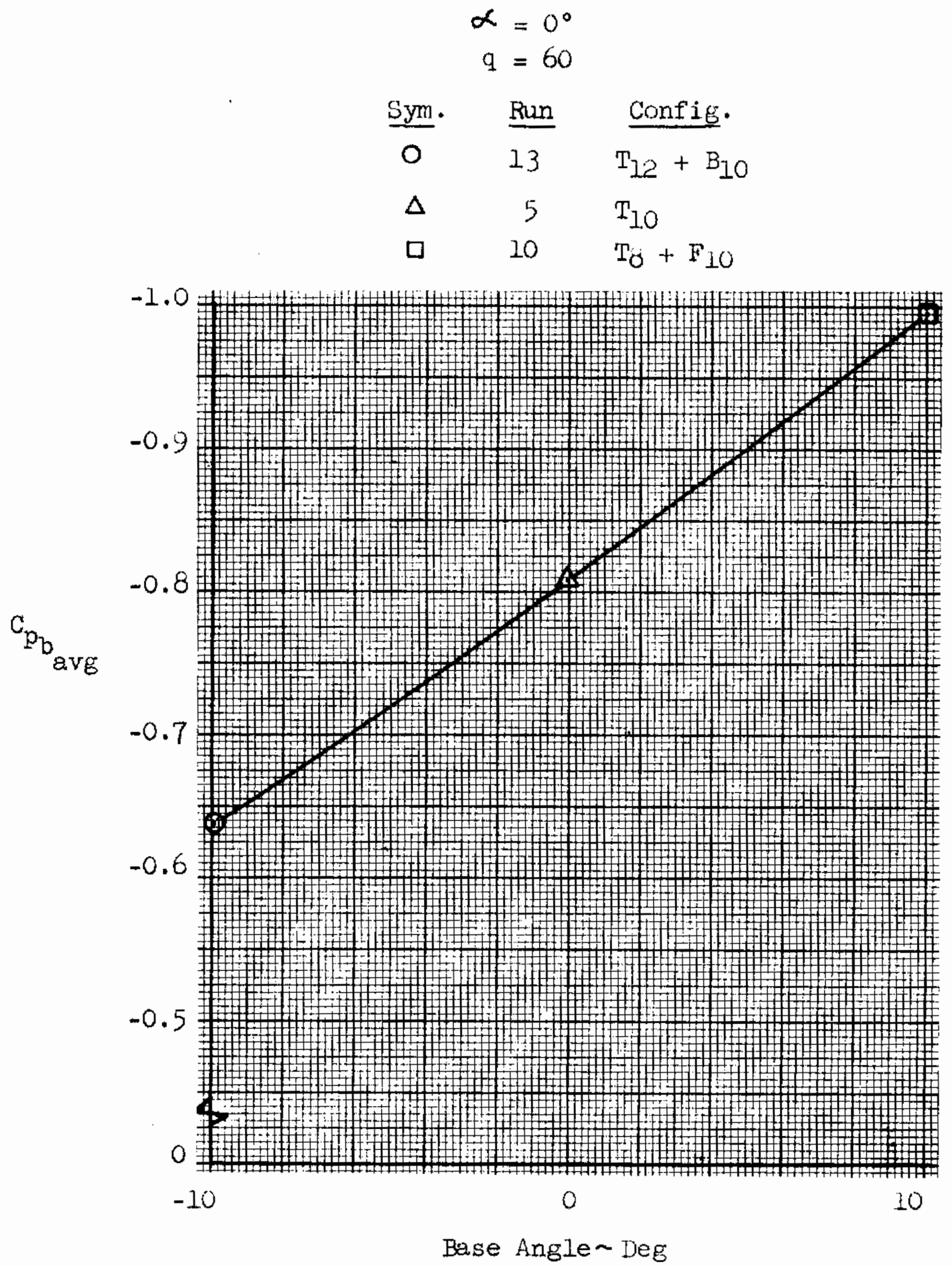


**FIGURE 31** **Effect of Base Angle on Average Base Pressure Coefficient - 2-D Configuration**

$\alpha = 0 \quad q = 60$

| Sym. | Run | Conf. |
|---|---|---|
| ○ | 13 | $T_{12} + B_{10}$ |
| △ | 5 | $T_{10}$ |
| ⬡ | 10 | $T_8 + F_{10}$ |
| □ | 11 | $T_{12} + B_{10} + P$ |
| ◺ | 7 | $T_{10} + P$ |
| ◇ | 9 | $T_8 + F_{10} + P$ |

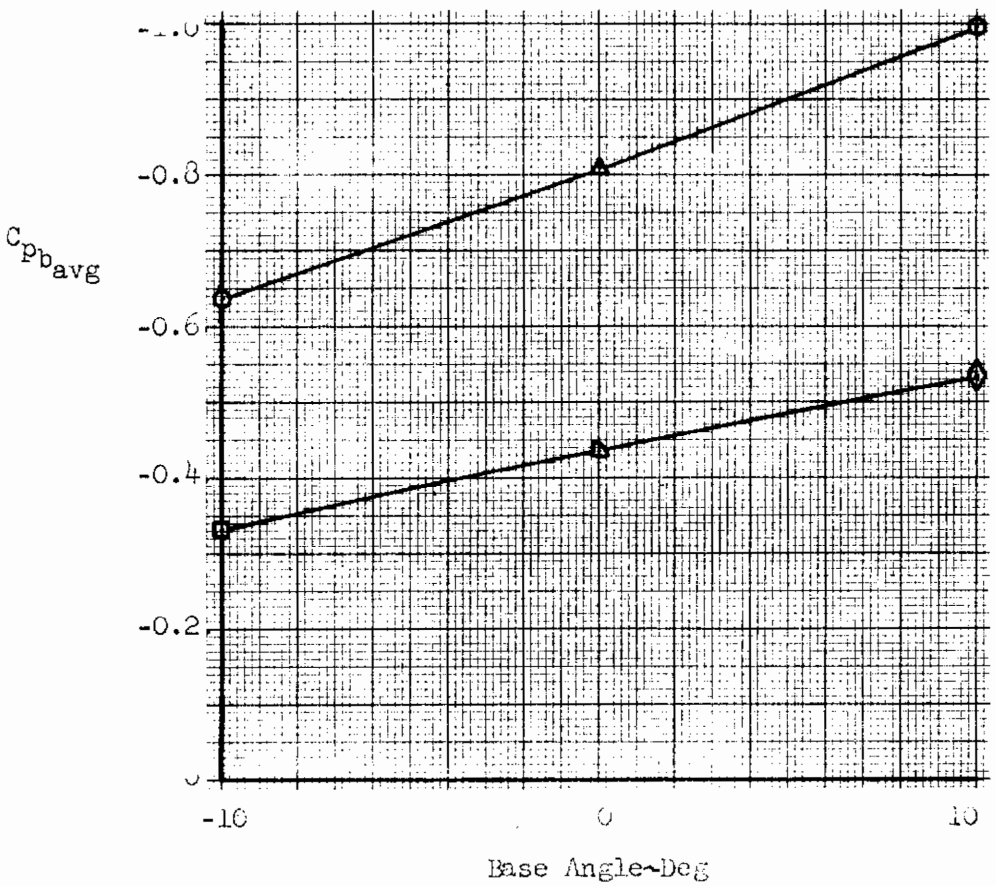


FIGURE 32 Effect of Splitter Plate and Base Angle on Average Base Pressure Coefficient - 2-D Configurations

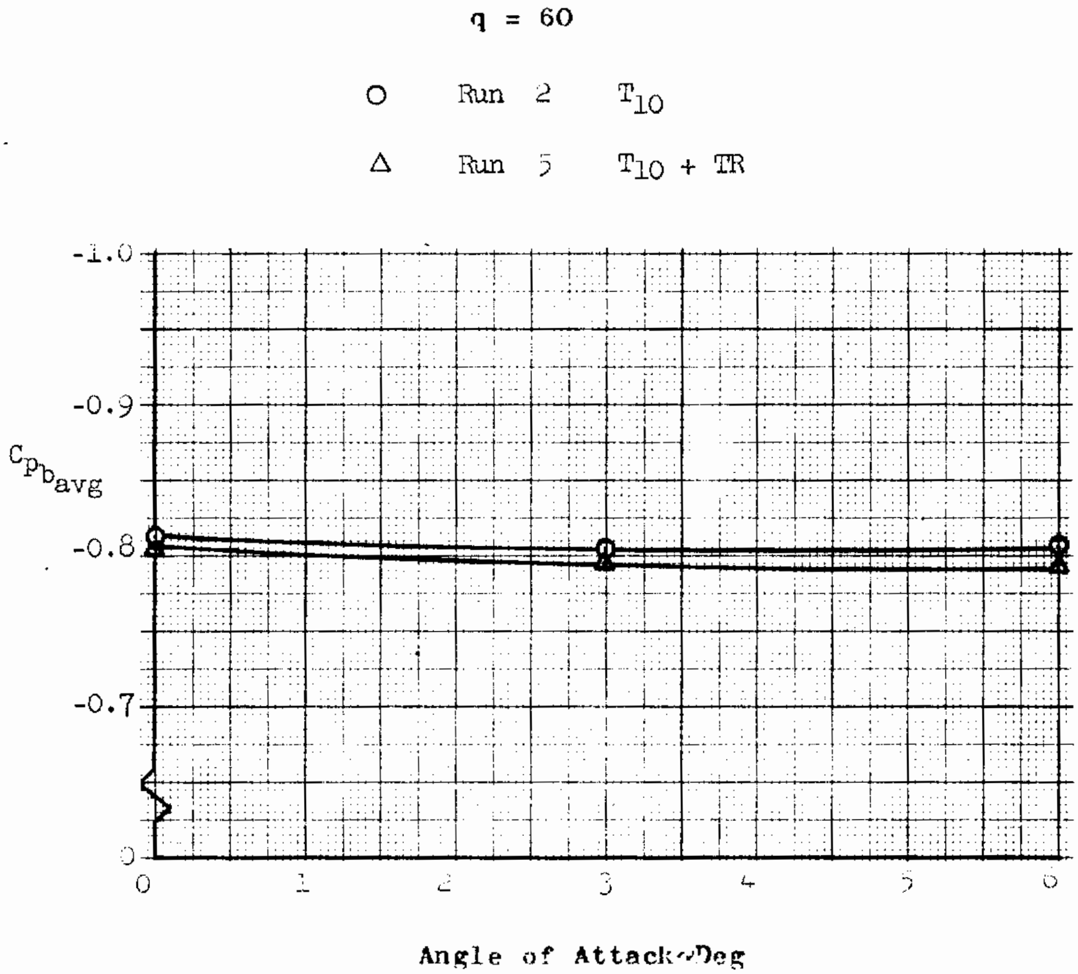


FIGURE 33 Effect of Transition Grit on Average Base Pressure Coefficient - 2-D Body $T_{10}$

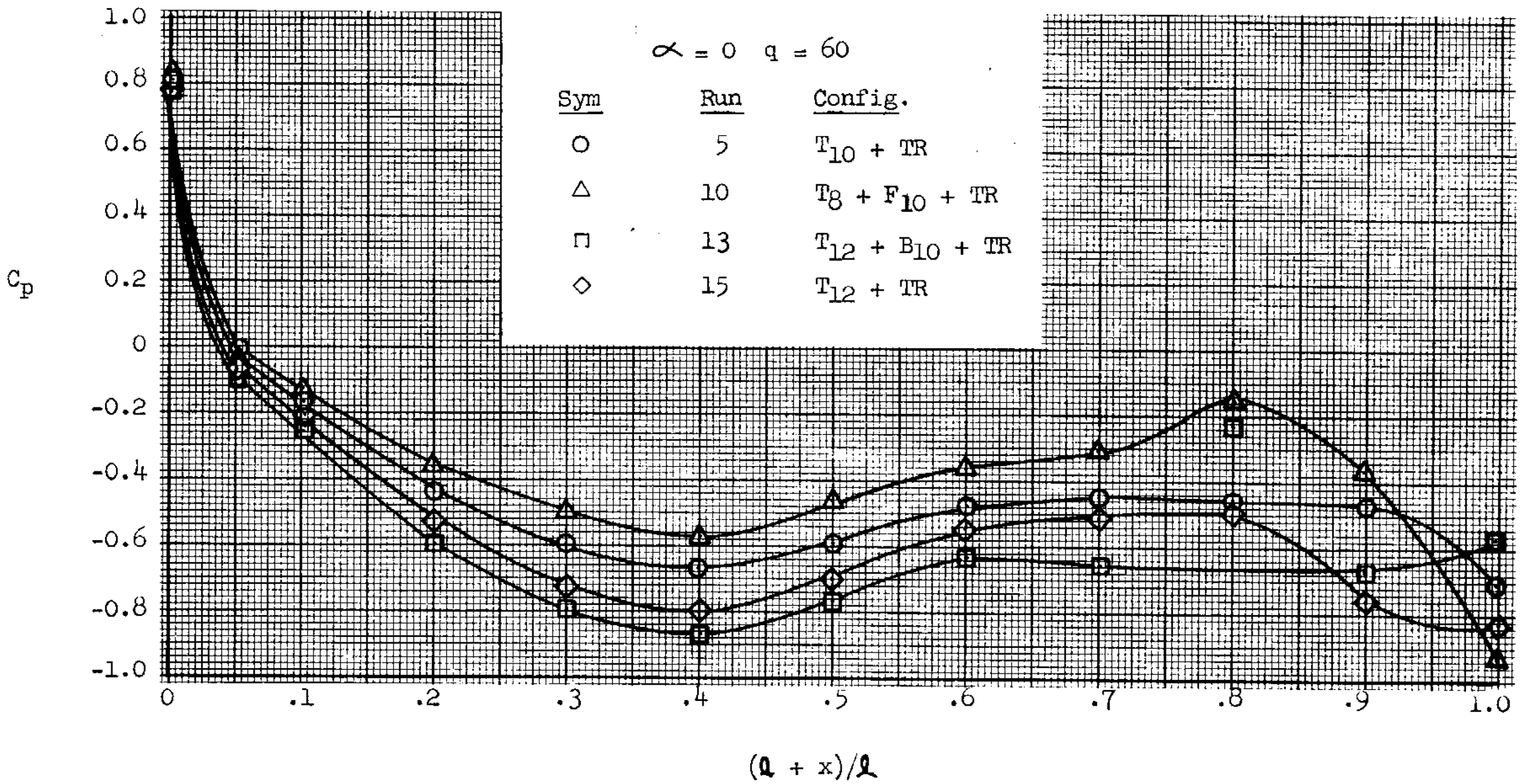


FIGURE 34 Effect of Configurations on Surface Pressure Coefficient
2-D Models

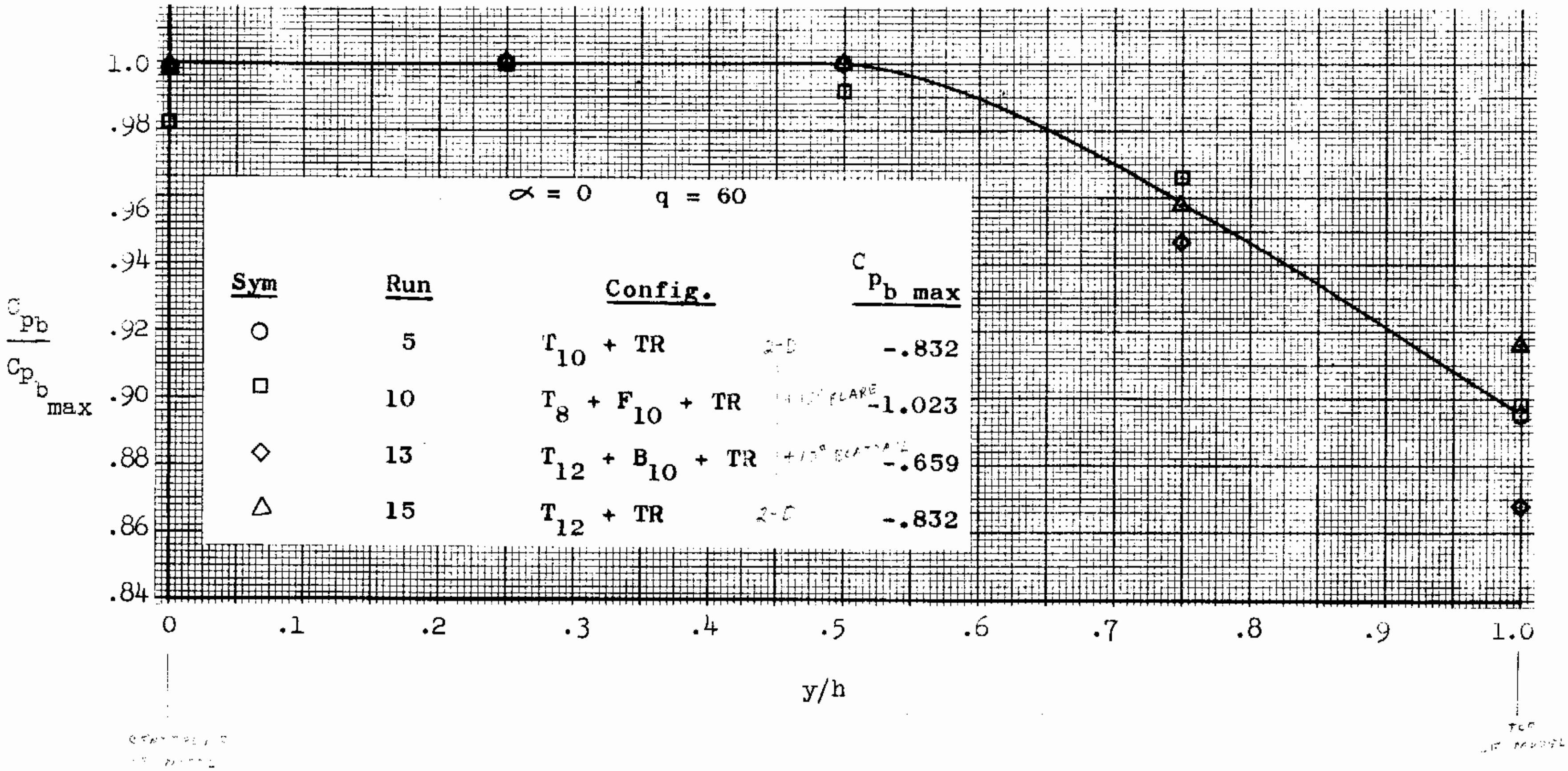


FIGURE 35    Effect of Configuration on Base Pressure
2-D Model

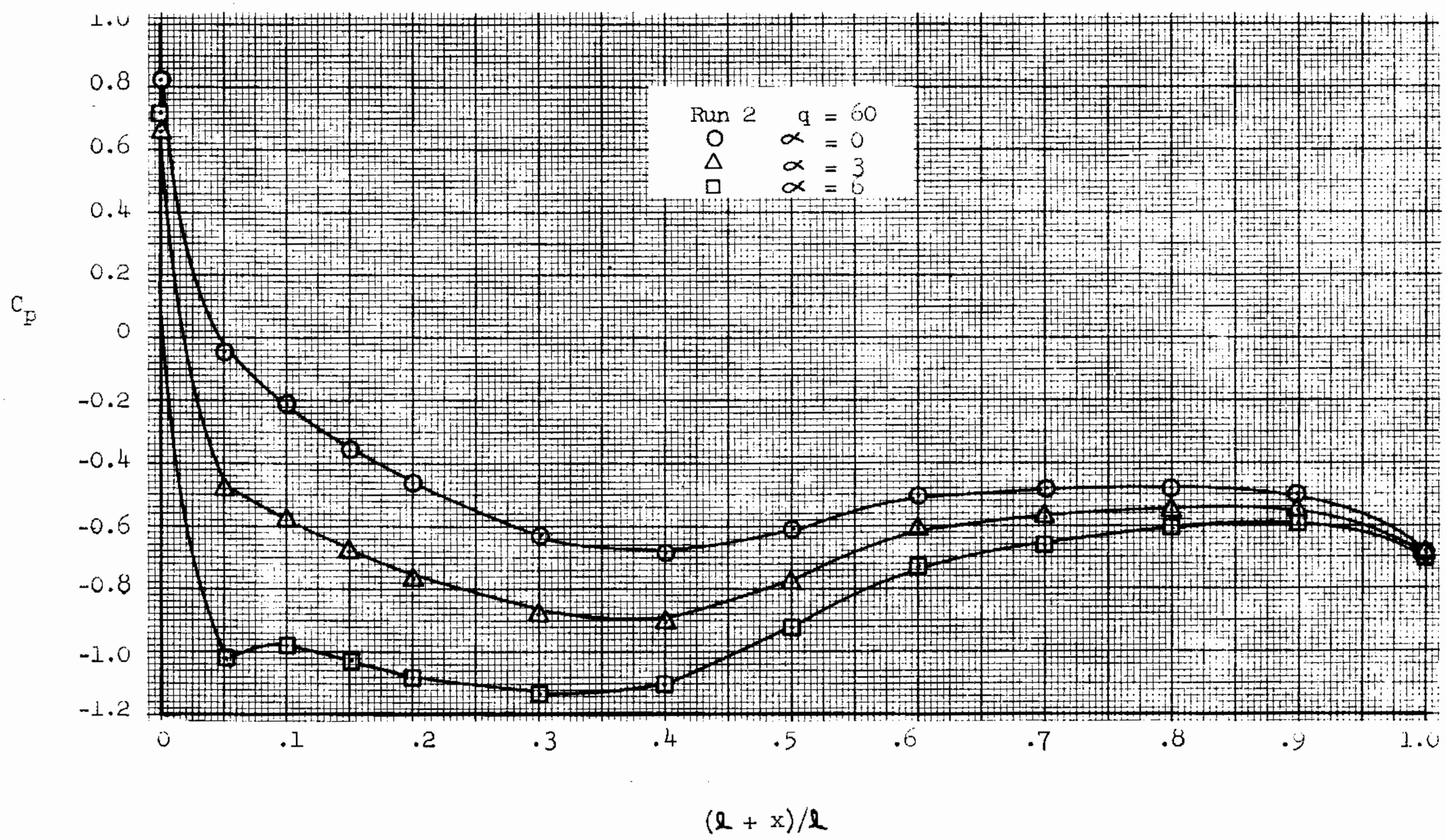


FIGURE 36 **Effect of Angle of Attack on Surface Pressure Coefficient**
**2-D Model $T_{10}$**

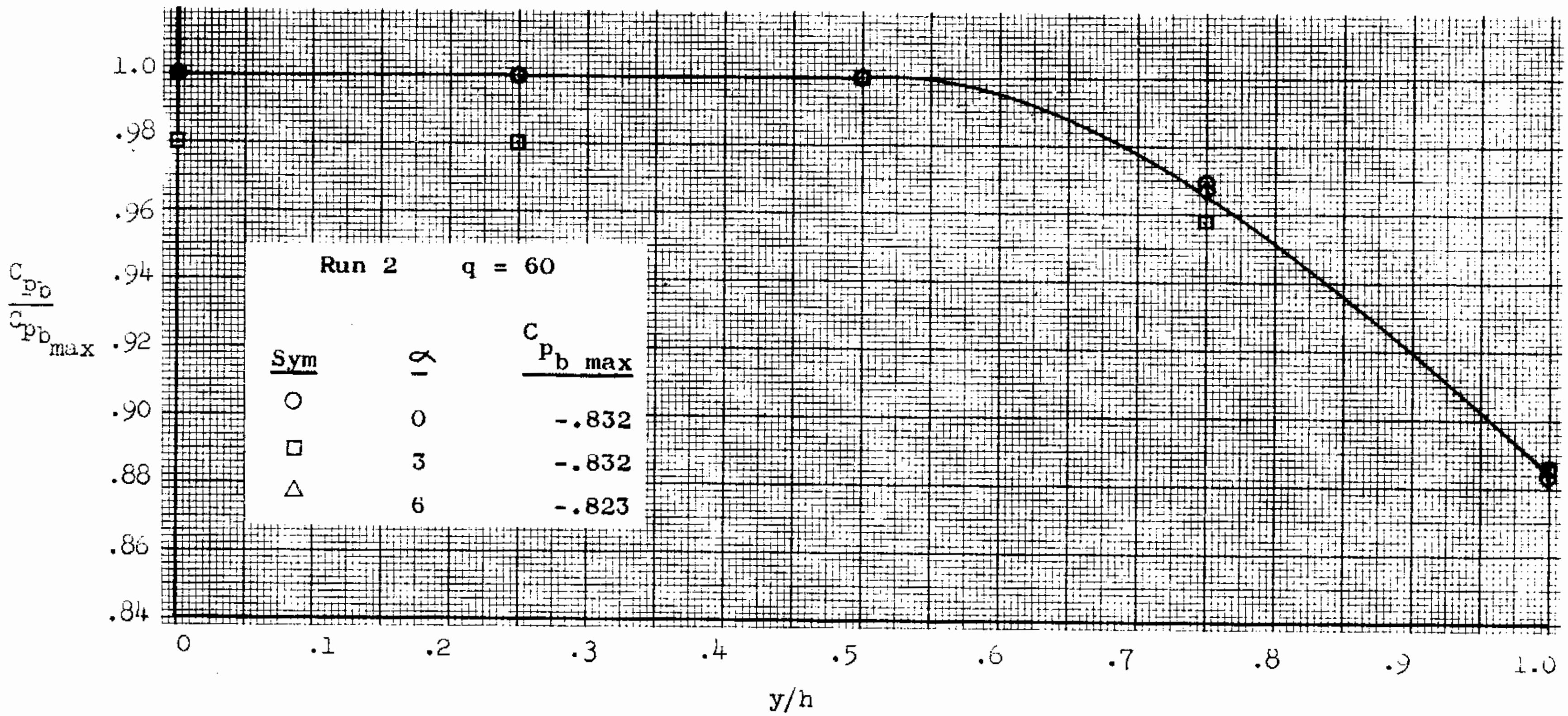


FIGURE 37 Effect of Angle of Attack on Base Pressure 2-D Model $T_{10}$

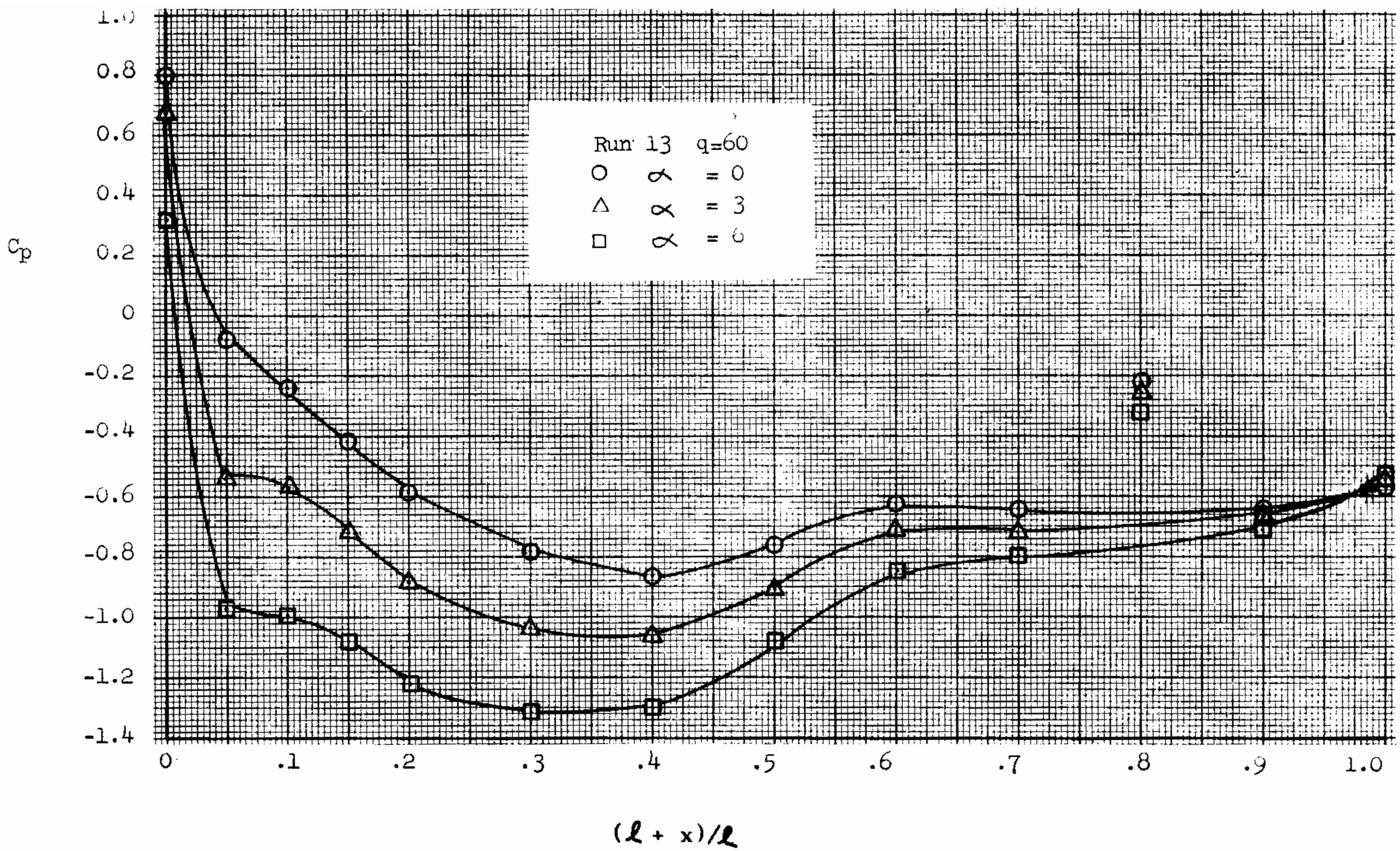


FIGURE 38 Effect of Angle of Attack on Surface Pressure Coefficient
2-D Model $T_{12} + B_{10}$

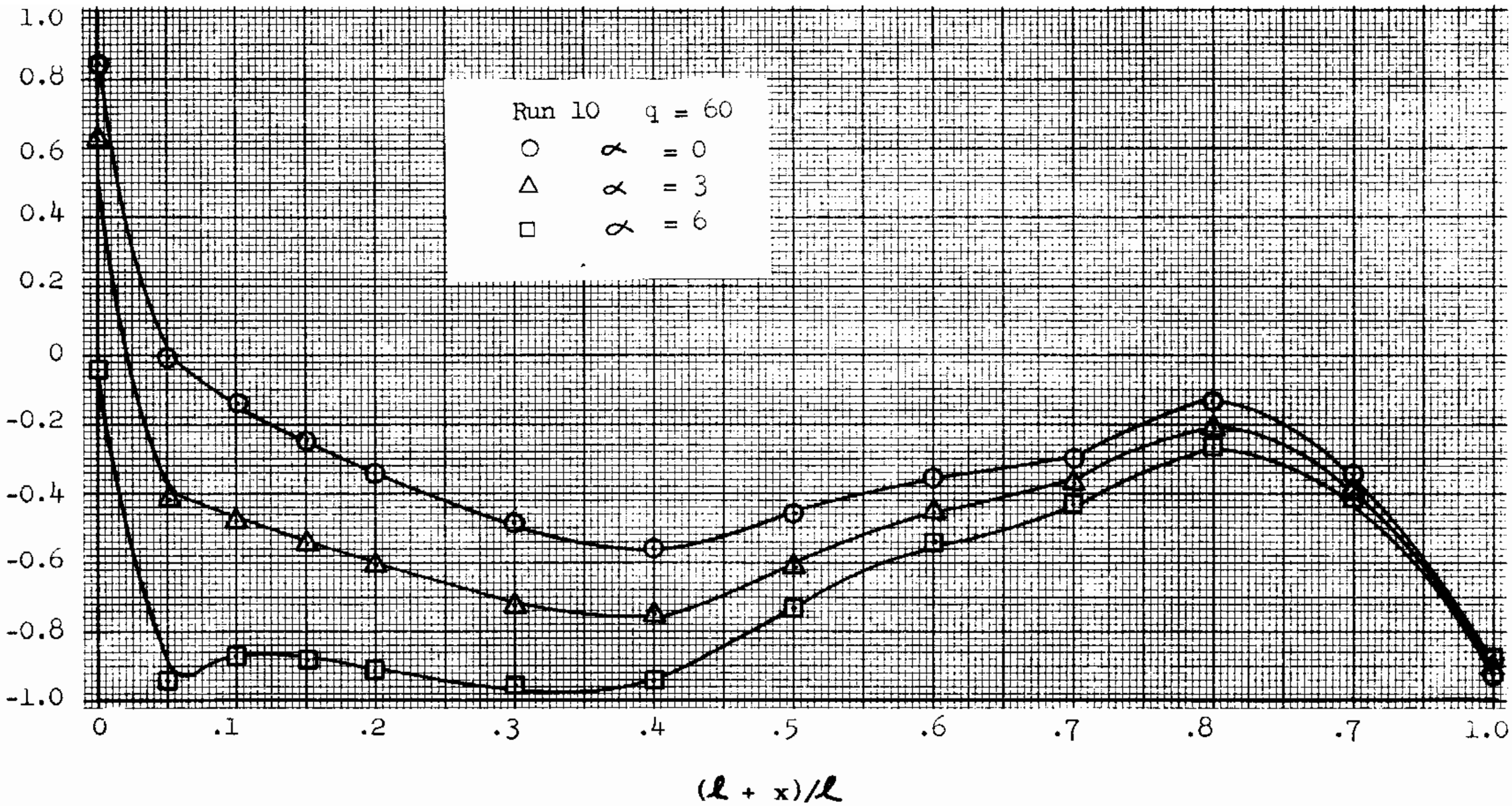


FIGURE 39 Effect of Angle of Attack on Surface Pressure Coefficient
2-D Model $T_8 + F_{10}$

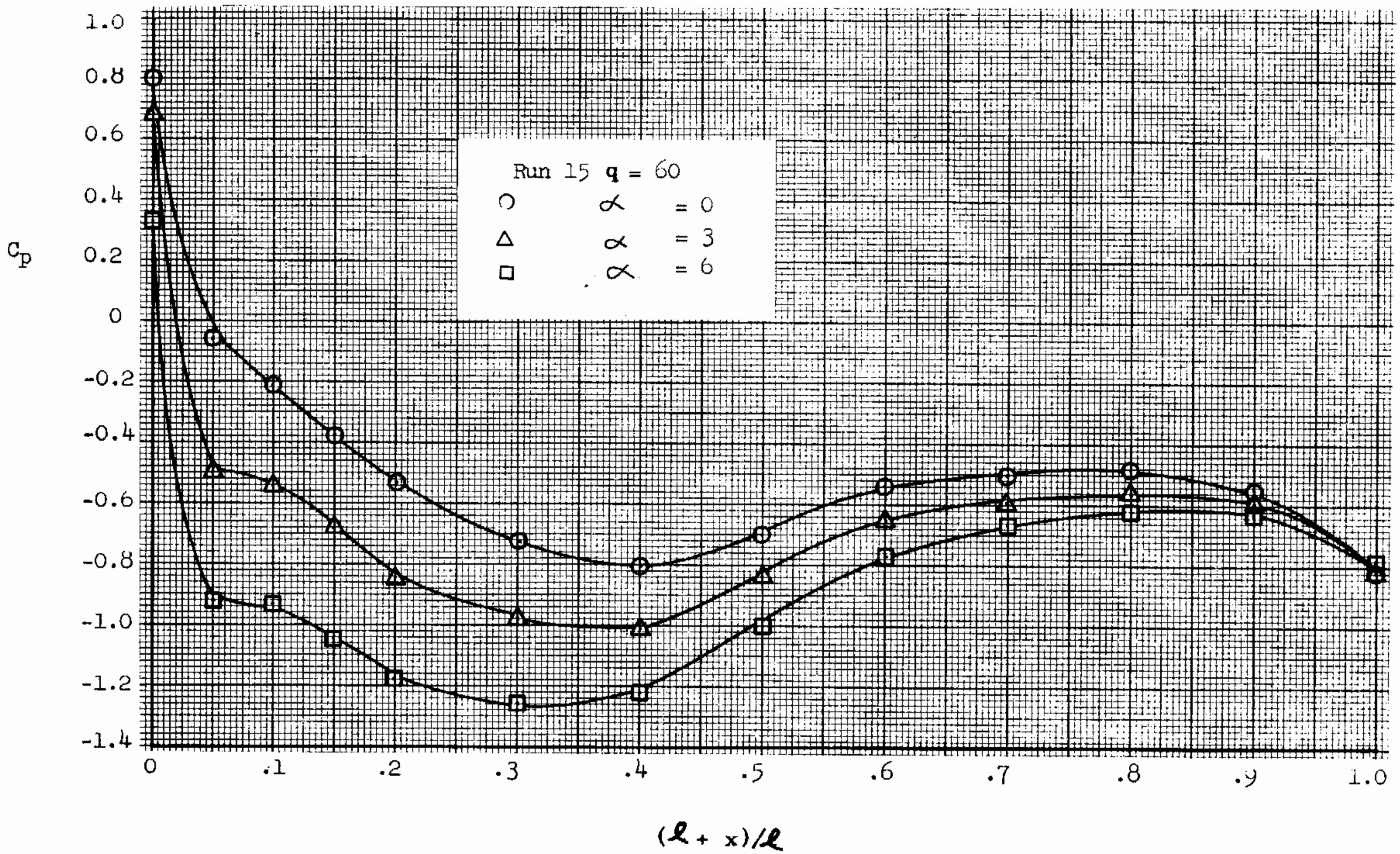


FIGURE 40 Effect of Angle of Attack on Surface Pressure Coefficient
2-D Model $T_{12}$

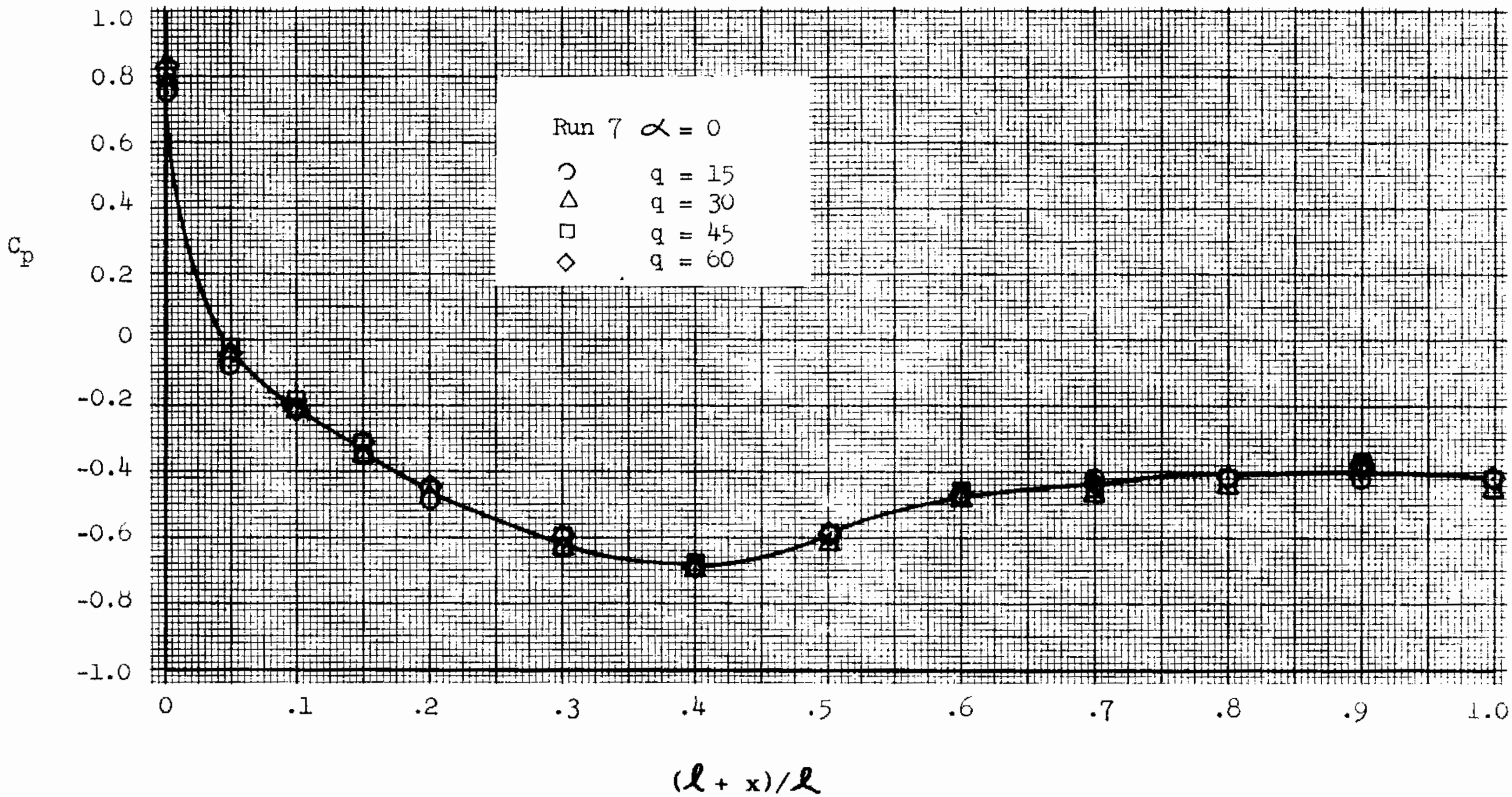


FIGURE 41 Effect of Reynolds Number on Surface Pressure Coefficient
2-D Model $T_{10}$ + P

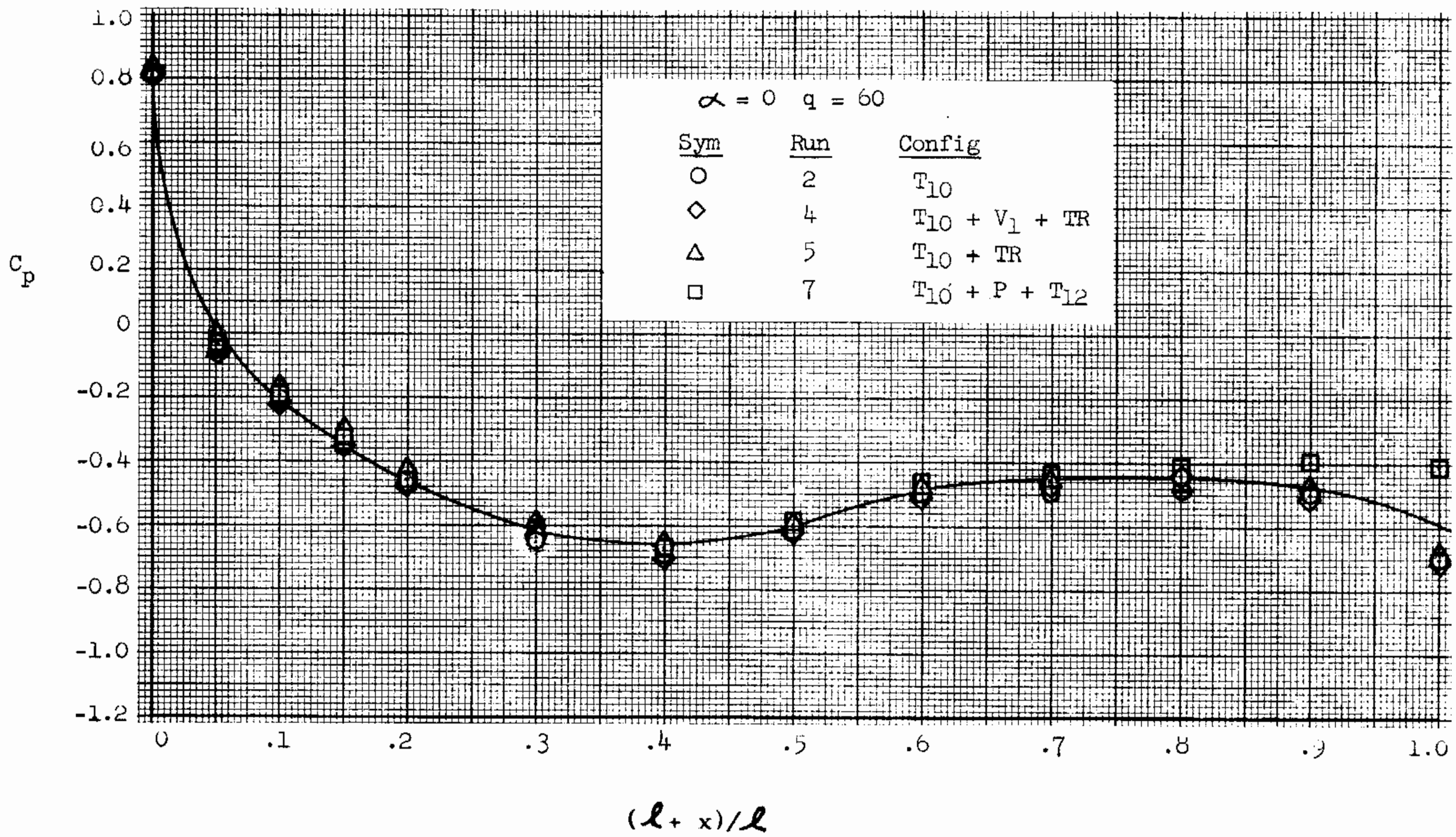


FIGURE 42 Effect of Splitter Plate, Vertical Plate and Transition Grit on Surface Pressure Coefficient

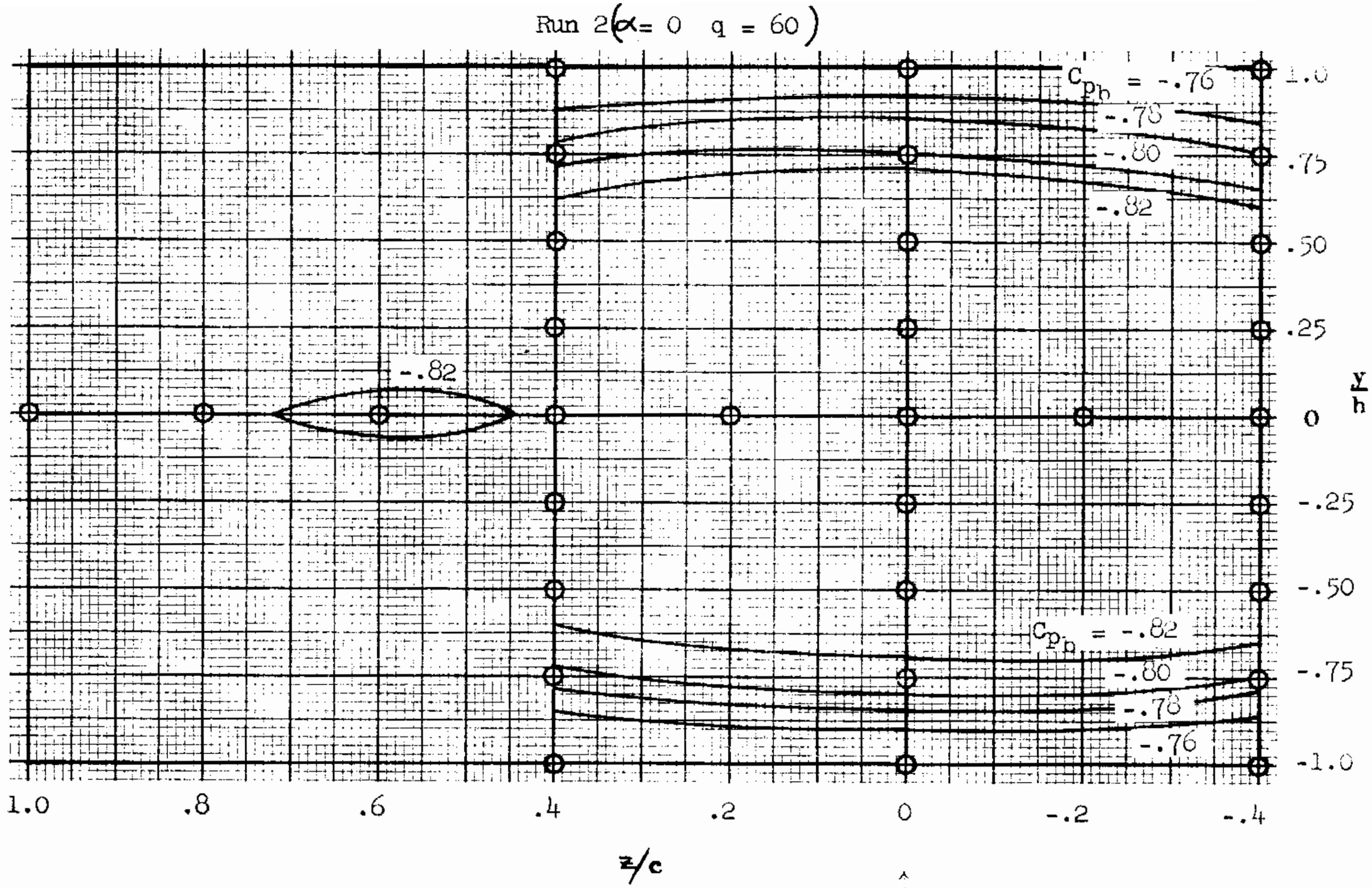


FIGURE 43 Base Pressure Contour Plot - 2-D Model $T_{10}$

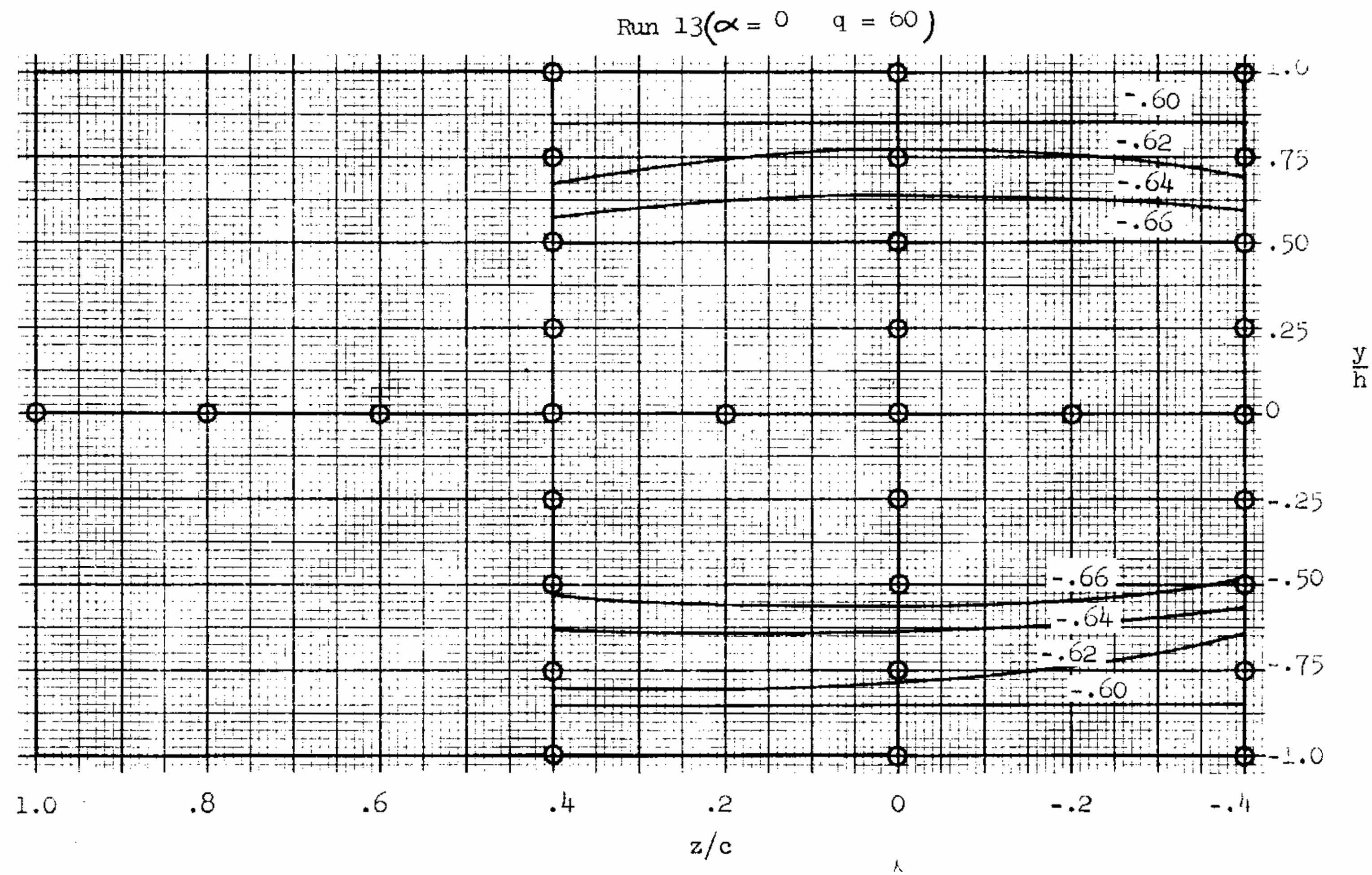


FIGURE 44 Base Pressure Contour Plot - 2-D Model $T_{12}$ + $B_{10}$

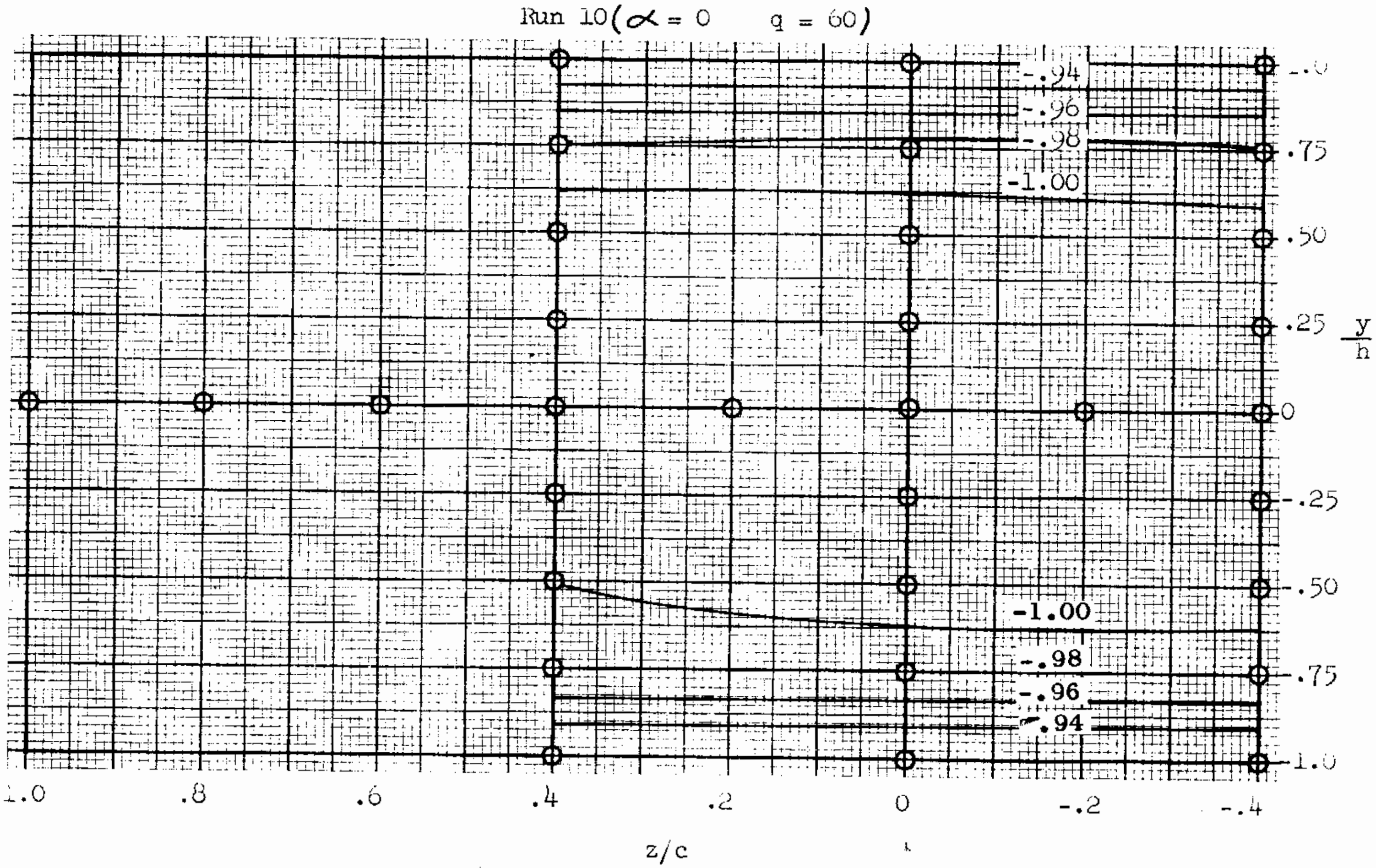


**FIGURE 45** Base Pressure Contour Plot - 2-D Model $T_8 + F_{10}$

$\alpha = 0 \qquad q = 45$

| Sym | Run | Config. |
|---|---|---|
| ○ | CT 3 | $M_1 + B_{10}$ |
| □ | CT 2 | $M_1$ |
| △ | CT 33 | $M_1 + F_{10}$ |

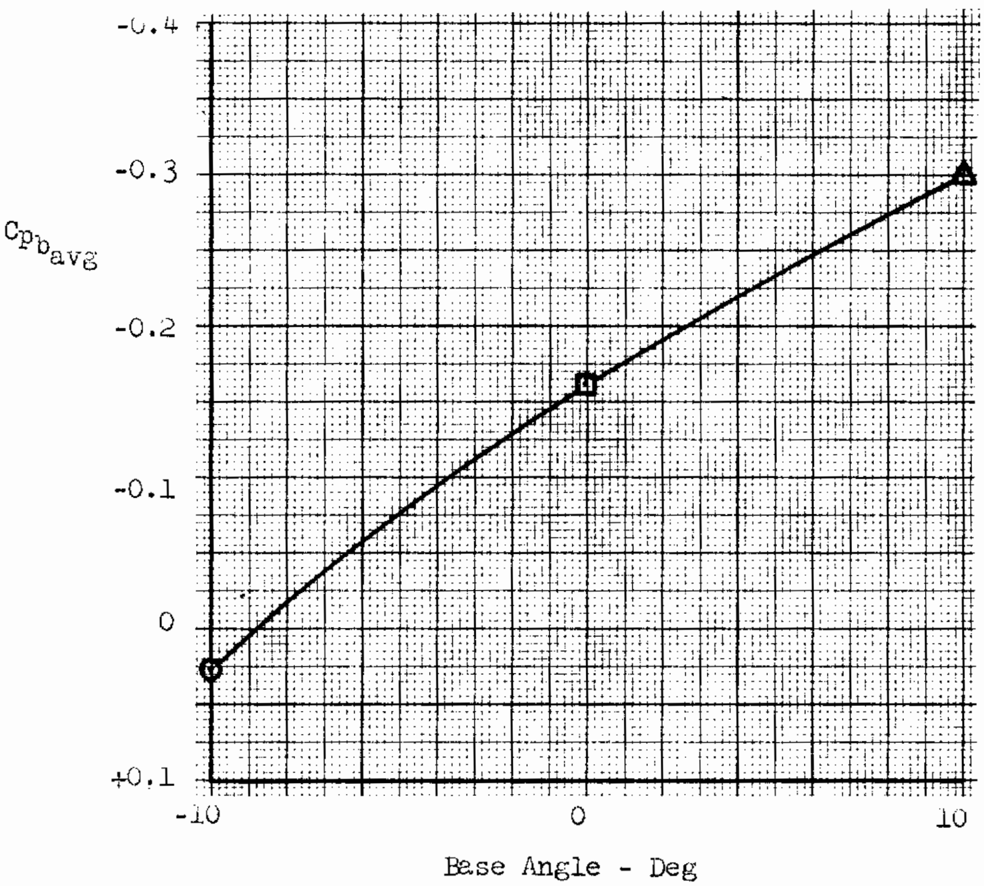


FIGURE 46 **Effect of Base Angle an Average Base Pressure Coefficient - 3D Body**

| Sym. | Run | Config. | q |
|---|---|---|---|
| O | CT 2 | $M_1$ | 45 |
| Δ | CT 1 | $M_1$ | 30 |
| O | CT 32 | $M_1 + R$ | 45 |
| Δ | CT 31 | $M_1 + R$ | 30 |
| O | CT 33 | $M_1 + F_{10}$ | 45 |
| Δ | CT 34 | $M_1 + F_{10}$ | 30 |
| O | CT 3 | $M_1 + B_{10}$ | 45 |
| Δ | CT 4 | $M_1 + B_{10}$ | 30 |

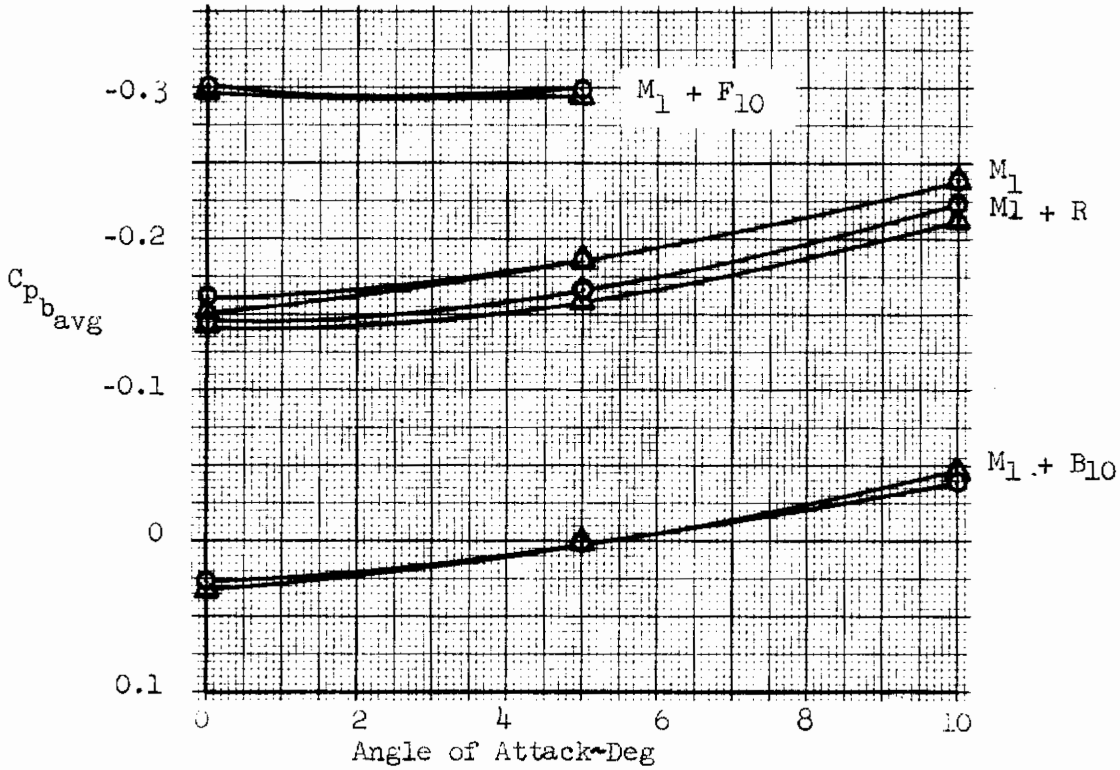


FIGURE 47 Effect of Angle of Attack and Reynolds Number on Average Base Pressure Coefficients - 3-D Body Configurations

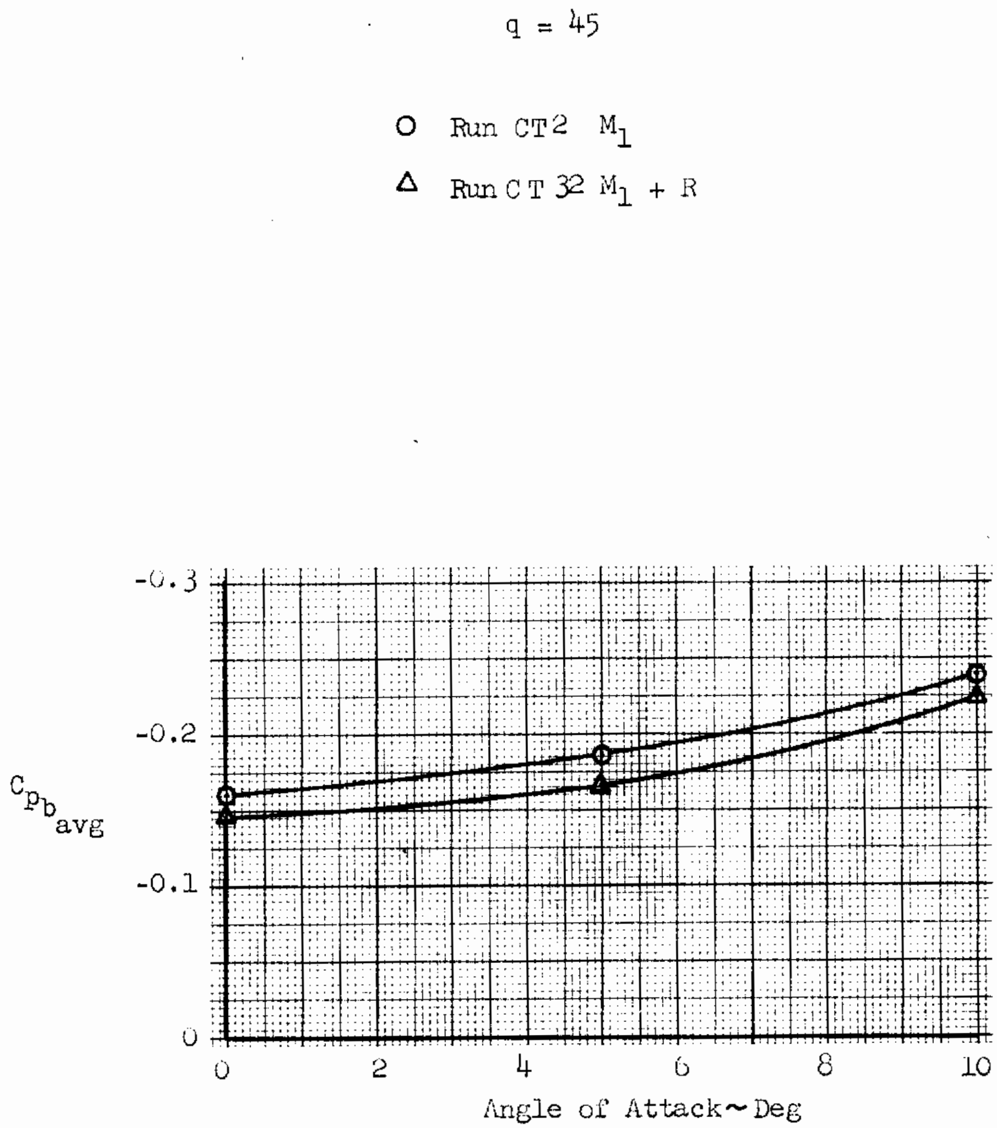


FIGURE 48 Effect of Nose Bluntness on Average Base Pressure Coefficient - 3-D Body

$q = 45$

| Sym | Run | Config. |
|---|---|---|
| ⬡ | CT 2 | $M_1$ |
| ○ | CT 23 | $M_1 + A_1$ |
| □ | CT 25 | $M_1 + 1/2\ A_1$ |
| ◇ | CT 28 | $M_1 + A_2$ |
| △ | CT 25 | $M_1 + 1/2\ A_2$ |

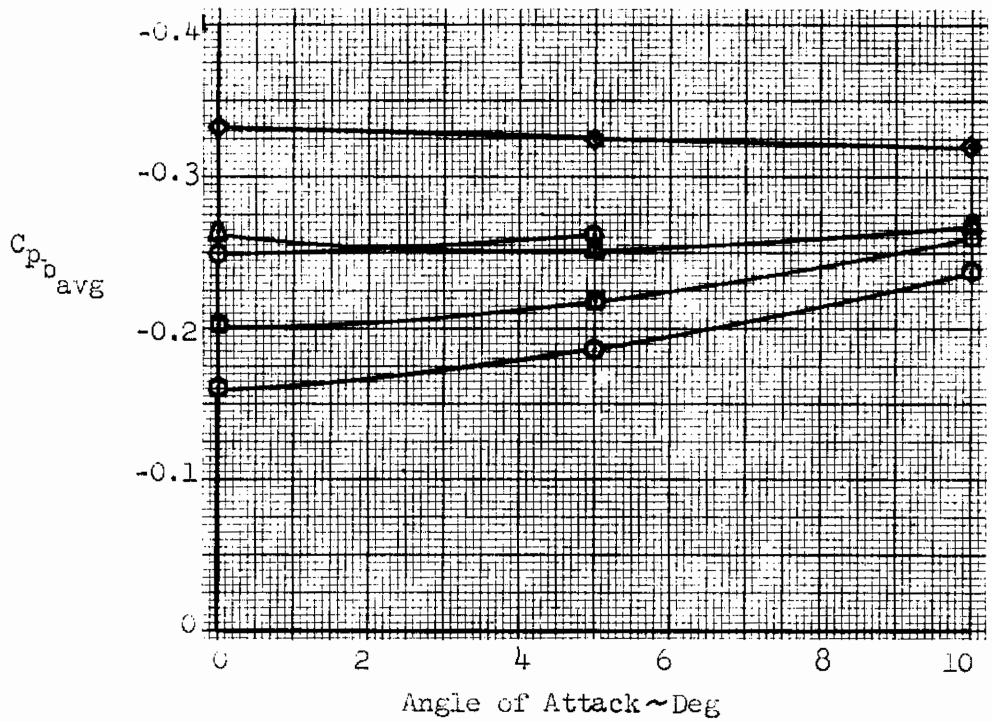


FIGURE 49 **Effect of Fin Configuration on Average Base Pressure Coefficient - 3D Body**

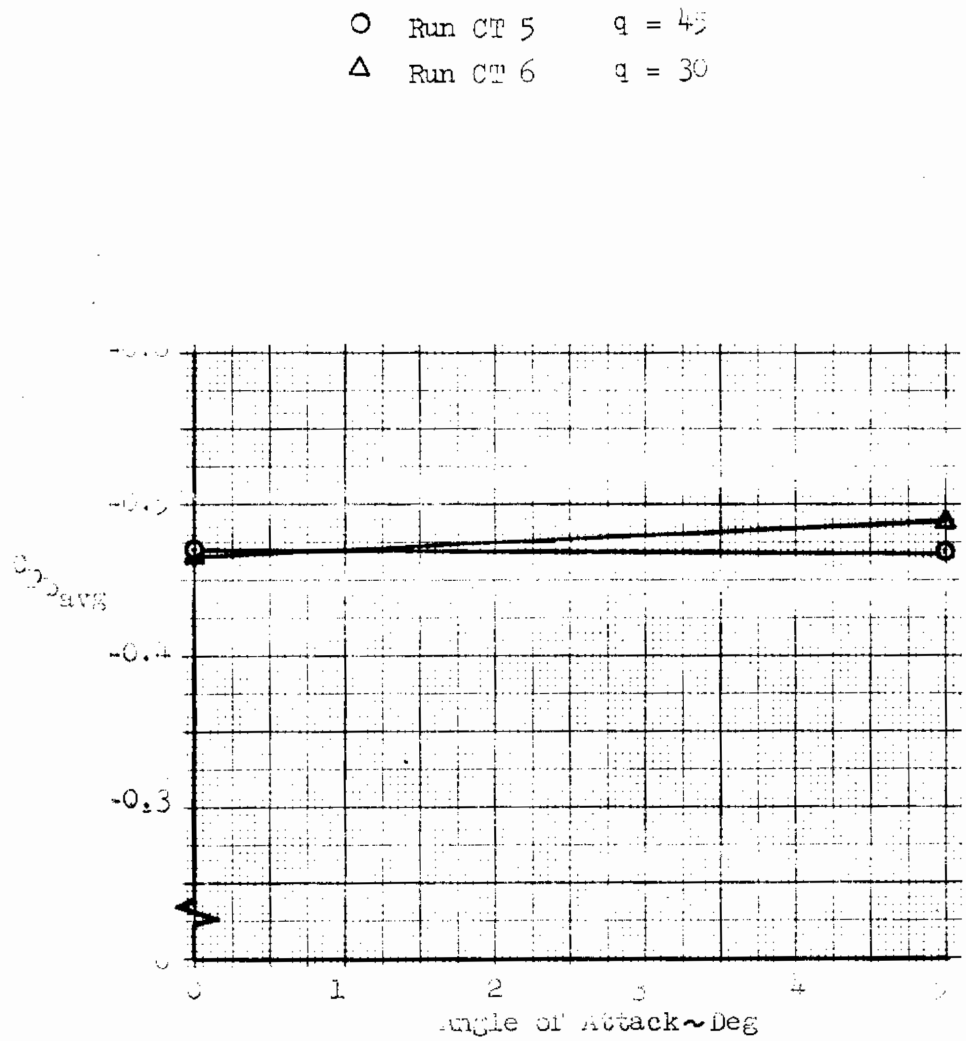


FIGURE 53 **Effect of Angle of Attack and Reynolds Number on Average Base Pressure Coefficient - 3 Inch Wing**

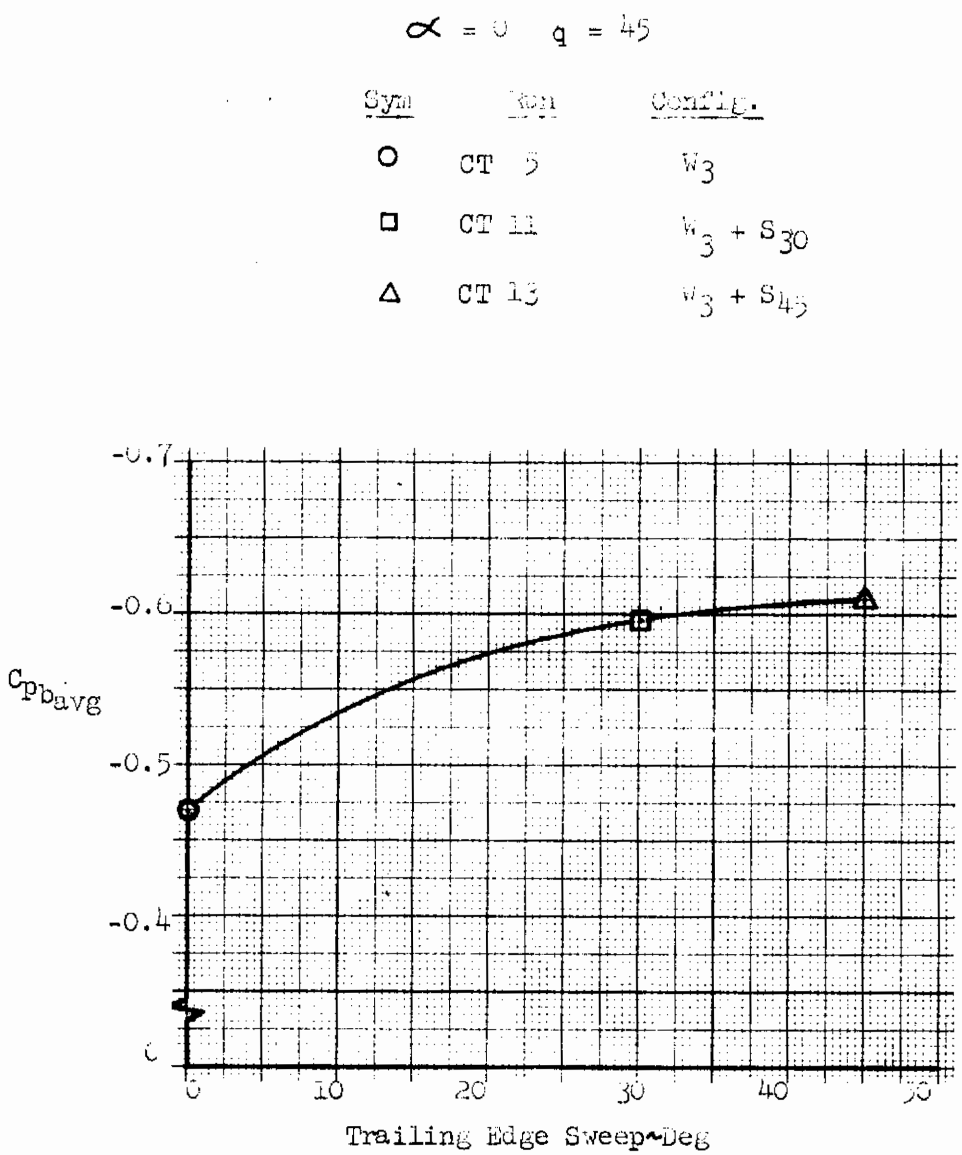


FIGURE 51 **Effect of Trailing Edge Sweep Angle on Average Base Pressure Coefficient - 3 Inch Wing**

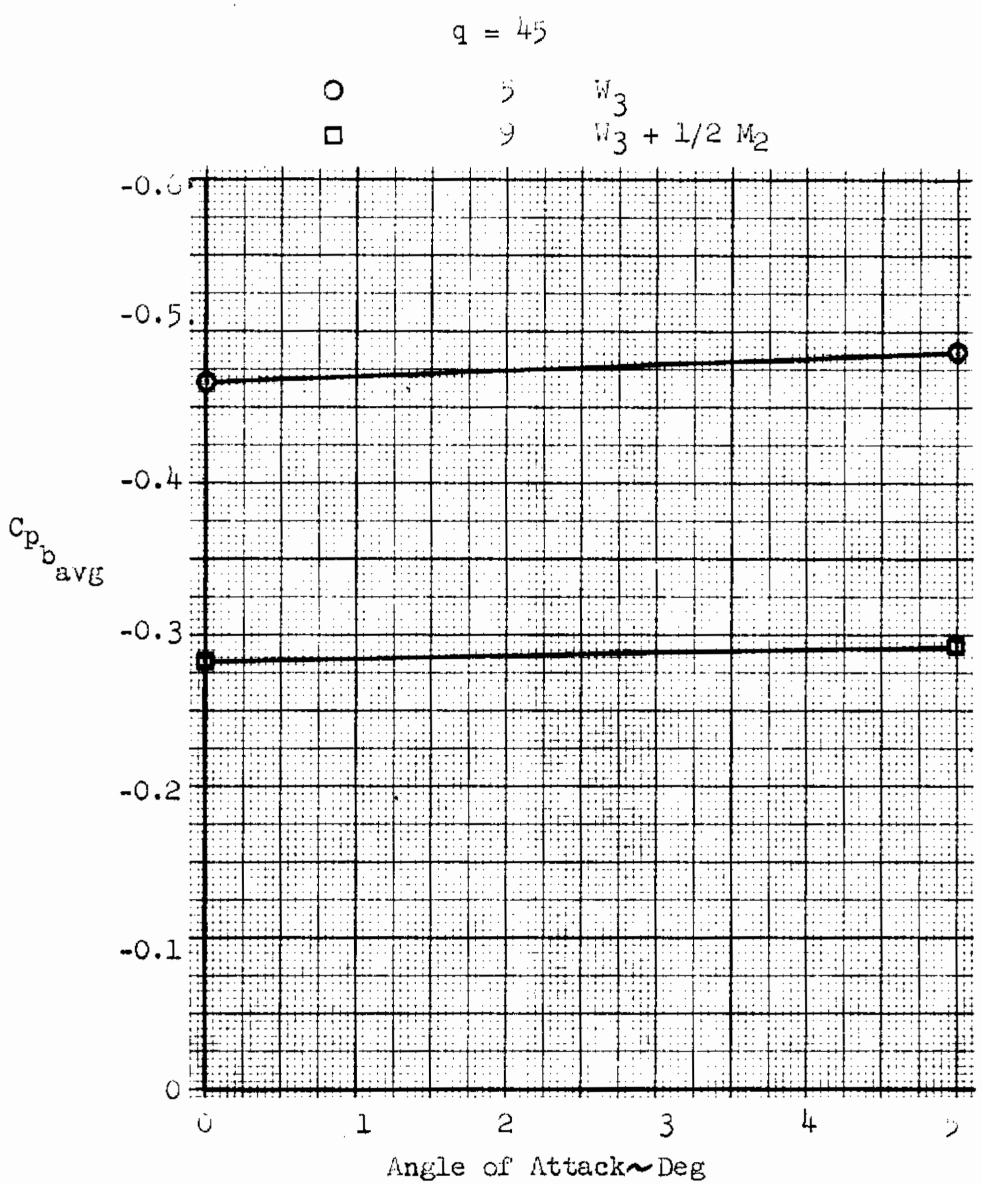


FIGURE 52 **Effect of Body on 3 Inch Wing on Average Base Pressure Coefficient**

| Sym. | Run | Config. | q |
|---|---|---|---|
| O | CT 17 | $W_4$ | 45 |
| △ | CT 18 | $W_4$ | 30 |
| O | CT 21 | $W_4 + U_5$ | 45 |
| △ | CT 22 | $W_4 + U_5$ | 45 |
| O | CT 19 | $W_4 + U_{10}$ | 45 |
| △ | CT 20 | $W_4 + U_{10}$ | 30 |

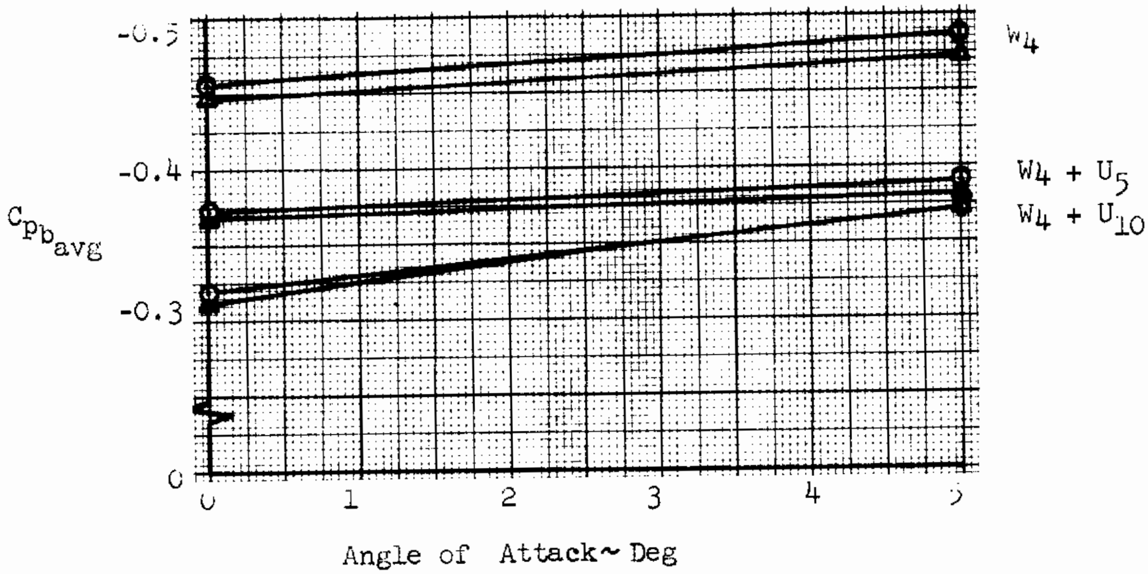


**FIGURE 53 Effect of Angle of Attack and Reynolds Number on Average Base Pressure Coefficient - 4 Inch Wing Configuration**

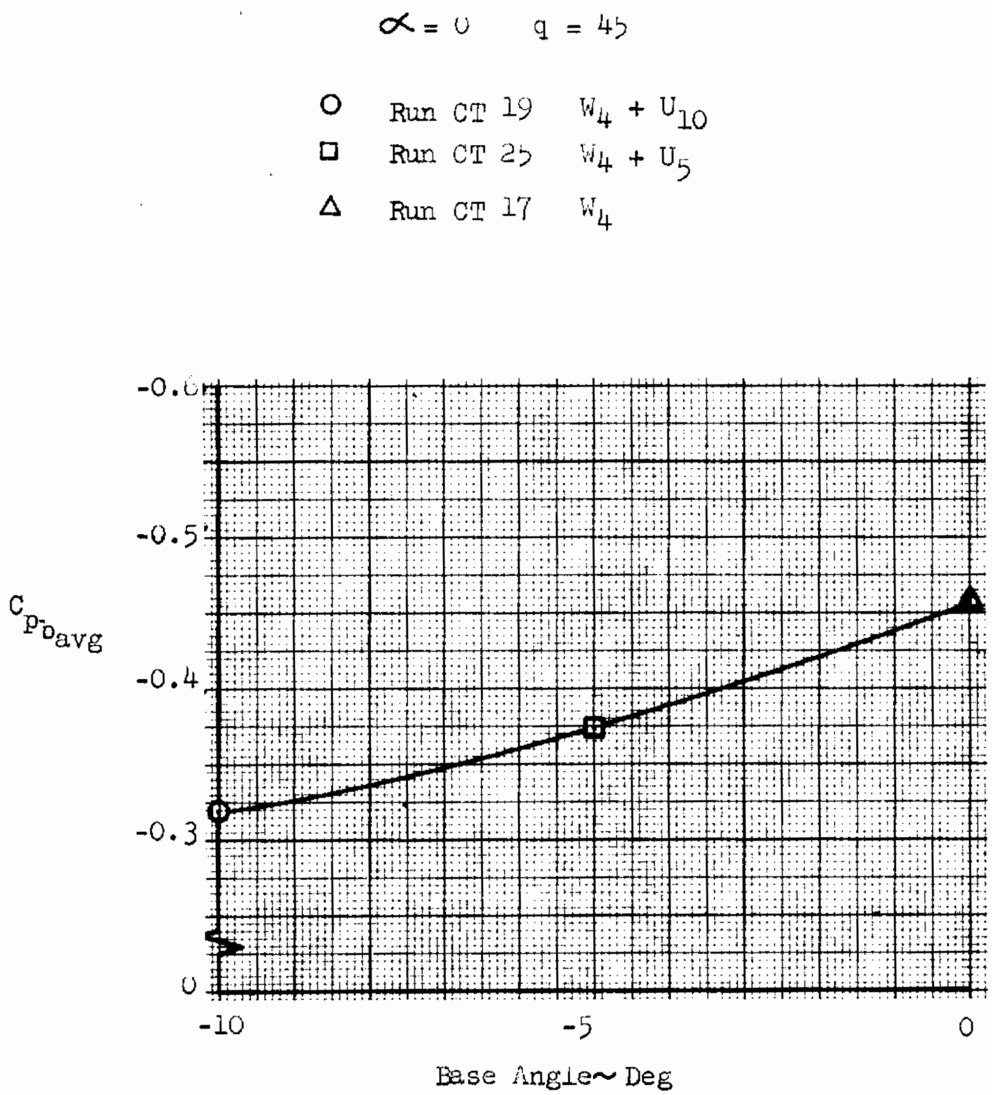


FIGURE 54 **Effect of Base Angle of 4-Inch Wings on Average Base Pressure Coefficient**

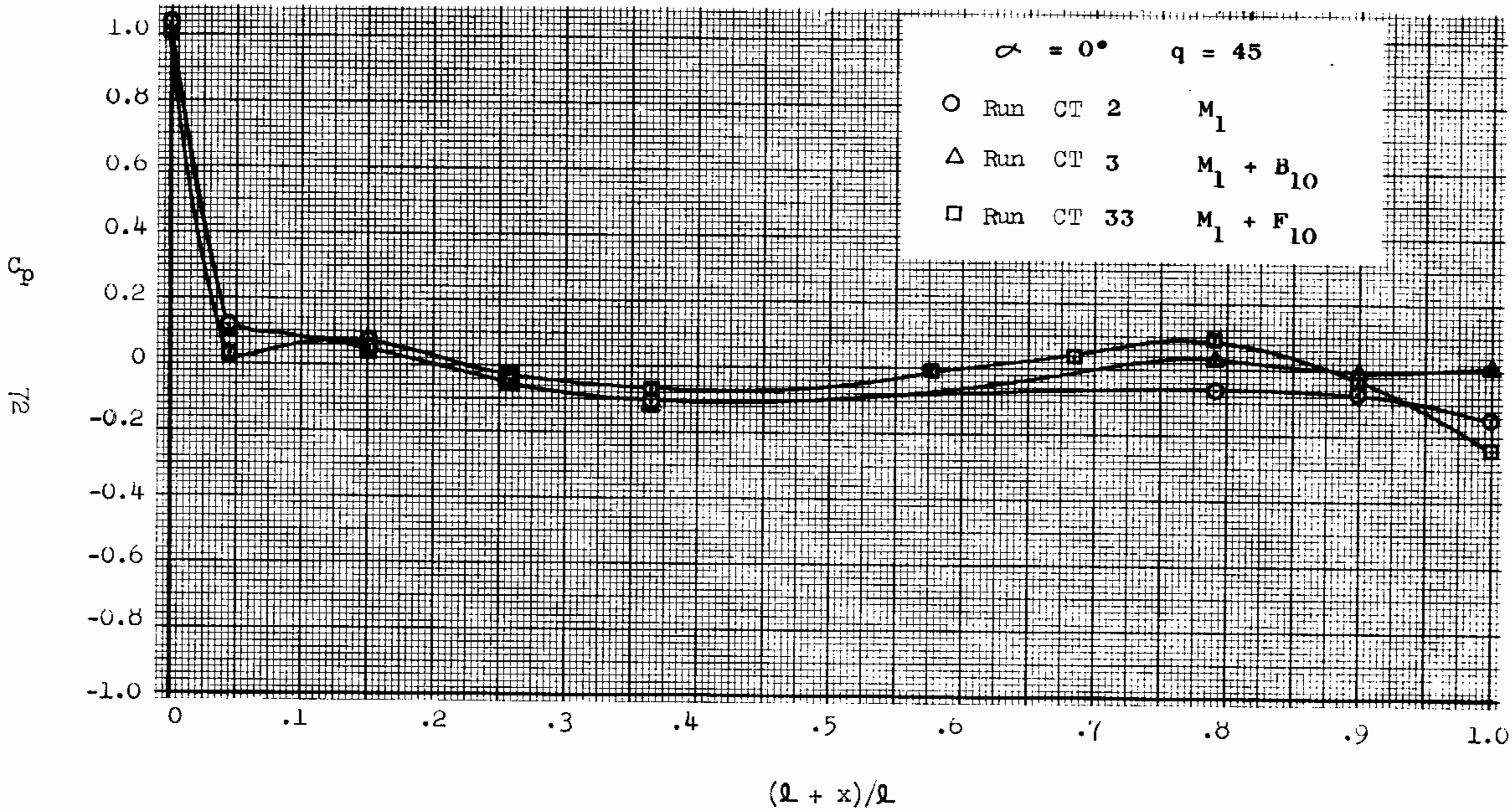


FIGURE 55 Comparison of 3-D Body Configurations on Surface Pressure Coefficients

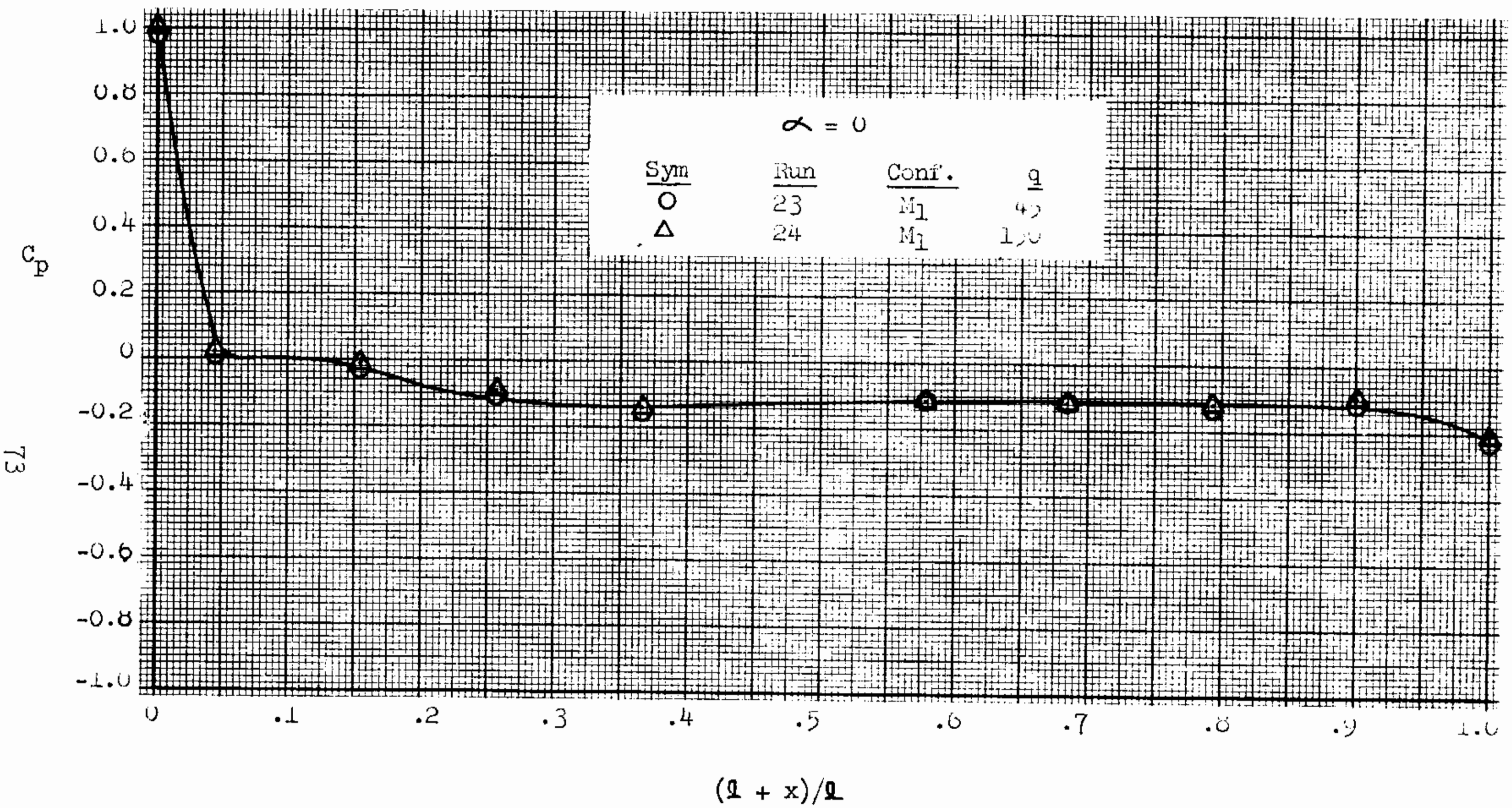


FIGURE 56 Effect of Reynolds Number on Surface Pressure Coefficients of 3-D Body

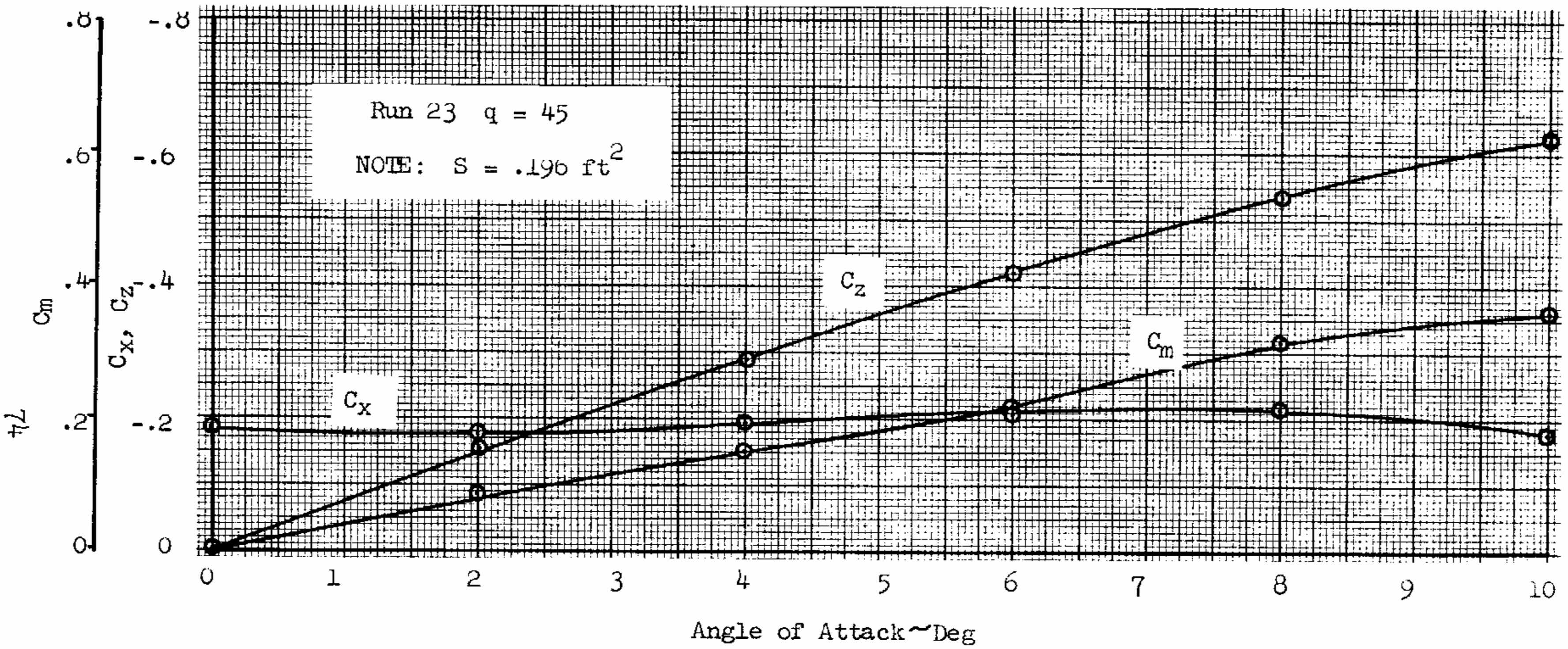


FIGURE 57 Force and Moment Data - 3-D Body

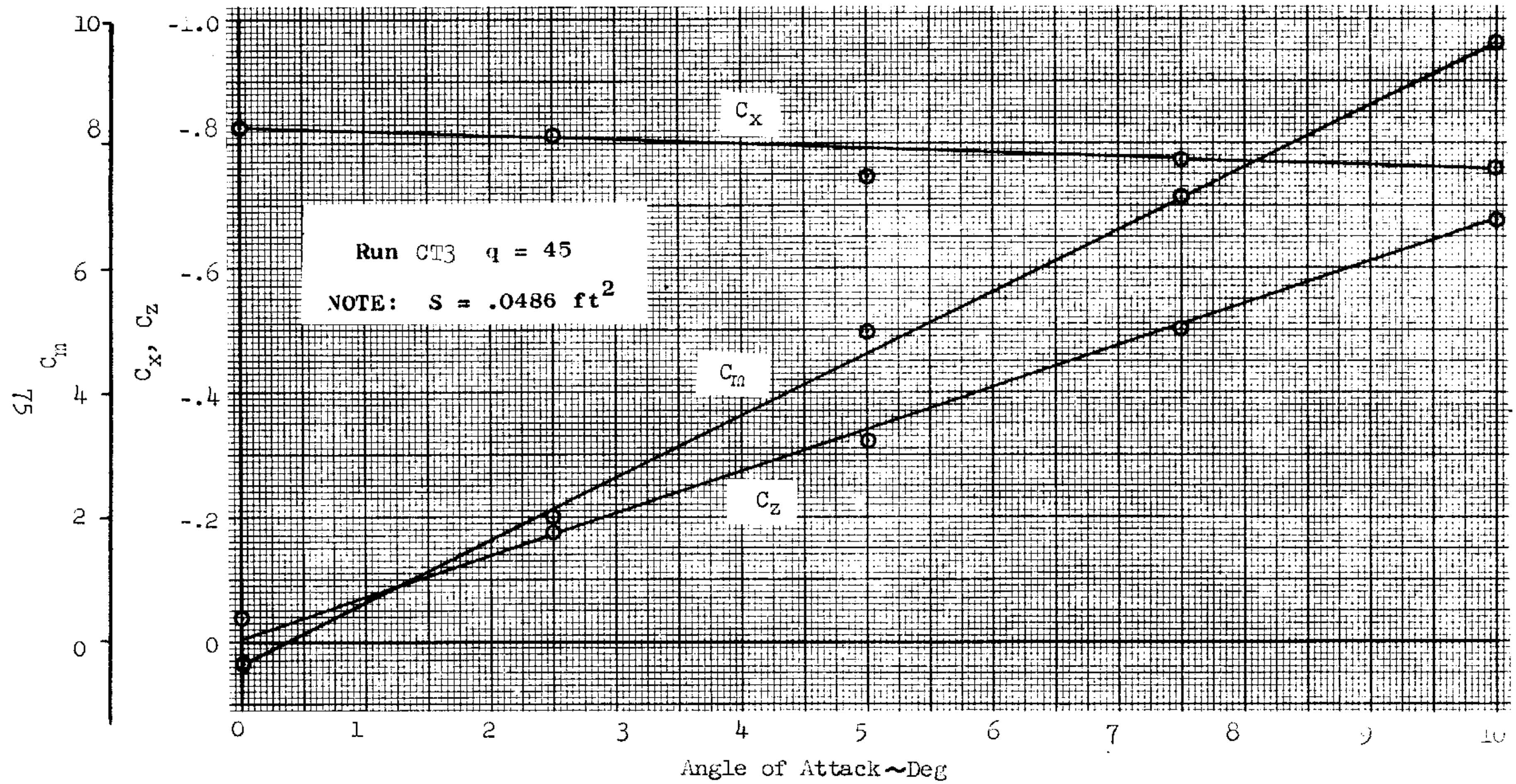


**FIGURE 58** **Force and Moment Data - 3-D Body With Boattail**

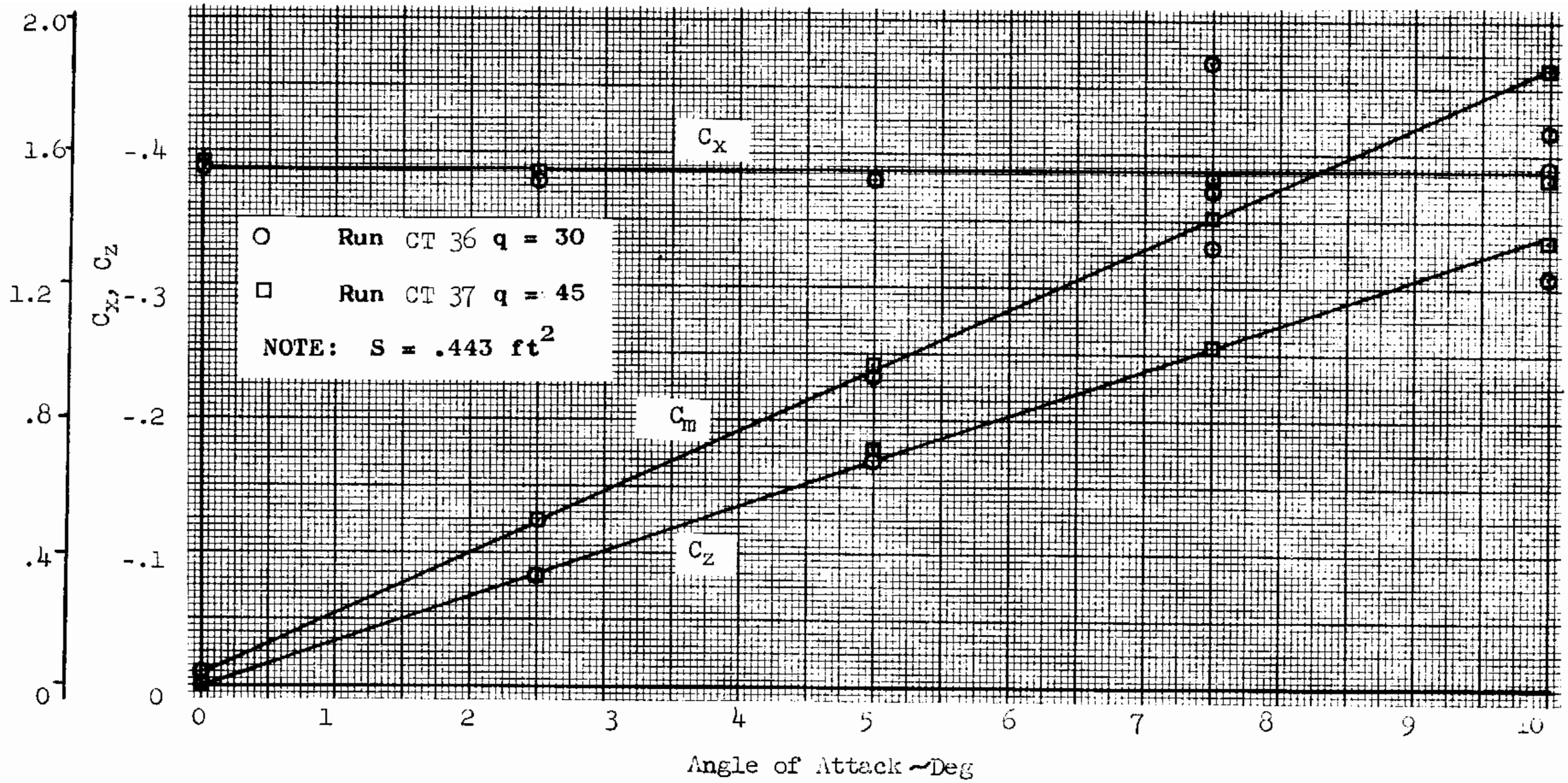


FIGURE 59 **Effect of Reynolds Number on Force and Moment Data - 3-D Body with Flare**

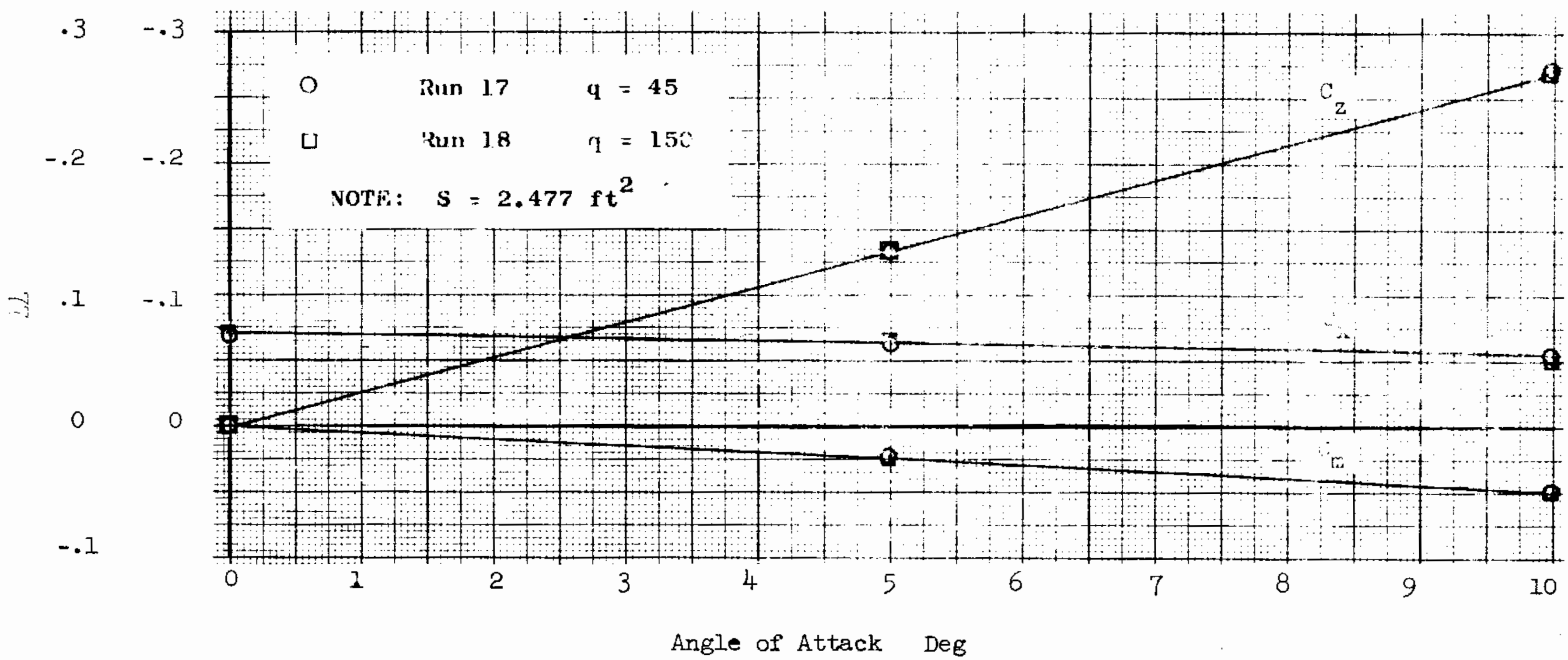


FIGURE 60 Effect of Reynolds Number on Force and Moment Data - 3 Inch Wing

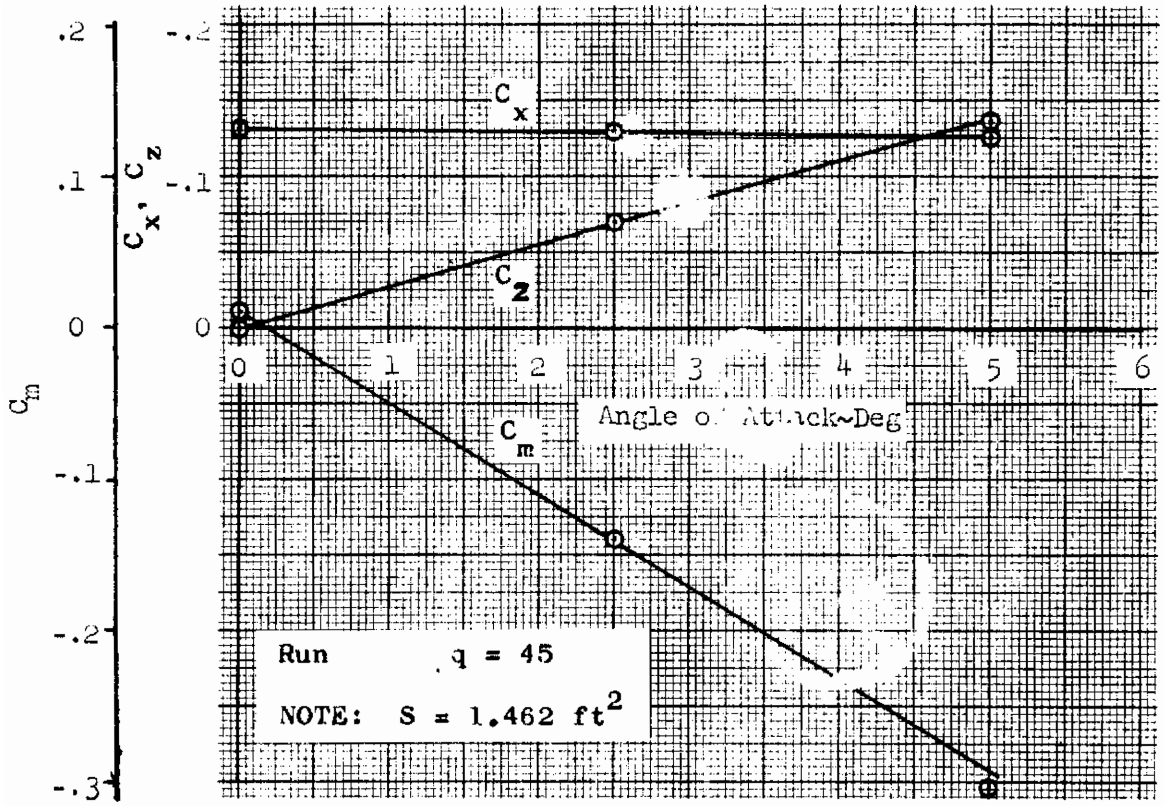


FIGURE 61 Force and Moment Data - 4 Inch Wing

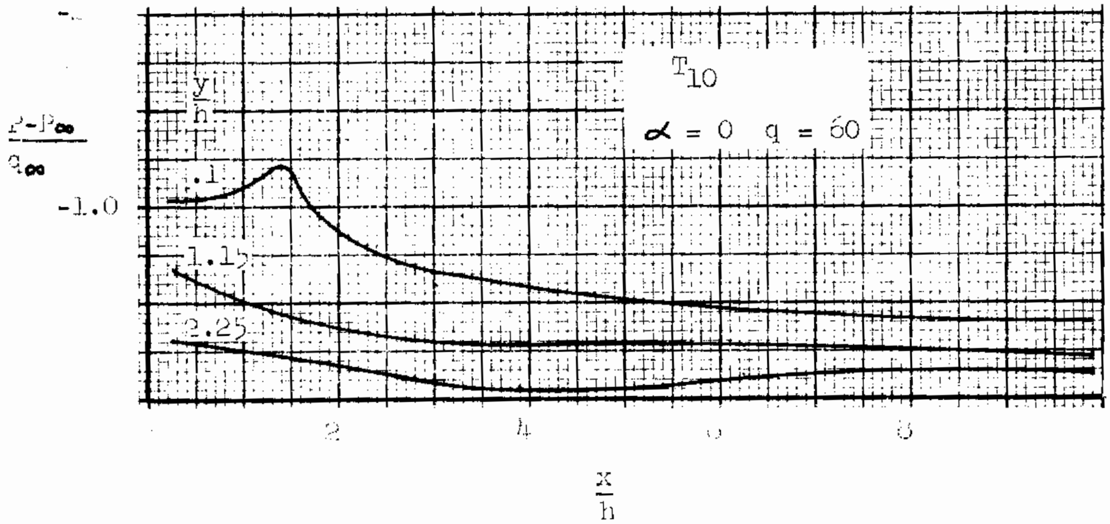


a. "Open" Wake

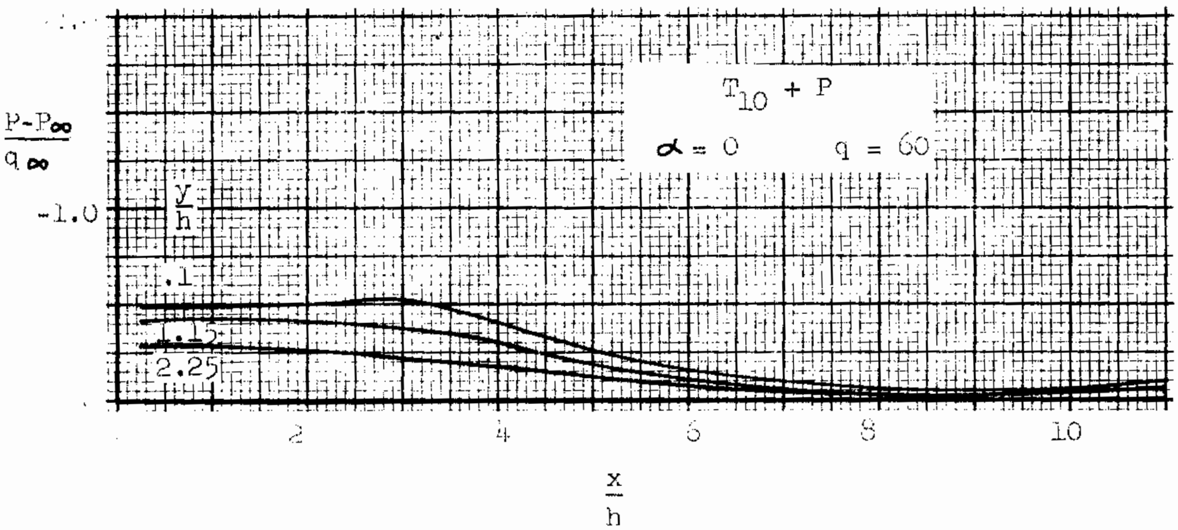


b. "Closed" Wake

FIGURE 62 Static Pressure Distribution in the Wakes of Configurations $T_{10}$ and $T_{10}$ + P.

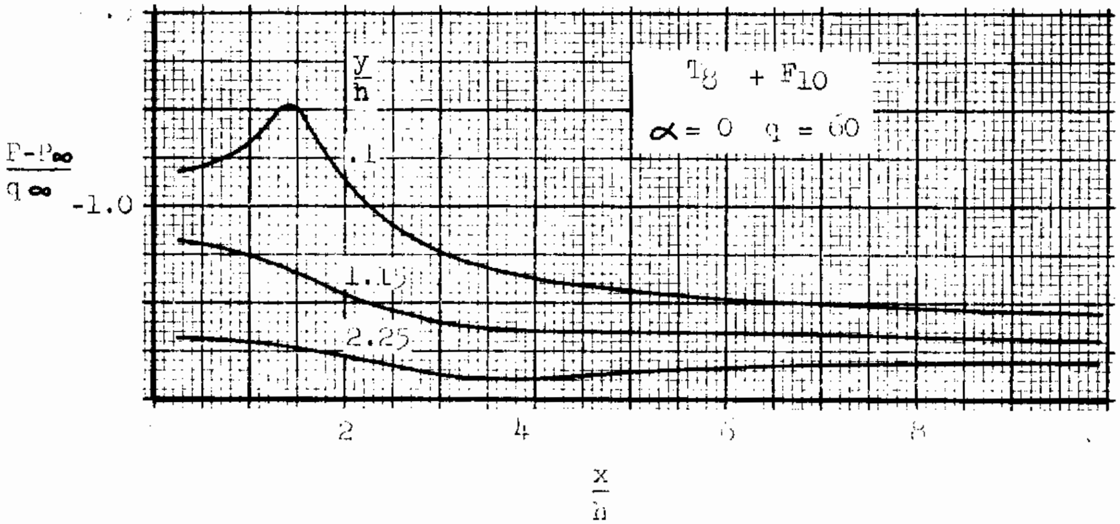


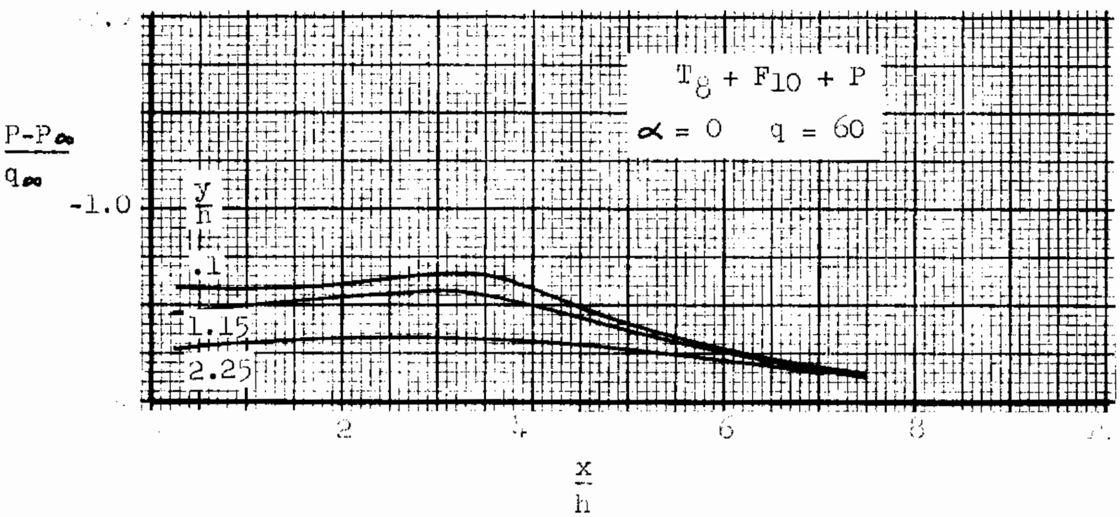


FIGURE 63 Static Pressure Distribution in the Wakes of Configurations $T_8 + F_{10}$ and $T_8 + F_{10} + P$.

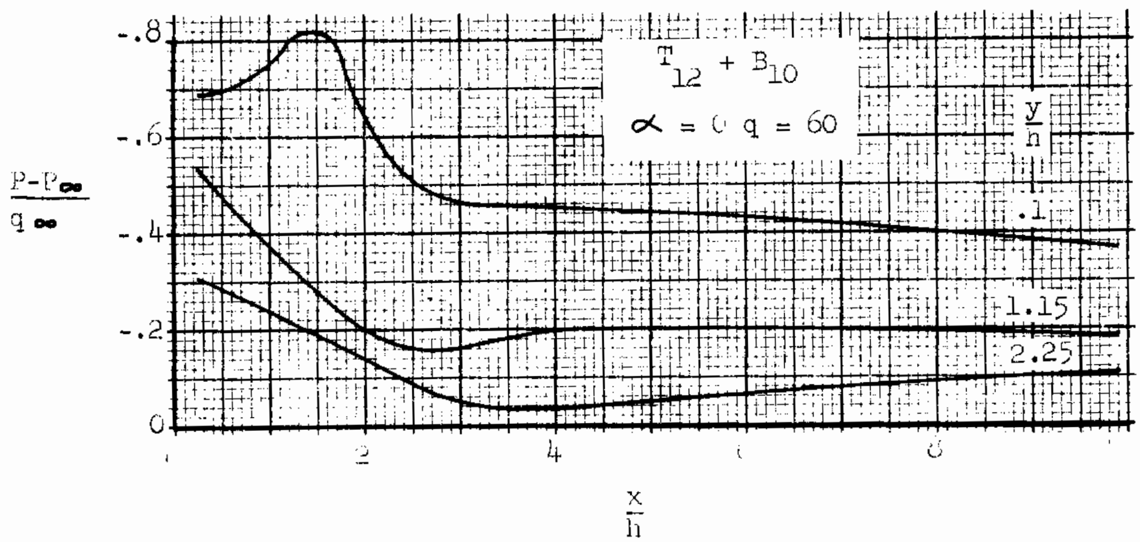


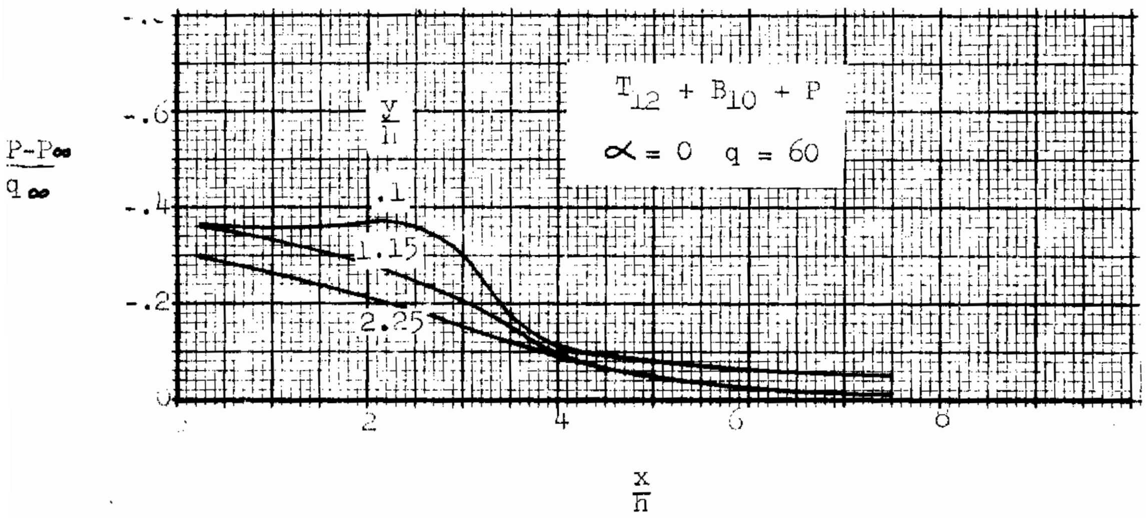


FIGURE 44 Static Pressure Distribution in the Wakes of Configurations $T_{12} + B_{10}$ and $T_{12} + B_{10} + P$.

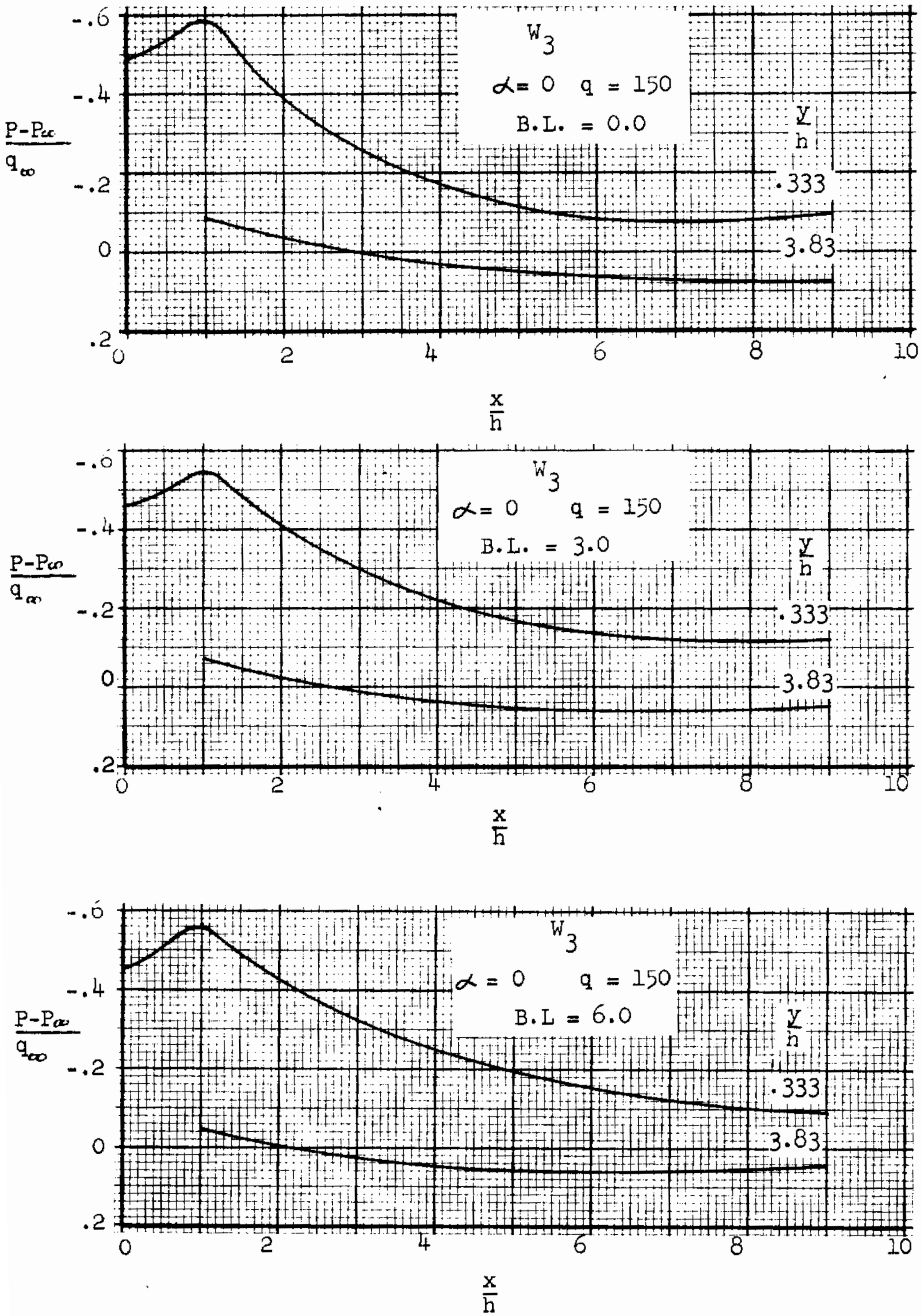


FIGURE 65 Spanwise Variation of Static Pressures in the Wake of Configuration $W_3$

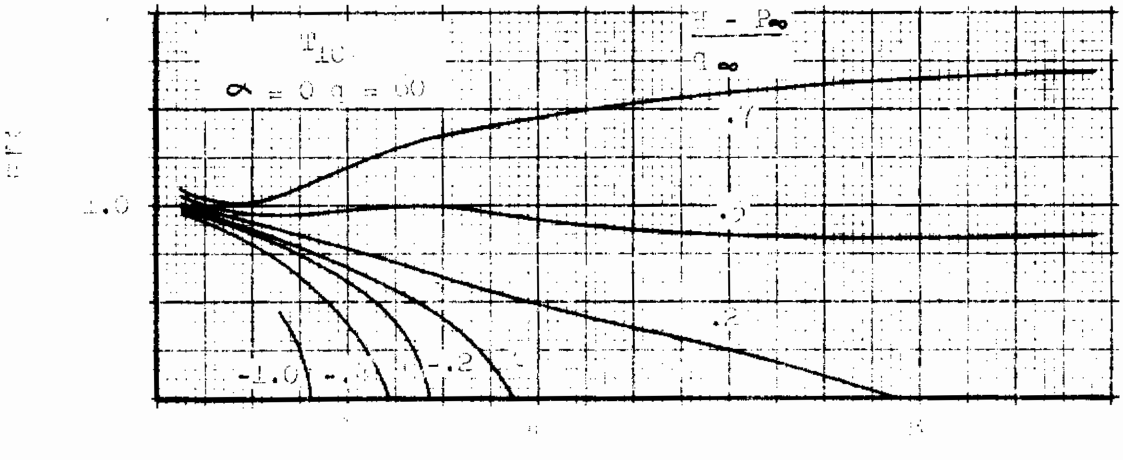


a. "Open" Wake

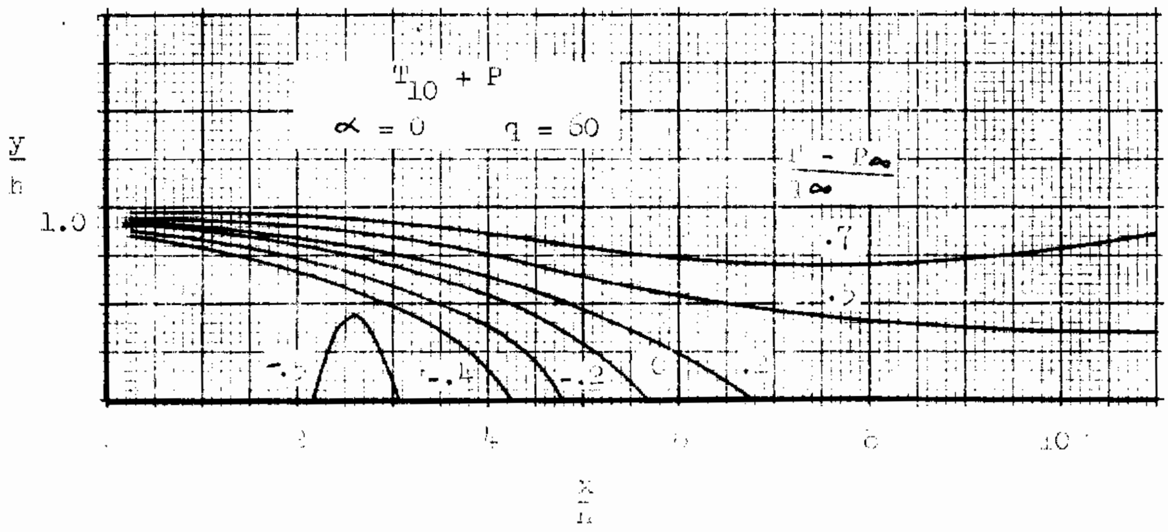


b. "Closed" Wake

FIGURE 6? Total Pressure Contours in the Wakes of Configurations $T_{10}$ and $T_{10}$ + P.

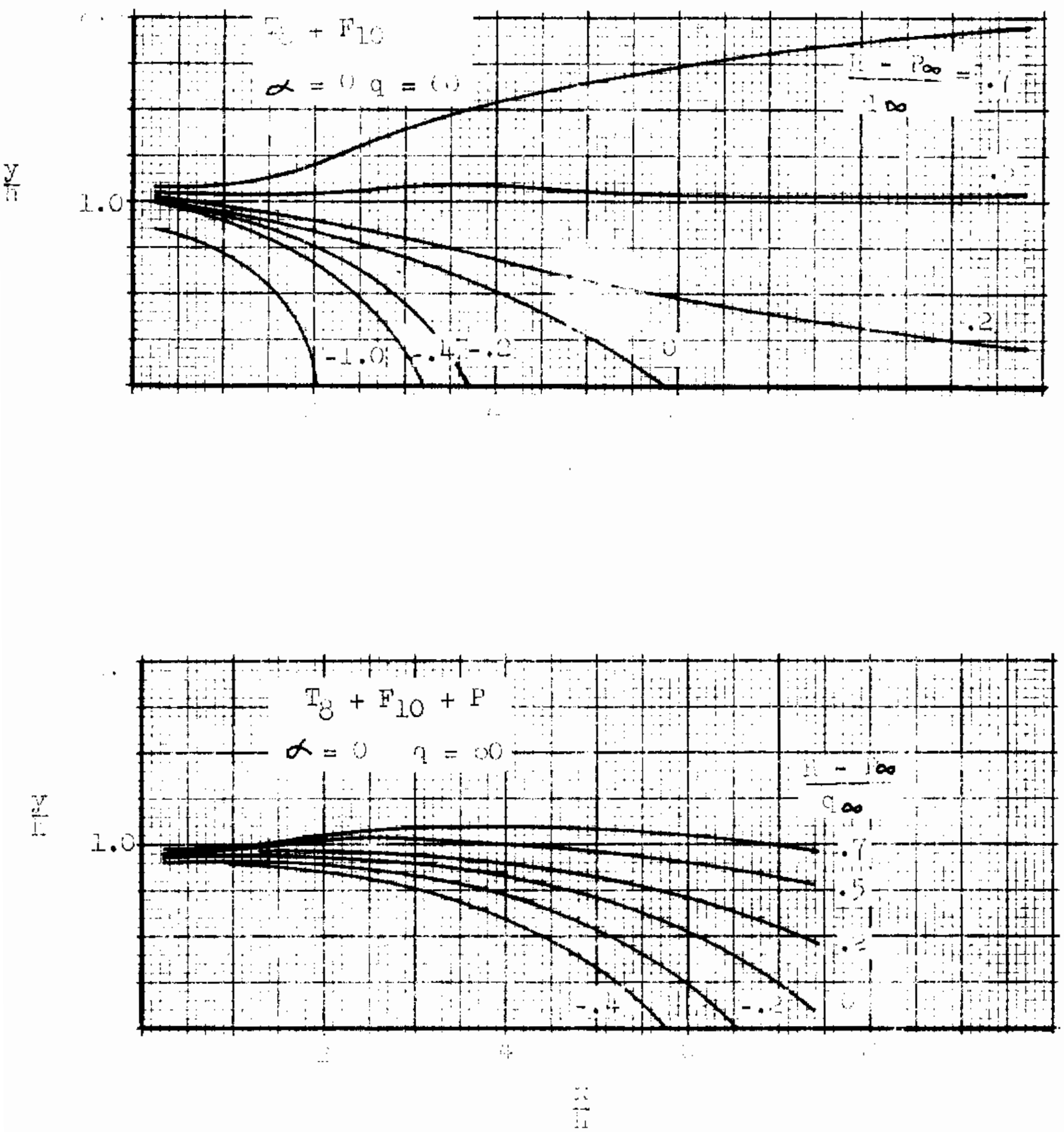


FIGURE 67 Total Pressure Contours in the Wakes of Configurations $T_8 + F_{10}$ and $T_8 + F_{10} + P$.

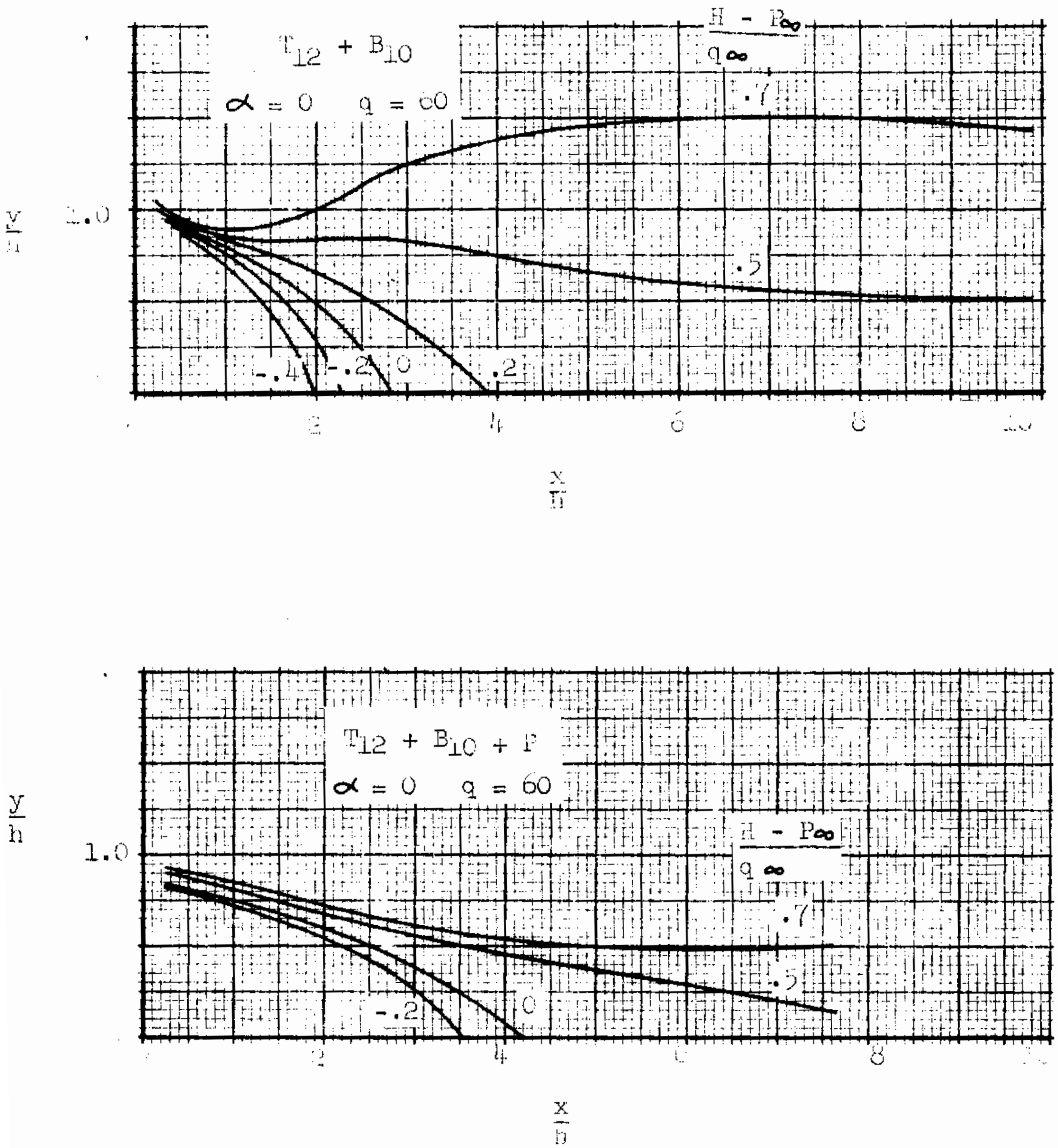


FIGURE 68 Total Pressure Contours in the Wakes of Configurations $T_{12} + B_{10}$ and $T_{12} + B_{10} + P$.

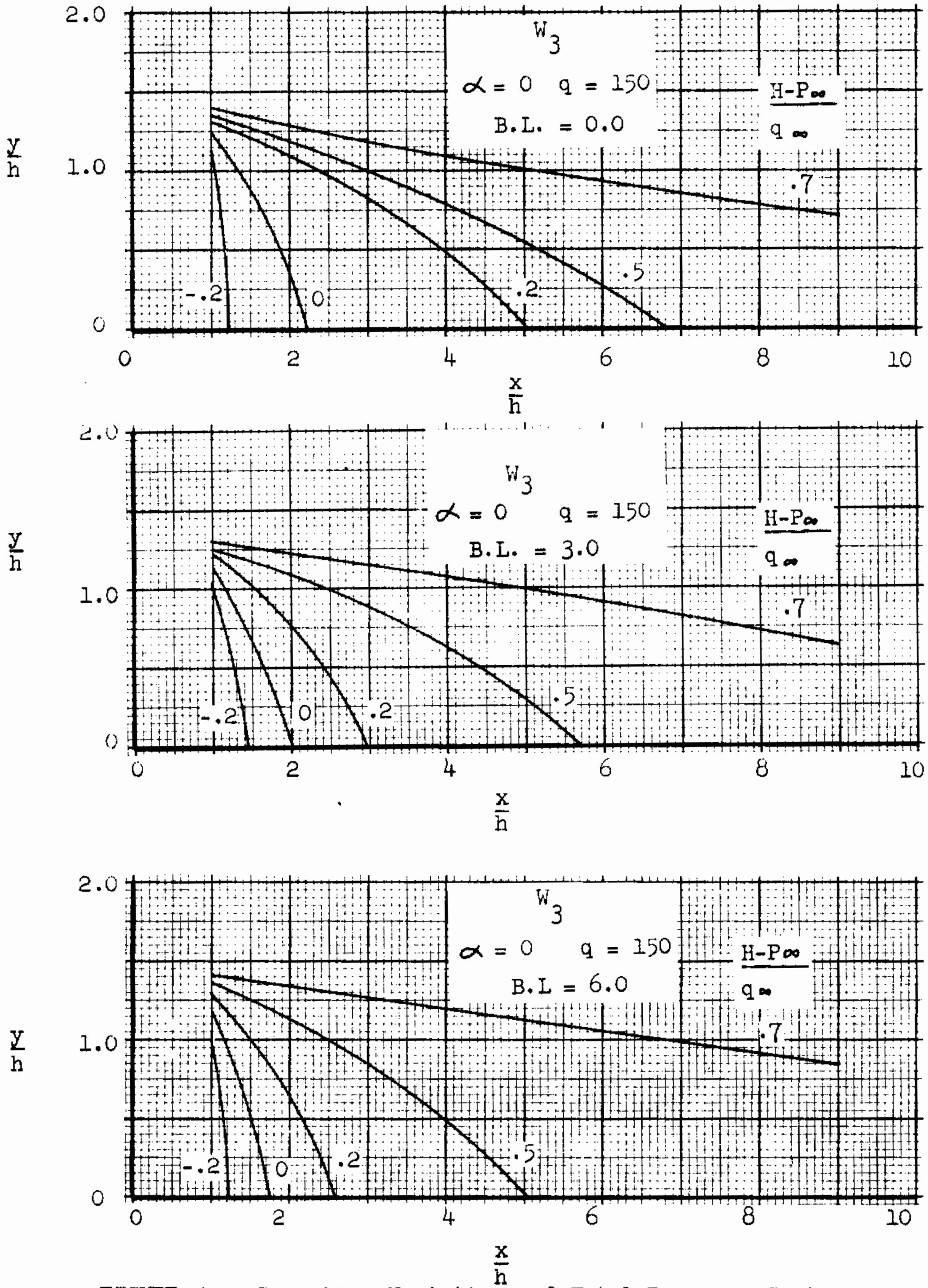


FIGURE 69 Spanwise Variations of Total Pressure Contours in the Wake of Configuration $W_3$

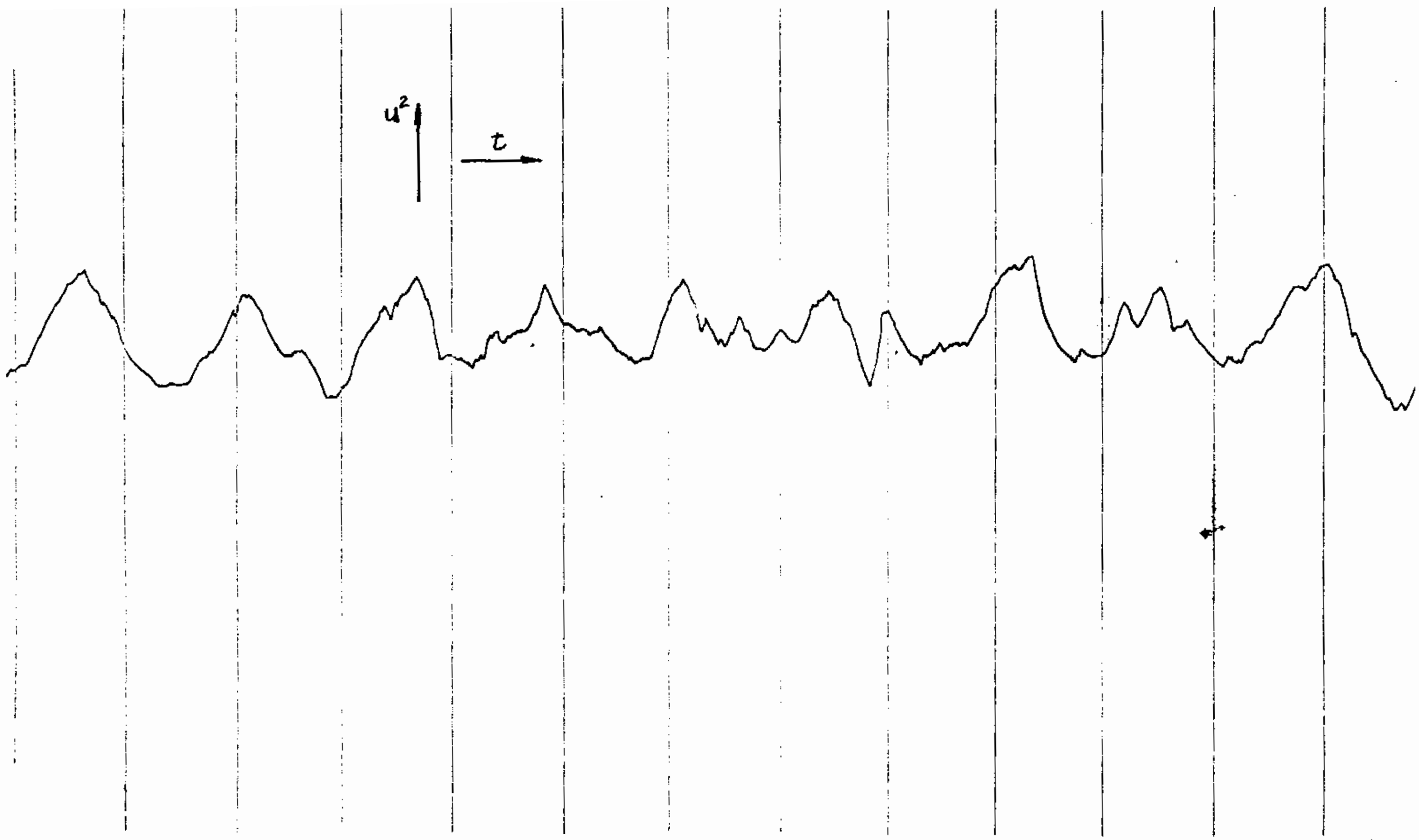


FIGURE 70

Velocity Fluctuations in the Wake of Configuration $T_{10}$

7-3/8" aft of base Time Lines = .01 sec

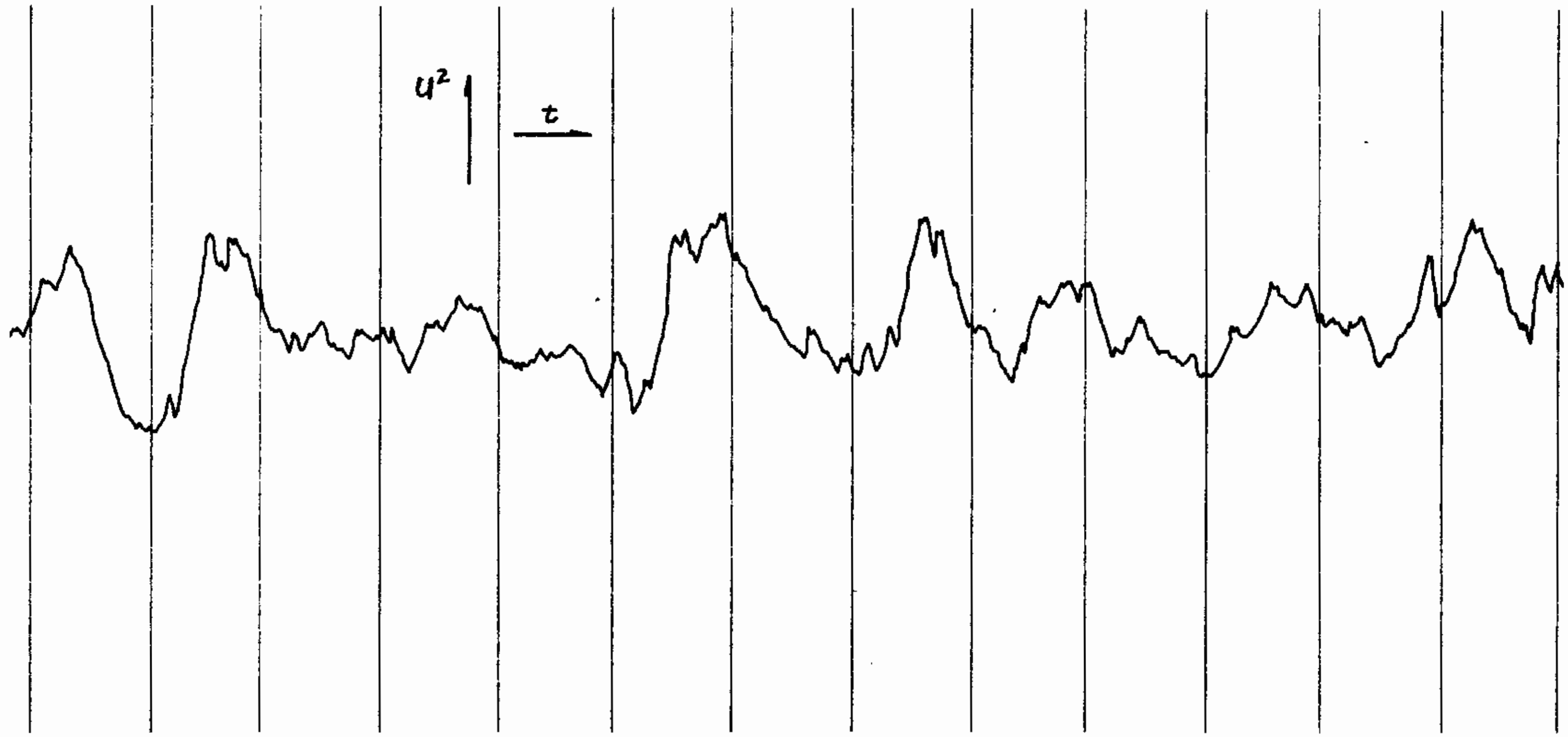


FIGURE 71

Velocity Fluctuations in the Wake of Configuration $T_{10} + P$

7-3/8" Aft of Base                Time Lines = .01 sec

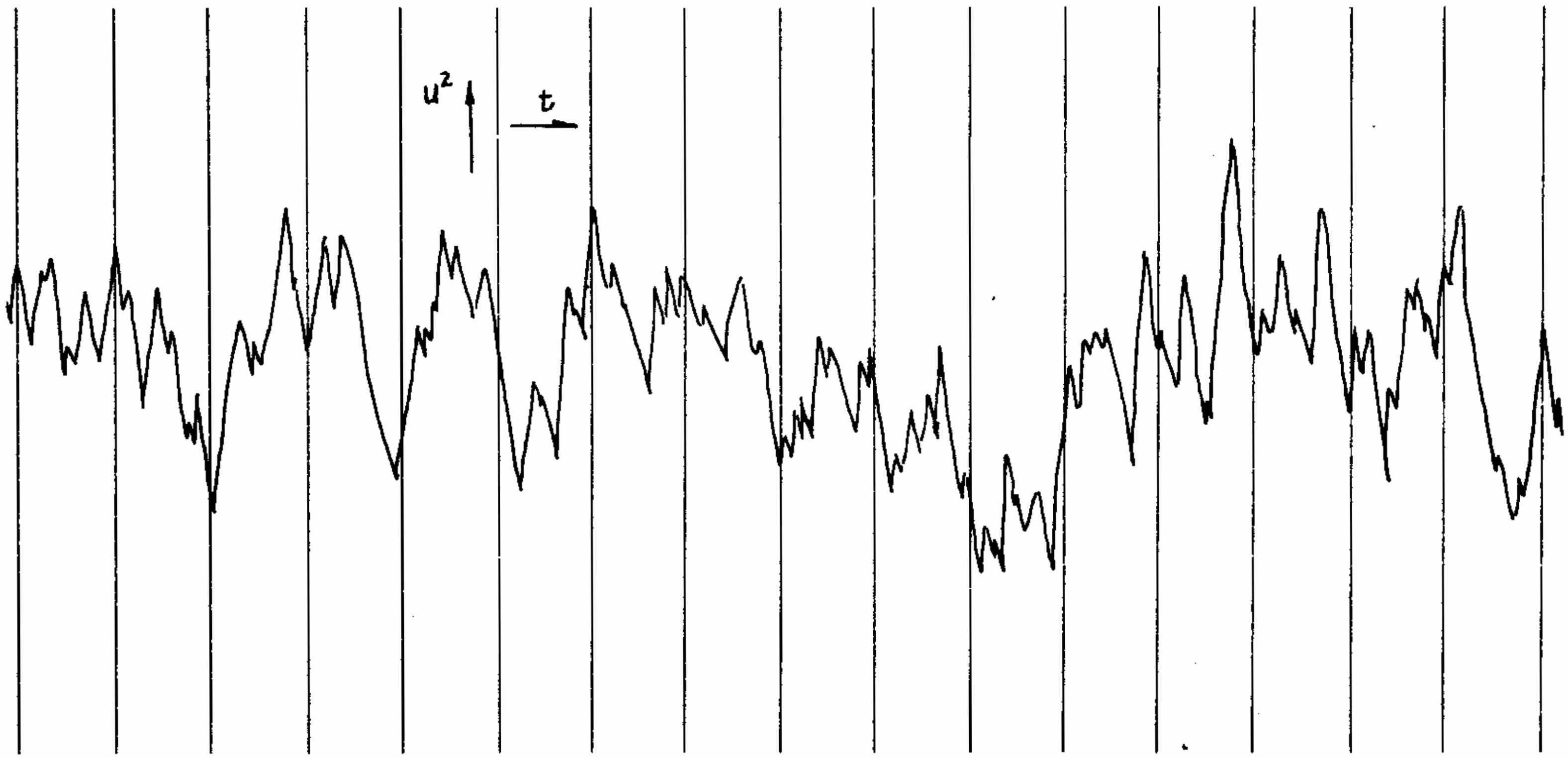


FIGURE 72

Velocity Fluctuations in the Wake of Configuration $M_1$

6" Aft of Base        Time Lines = .01 sec

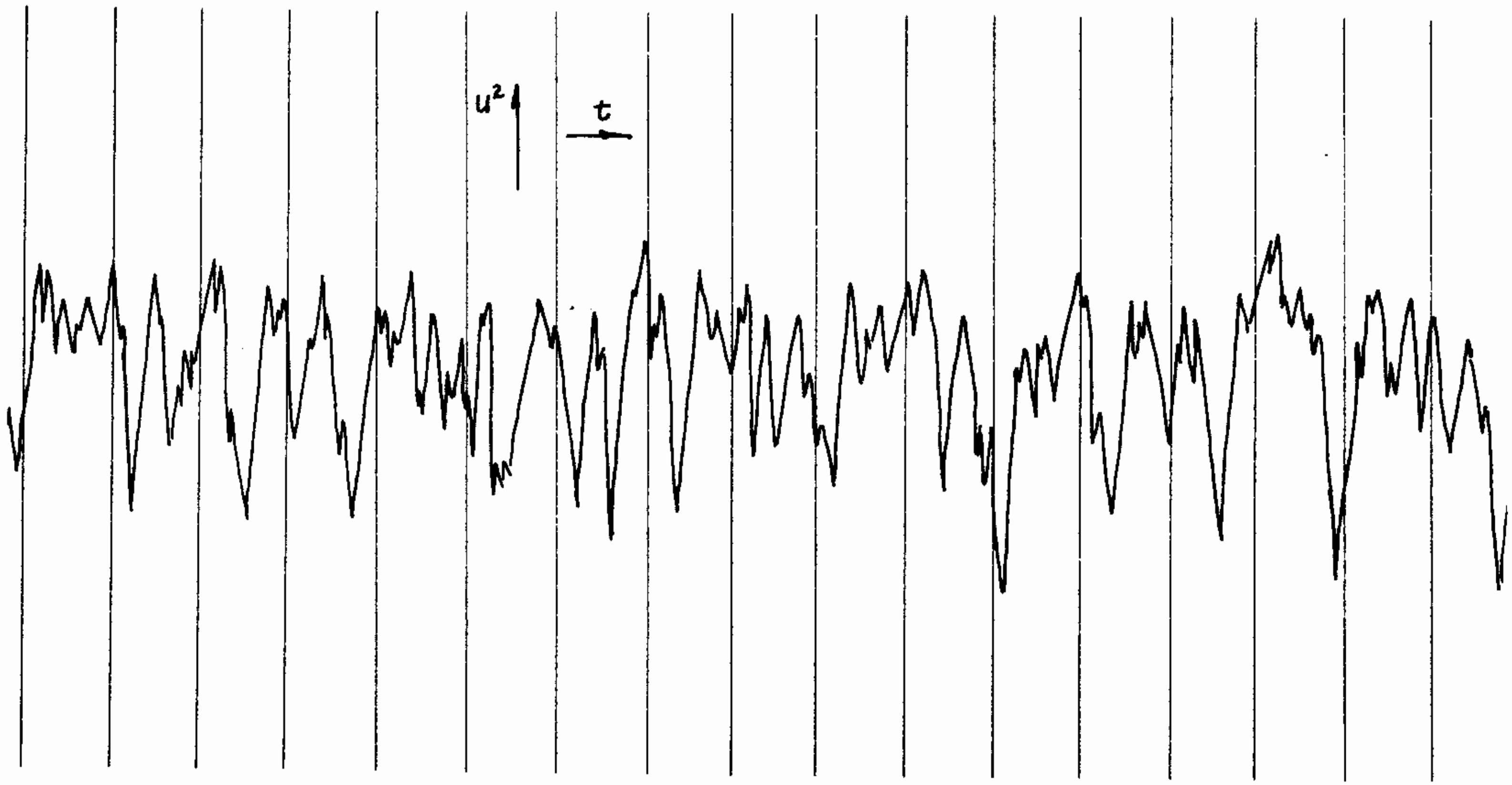


FIGURE 73

Velocity Fluctuations in the Wake of Configuration $W_4$

8" Aft of Base Time Lines = .01 sec

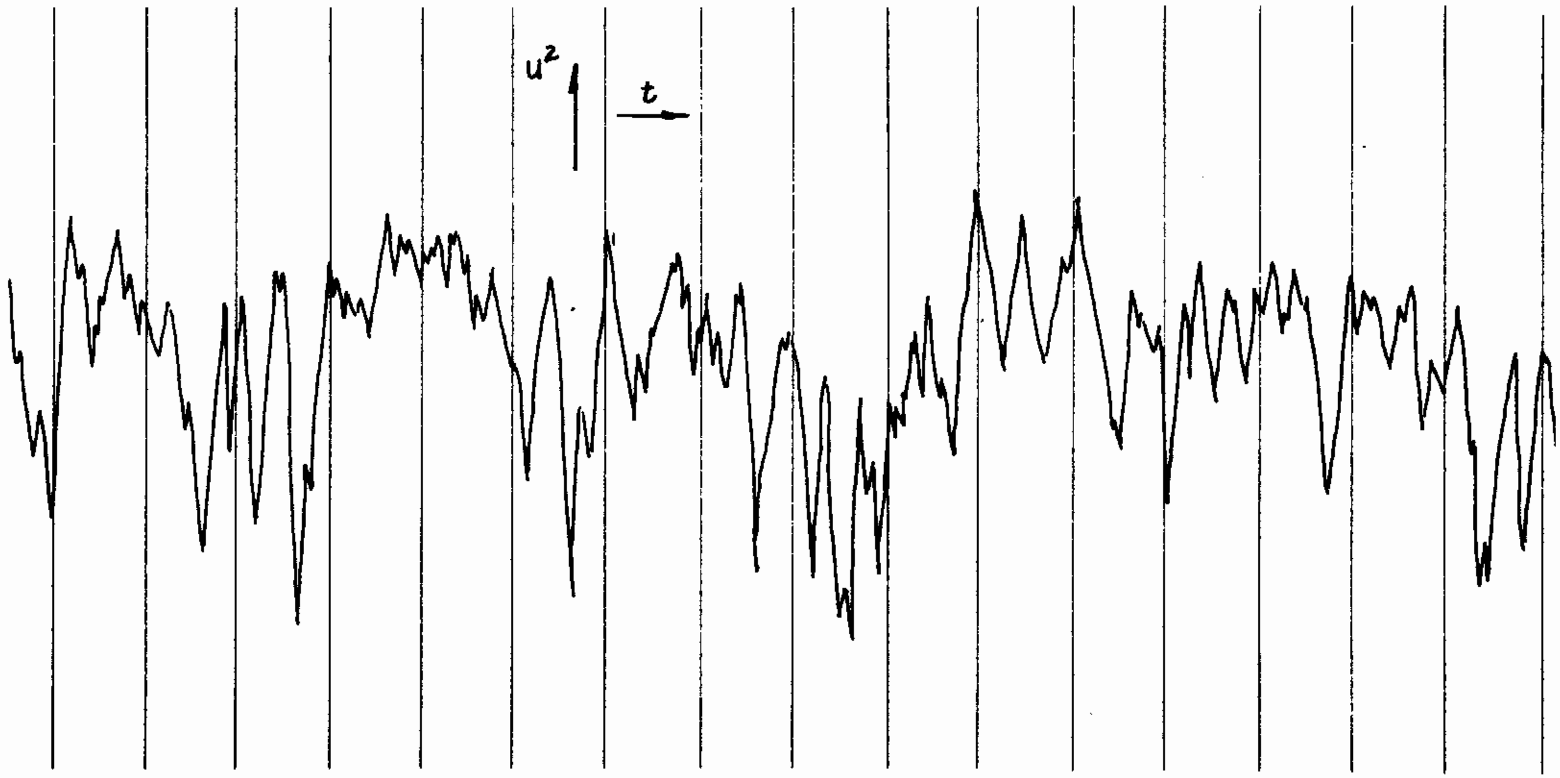


FIGURE 74

Velocity Fluctuations in the Wake of Configuration $W_3$

5" Aft of Base Time Lines = .01 sec

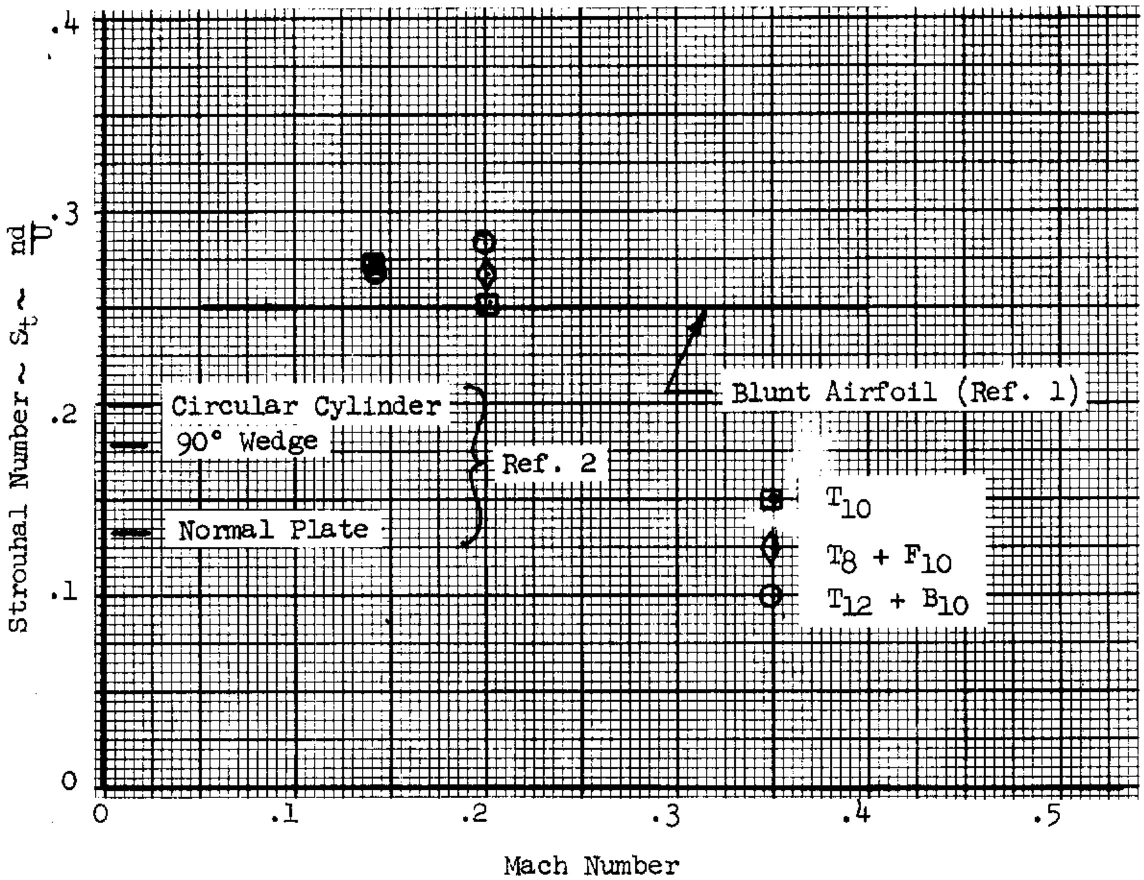


FIGURE 75

Correlation of Non-Dimensional Wake Periodicity of Two-Dimensional Isolated Blunt Bases in Subsonic Flow

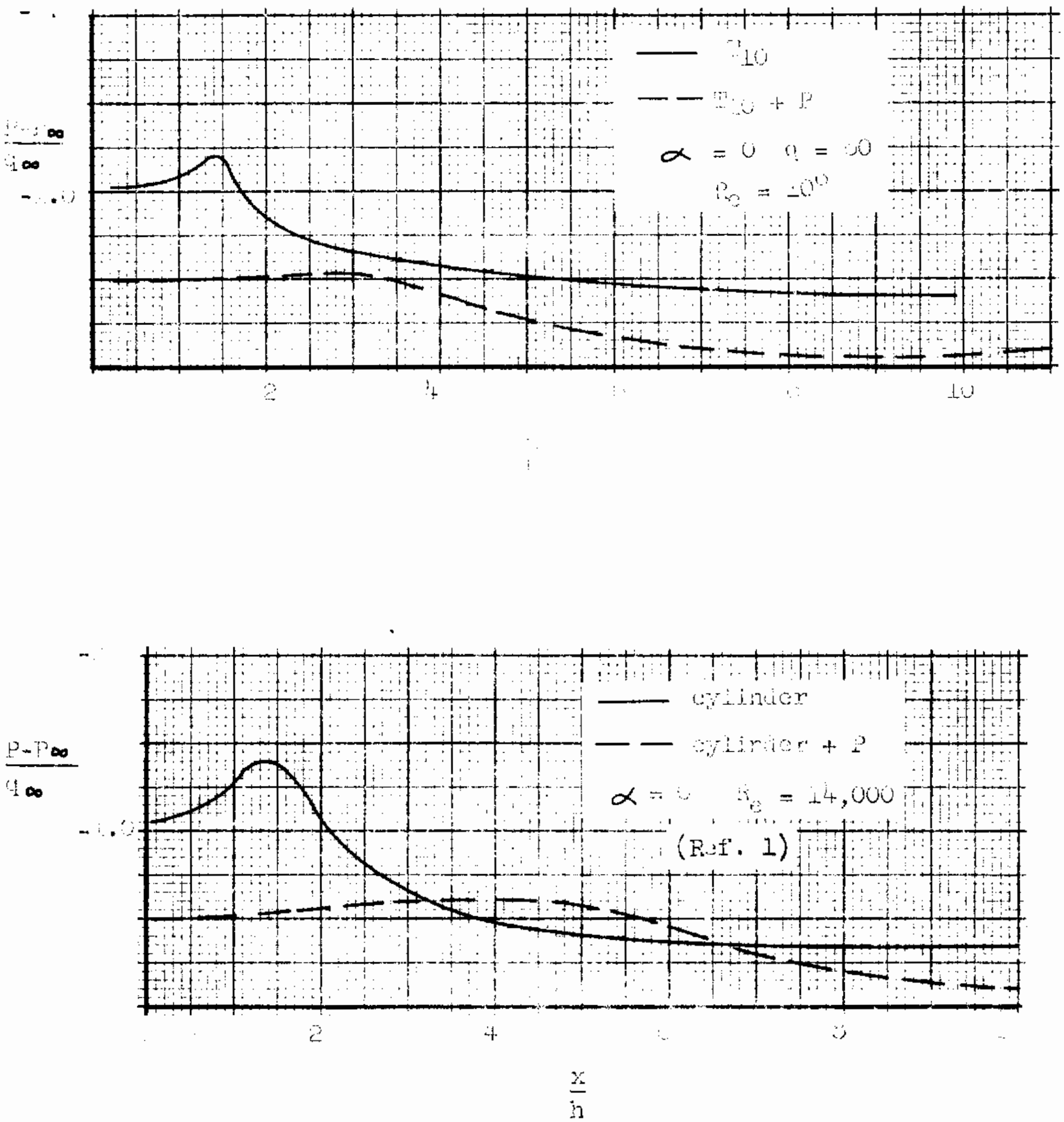


FIGURE 76 Effect of Horizontal Splitter Plate on Centerline Static Pressure Behind Two-Dimensional Blunt Base Configuratons in Subsonic Flow.

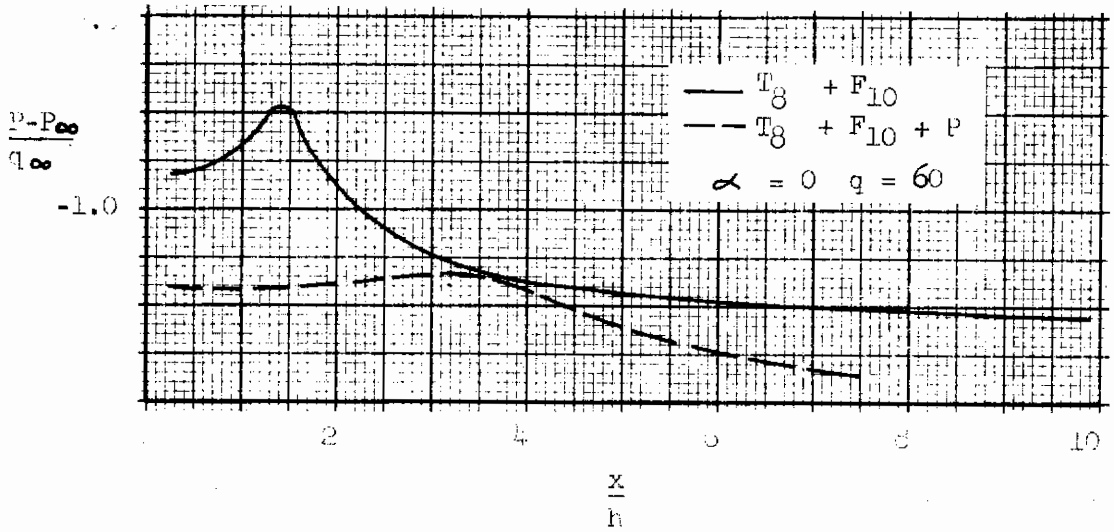


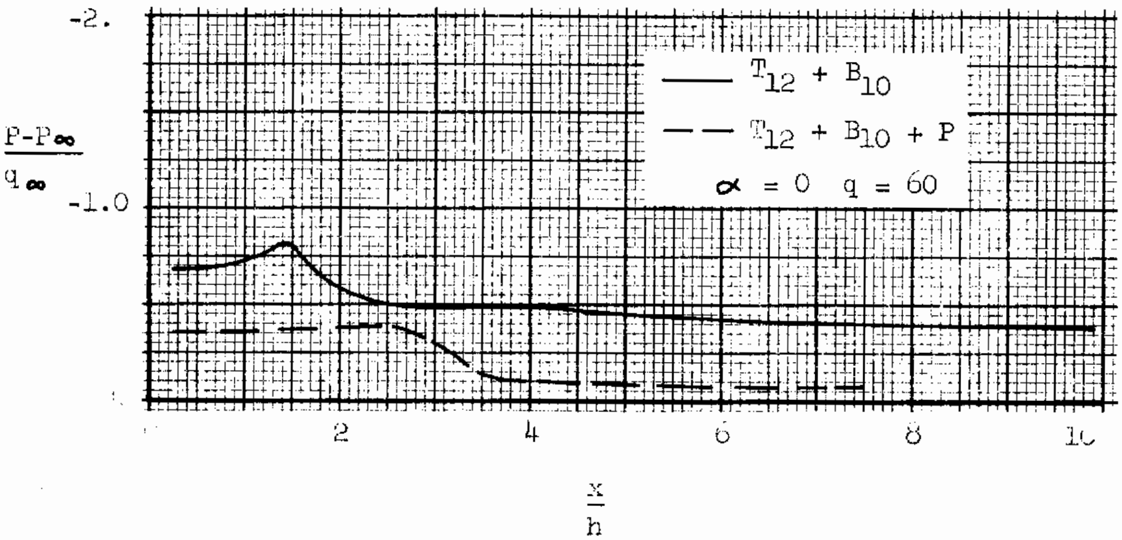


FIGURE 77 Effect of Horizontal Splitter Plate on Centerline Static Pressure Behind Two-Dimensional Blunt base configurations in Subsonic Flow.

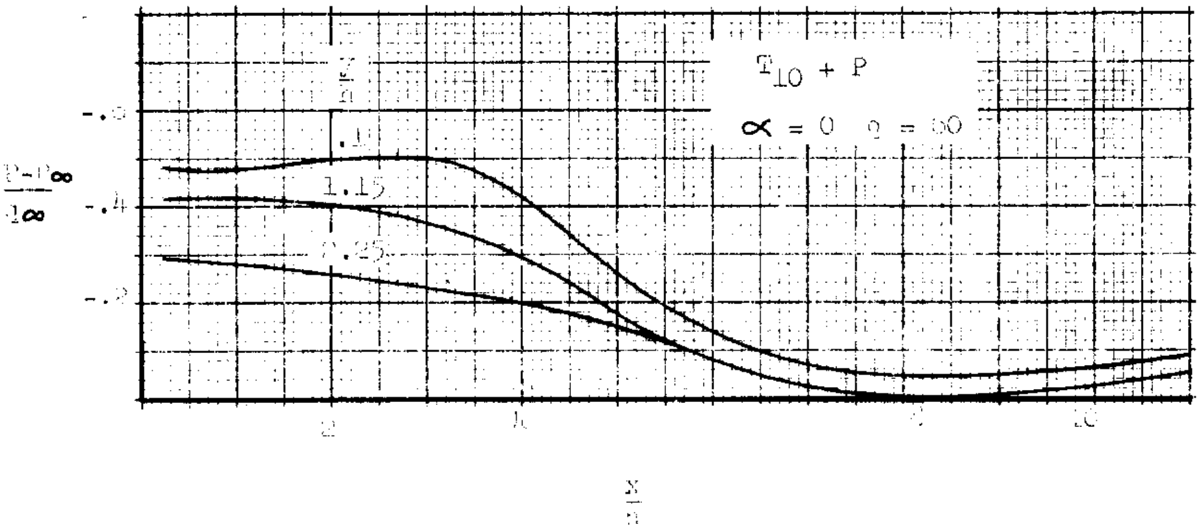


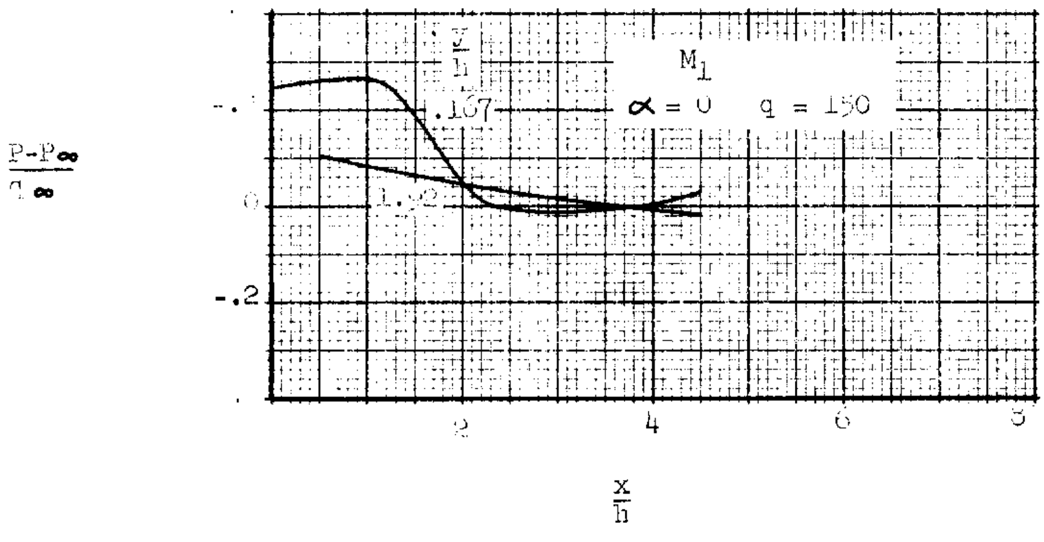


FIGURE 78 Comparison of Static Pressure Distributions in the Wakes of Configurations $M_1$ and $T_{10} + P$.

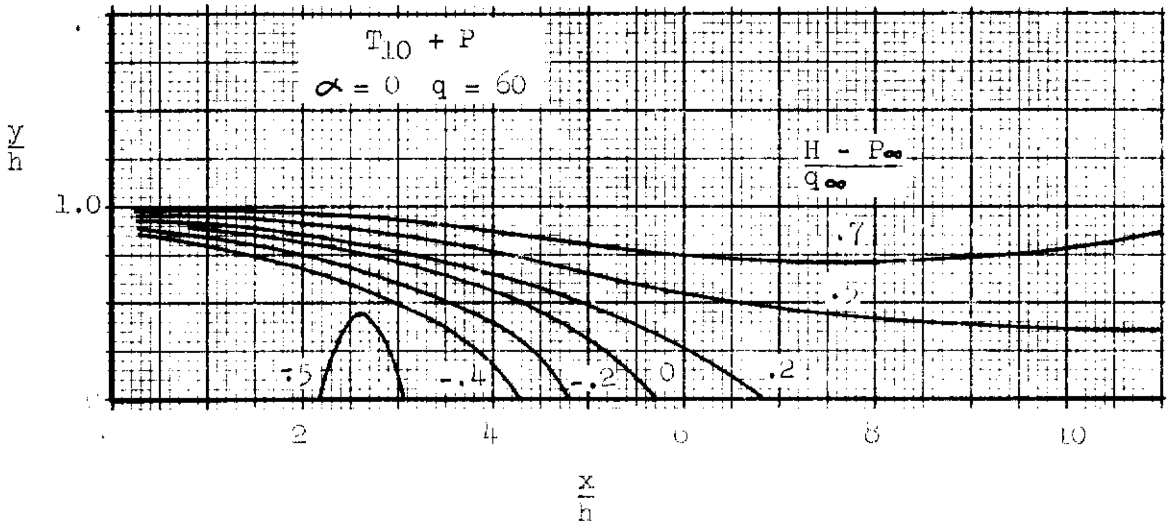


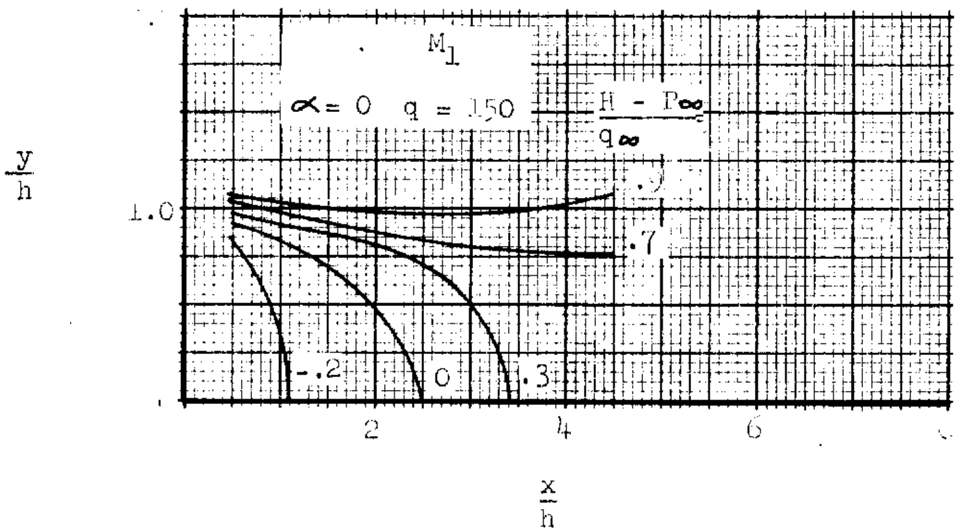


FIGURE 79 Comparison of Total Pressure Contours in the Wakes of Configurations $M_1$ and $T_{10}$ + P

## 10/ TABLES

The following tables include data reduction constants, base pressures from the smoke tunnel test and average base pressures for the two and three dimensional models tested in the Convair and Cal Tech Tunnels.

TABLE 1

RUN INDEX

San Diego State College Smoke Wind Tunnel

| Run No. | Configuration | Angle of Attack Range (Degrees) | Velocity (Ft/Sec) | Base Pressure Data | Photos |
|---|---|---|---|---|---|
| 1 | $T_1$ | 0,5,10,15 | 29.2 | X | |
| 2 | $T_1$ | 0,5,15 | 9.5 | | X |
| 3 | $T_1 + B_{5^\circ}$ | 0,5,10,15 | 29.2 | X | |
| 4 | $T_1 + B_{5^\circ}$ | | 9.5 | | X |
| 5 | $T_1 + B_{10^\circ}$ | | 29.2 | X | |
| 6 | $T_1 + B_{10^\circ}$ | | 9.5 | | X |
| 7 | $T_1 + F_{5^\circ}$ | | 29.2 | X | |
| 8 | $T_1 + F_{5^\circ}$ | | 9.5 | | X |
| 9 | $T_1 + F_{10^\circ}$ | | 29.2 | X | |
| 10 | $T_1 + F_{10^\circ}$ | | 9.5 | | X |
| 11 | $T_2$ | 0,5,10,15 | 29.2 | X | |
| 12 | $T_2$ | | 10.5 | | X |
| 13 | $T_2 + B_{5^\circ}$ | | 29.2 | | |
| 14 | $T_2 + B_{5^\circ}$ | | 10.5 | | X |
| 15 | $T_2 + B_{10^\circ}$ | | 29.2 | X | |
| 16 | $T_2 + B_{10^\circ}$ | | 10.5 | | X |
| 17 | $T_2 + F_{5^\circ}$ | | 29.2 | X | |
| 18 | $T_2 + F_{5^\circ}$ | | 10.5 | | X |
| 19 | $T_2 + F_{10^\circ}$ | | 29.2 | X | |
| 20 | $T_2 + F_{10^\circ}$ | | 10.5 | | X |
| 21 | $T_{2R}$ | | 29.2 | X | |
| 22 | $T_{2R}$ | | 10.5 | | X |
| 23 | $T_3$ | | 29.2 | X | |
| 24 | $T_3$ | | 9.5 | | X |
| 25 | $T_3 + B_{5^\circ}$ | | 29.2 | X | |
| 26 | $T_3 + B_{5^\circ}$ | | 9.5 | | X |
| 27 | $T_3 + B_{10^\circ}$ | | 29.2 | X | |
| 28 | $T_3 + B_{10^\circ}$ | | 9.5 | | X |
| 29 | $T_3 + F_{10}$ | | 29.2 | X | |
| 30 | $T_3 + F_{10}$ | | 9.5 | | x |

TABLE 2

Model Configurations Smoke Tunnel Test

| Symbol | | | | Definition |
|---|---|---|---|---|
| $T_1$ | 1" Thick Body with Ogive Nose | | | |
| $T_1 + B_{5°}$ | " | " | " | + 5° Boattail |
| $T_1 + B_{10°}$ | " | " | " | + 10° Boattail |
| $T_1 + F_{5°}$ | " | " | " | + 5° Flare |
| $T_1 + F_{10}$ | " | " | " | + 10° Flare |
| $T_2$ | 2" Thick Body with Ogive Nose | | | |
| $T_2 + B_{5°}$ | " | " | " | + 5° Boattail |
| $T_2 + B_{10°}$ | " | " | " | + 10° Boattail |
| $T_2 + B_{10°S}$ | " | " | " | + small 10° Boattail |
| $T_2 + F_{5°}$ | " | " | " | + 5° Flare |
| $T_2 + F_{10°}$ | " | " | " | + 10° Flare |
| $T_2 + F_{10°S}$ | " | " | " | + Small 10° Flare |
| $T_{2R}$ | 2" Thick Body with Radius Nose | | | |
| $T_3$ | 3" Thick Body with Ogive Nose | | | |
| $T_3 + B_{5°}$ | " | " | " | + 5° Boattail |
| $T_3 + B_{10°}$ | " | " | " | + 10° Boattail |
| $T_3 + F_{10°}$ | " | " | " | + 10° Flare |

TABLE 3

RUN INDEX

Convair 8' x 12' Wind Tunnel

| RUN | CONFIGURATION | TEST | q | $\alpha$ | RAKE POSIT. | REMARKS |
|---|---|---|---|---|---|---|
| 1 | None | Hot Wire & Rake | A | - | 24"&54" | 24"&54" Aft of Trunnion Ctr. |
| 2 | $T_{10}$ | (F.P.)(H.W.) (P.R.) | 60 | 0,3,6 | A | Force & Press. Only @ $\alpha$ = 3° & 6° |
| 3 | $T_{10}$ | " | 30 | " | A | " " " " " |
| 4 | $T_{10}$+V | Press Kero Talc | 60 | 0 | - | |
| 5 | $T_{10}$ | (F.P.)(H.W.) P.R. | 60 | 0,3,6 | C | Force & Press. Only @ $\alpha$ = 3, & 6° |
| 5A | $T_{10}$ | " | 60 | 0 | 1 3/8 | |
| 6 | $T_{10}$ | " | 30 | 0,3,6 | C | Force & Press. Only @ $\alpha$ = 3° & 6° |
| 7 | $T_{10}$+P | P.(H.W.) P.R. | B | 0 | B | |
| 8 | $T_8$+$F_{10}$+V | Press Kero Talc | 60 | 0 | - | Airflow Visualization |
| 9 | $T_8$+$F_{10}$+P | P.(H.W.) P.R. | 30&60 | 0 | B to 36" | |
| 10 | $T_8$+$F_{10}$ | F.P.(H.W.) P.R. | 60 | 0,3,6 | C | Force & Press. Only @ $\alpha$ = 3° & 6° |
| 11 | $T_{12}$+$B_{10}$+P | P.(H.W.) P.R. | 30&60 | 0 | B to 36" | |
| 12 | $T_{12}$+$B_{10}$+V | Press Kero Talc | 60 | 0 | - | Airflow Visualization |

| RUN | CONFIGURATION | TEST | q | $\alpha$ | RAKE POSIT. | REMARKS |
|---|---|---|---|---|---|---|
| 13 | $T_{12}+B_{10}$ | F.P.(H.W.) P.R. | 60 | 0,3,6 | C | Force & Press. Only @ $\alpha$= + 3° & 6° |
| 14 | $T_{12}+B_{10}$ | " | 30 | " | " | " " " " |
| 15 | $T_{12}$ | " | 60 | " | 13 3/8 | " " " " |
| 16 | $T_{12}$ | " | 30 | " | " | " " " " |
| 17 | $W_3$ | P.(H.W.) P.R. | 45 | 0,5,10 | D | Press. Only @ $\alpha$ = 5° & 10° |
| 18 | $W_3$ | " | 150 | " | " | " " " " " |
| 19 | $W_3$+I | Force & Press | 45 | 0 | - | Image Bayonet Only |
| 20 | $W_3$+I | " | 150 | " | - | " " " |
| 21 | $W_3$ | Force | 45 | 0,5,10 | - | Force Only |
| 22 | $W_3$ | Force | 150 | " | - | " " |
| 23 | $M_1$ | F.P.(H.W.) P.R. | 45 | " | D | Force & Press. Only @ $\alpha$= 5° & 10° |
| 24 | $M_1$ | " | 150 | " | D | " " " " |
| 25 | $M_1$+I | Force & Press | 45 | 0 | - | |
| 26 | $M_1$+I | " | 150 | 0 | - | |

F.P. = Force & Surface Press.
H.W. = Hot Wire
P.R. = Press. Rake

TABLE 4

RUN INDEX

CAL Tech Merrill Wind Tunnel

| RUN | CONFIGURATION | TEST | q | α | REMARKS |
|---|---|---|---|---|---|
| 1 | $M_1$ | F.P. (H.W.) | 30 | 0,5,10 | |
| 2 | $M_1$ | Press. (H.W.) | 45 | " | |
| 3/3A | $M_1+B_{10}$ | " | 45 | " | (3A Tuft Photos Only) |
| 4 | " | " | 30 | " | |
| 5 | $W_3$ | " | 45 | 0,5 | |
| 6 | " | " | 30 | 0,5 | |
| 7 | $W_3+I$ | Press. | 45 | 0 | |
| 8 | " | " | 30 | " | |
| 9 | $W_3+1/2M_2$ | Press. H.W. | 45 | 0,5 | |
| 10 | " | " | 30 | " | |
| 11 | $W_3+S_{30}$ | " | 45 | " | |
| 12 | " | " | 30 | " | |
| 13 | $W_3+S_{45}$ | " | 45 | 0 | |
| 14 | " | " | 30 | 0 | |
| 15 | $W_4+I$ | " | 45 | 0 | |
| 16 | " | " | 30 | 0 | |
| 17 | $W_4$ | " | 45 | 0,5 | |
| 18 | " | " | 30 | " | |

| RUN | CONFIGURATION | TEST | q | $\alpha$ | REMARKS |
|---|---|---|---|---|---|
| 19 | $W_4+U_{10}$ | Press.<br>H.W. | 45 | 0,5 | |
| 20 | " | " | 30 | " | |
| 21 | $W_4+U_5$ | " | 45 | " | |
| 22 | " | " | 30 | " | |
| 23 | $M_1+A_1$ | " | 45 | " | |
| 24 | " | " | 30 | " | |
| 25 | $M_1+1/2A_1$ | " | 45 | 0,5,10 | |
| 26 | " | " | 30 | " | |
| 27 | $M_1+A_2$ | " | 30 | " | |
| 28 | " | " | 45 | " | |
| 29 | $M_1+1/2A_2$ | " | 45 | " | |
| 30 | " | " | 30 | " | |
| 31 | $M_1+R$ | " | 30 | " | |
| 32 | " | " | 45 | " | |
| 33 | $M_1+F_{10}$ | " | 45 | 0,5 | |
| 34 | " | " | 30 | " | |
| 35 | None | H.W. | 30,45 | - | Hot Wire With Clear Tunnel |
| 36 | $M_1+F_{10}$ | 3 Comp. | 30 | 0,2 1/2,5<br>7 1/2,10 | |
| 37 | " | " | 45 | " | |
| 38 | $M_1+B_{10}$ | " | 45 | " | |
| 39 | $W_4$ | " | 45 | 0,2 1/2,5 | |
| 40 | $W_4+I$ | " | 45 | 0 | |

(F.P. = Force & Surface Press.)
(H.W. = Hot Wire)
(P.R. = Press. Rake)

TABLE 5

Description of Model Components
For Convair and Cal Tech Tests

| Symbol | Description |
| --- | --- |
| $A_1$ | Four rectangular fins with a span of 4.50 inches, chord of 7.79 inches and 1.00 inches thick. Fins are located in the y and z planes of the model. |
| $1/2A_1$ | Same as $A_1$ except only two fins are used located in the y plane of the model. |
| $A_2$ | Four delta fins with a span of 4.50 inches, a root chord of 7.79 inches, and 1.00 inch thick. Fins are located in the y and z planes of the model. |
| $1/2A_2$ | Same as $A_2$ except only two fins located in the y plane of the model. |
| $B_{10}$ | Boattail Trailing Edge; modification to $T_{12}$ and $M_1$ which boattails the upper and lower surfaces of the model 10° at the trailing edge. |
| $F_{10}$ | Flare Trailing Edge; modification to model $T_8$ and $M_1$ which flares the upper and lower surfaces of the model 10° at the trailing edge. |
| $I_1$ | Image system; image bayonets and pressure tubing installed at the model upper surface, on $W_3$. |
| $I_2$ | Image System; image bayonet and pressure tubing installed at the model upper surface, on $M_1$. |
| $M_1$ | Three-dimensional body; six inch diameter body with a blunted tangent ogive nose and a blunt base, model length = 30.55 inches. |
| $1/2M_2$ | One half of body $M_1$ mounted on the top of wing $W_3$. |
| P | Splitter Plate; a .25-inch thick plate, 36 inches wide, 60 inches long, mounted on the model chord plane with one end at the model base, and extending 60 inches aft of the model base. |

| Symbol | Description |
|---|---|
| R | Blunt nose to model $M_1$. The nose has a radius of 3.00 inches. |
| $S_{30}$ | Trailing edge modification to wing $W_3$ that sweeps the trailing edge 30 degrees. |
| $S_{45}$ | Trailing edge modification to wing $W_3$ that sweeps the trailing edge 45 degrees. |
| $T_8$ | Two-dimensional model with 36.000 inch span, 32.000 inch chord, and 8.00 inch thickness. Model is of constant symmetrical section with a parabolic nose and a blunt base. |
| $T_{10}$ | Two-dimensional model; same as $T_8$ except 10 inches thick. |
| $T_{12}$ | Two-dimensional model; same as $T_8$ except 12 inches thick. |
| TR | Transition grit, #180 carborundum grit applied to the models. |
| $U_5$ | Upper surface modification to wing $W_4$ which boattails the model 5 degrees at the trailing edge. |
| $U_{10}$ | Upper surface modification to wing $W_4$ which boattails the model 10 degrees at the trailing edge. |
| $V_1$ | Vertical Plate used with Model $T_{10}$, plate is 18 inches high, 54 inches long, mounted on the model centerline, and extending 50 inches aft of the model base. |
| $V_2$ | Vertical Plate used with Model $T_8F_{10}$; plate is 20 inches high, 44 inches long, mounted on the model centerline, and extending 40 inches aft of the model base. |
| $V_3$ | Vertical Plate used with Model $T_{12}B_{10}$; plate is 20 inches high, 44 inches long, mounted on the model centerline, and extending 36 inches aft of the model base. |

| Symbol | Description |
| --- | --- |
| $W_3$ | Three-dimensional wing; wing of delta planform with leading edge sweep of 75° and a span of 19.55 inches. The wing has a constant thickness of 3.00 inches, a leading edge radius of 1.5 inches and a blunt trailing edge. |
| $W_4$ | Three-dimensional wing; wing of delta planform with leading edge sweep of 75° and a span of 15.02 inches. The wing has a constant thickness of 4.00 inches, a leading edge radius of 2 inches and a blunt trailing edge. |

TABLE 6
Data Reduction Constants
for Convair 8' x 12' Tunnel Tests

| Config. | S Planform Area (sq.ft.) | h Base Height (ft.) | $A_b$ Base Area (sq.ft.) | $l_m$ Model Lgth. (ft.) | $l_p$ Splitter Length (ft.) | RMC From $BMC_x$ (ft.) | $BMC_y$ From RMC (ft.) |
|---|---|---|---|---|---|---|---|
| $T_8$ | 8.0 | .667 | 2.0 | 2.667 | 5.00 | .667 | .031 |
| $T_8+F_{10}$ | " | .833 | 2.5 | " | " | " | " |
| $T_{10}$ | " | " | 2.5 | " | " | " | " |
| $T_{12}+B_{10}$ | " | " | 2.5 | " | " | " | " |
| $T_{12}$ | " | 1.000 | 3.0 | " | " | " | " |
| $W_3$ | 2.477 | .25 | .315 | 2.683 | - | .105 | 0 |
| $M_1$ | .76 | .5 | .196 | 2.546 | - | 1.3375 | 0 |

NOTE: RMC - Reference Model Center
BMC - Balance Moment Center

$K_1$ through $K_7$ are wall and blockage correction constants. Values are not included as these corrections are applied during the wind tunnel data reduction process and depend on model blockage and test conditions.

TABLE 7
Data Reduction Constants
for Cal. Tech.Merrill Tunnel Tests

| Config. | S<br>Planform Area<br>(sq. ft.) | h<br>Base Height<br>(ft.) | $A_b$<br>Base Area<br>(sq. ft.) | $l_m$<br>Model Lgth.<br>(ft.) | RMC<br>From $BMC_x$<br>(ft.) | $BMC_y$<br>From RMS<br>(ft.) |
|---|---|---|---|---|---|---|
| $M_1$ | .76 | .5 | .196 | 2.546 | 1.3375 | 0.0 |
| $M_1 + B_{10}$ | .671 | .249 | .048 | 2.546 | 1.3375 | 0.0 |
| $M_1 + F_{10}$ | .849 | .75 | .443 | 2.546 | 1.3375 | 0.0 |
| $W_4$ | 1.462 | .33 | .393 | 1.858 | - .078 | 0.0 |
| $W_3$ | 2.477 | .25 | .394 | 2.683 | .105 | 0.0 |

NOTE: RMC - Reference Model Center
BMC - Balance Moment Center

TABLE 8

Base Pressure Coefficients for $T_1$ Series of Configurations for Smoke Tunnel Test

| Configuration | Angle of Attack (Degrees) | $P_{b_g}$ (lb/ft$^2$) | $C'_{pb}$ |
|---|---|---|---|
| $T_1$ | 0 | -1.562 | -.307 |
| | 5 | -1.480 | -.227 |
| | 10 | -1.535 | -.281 |
| | 15 | -1.816 | -.558 |
| $T_1 + B_{5°}$ | 0 | -1.343 | -.092 |
| | 5 | -1.296 | -.045 |
| | 10 | -1.405 | -.153 |
| | 15 | -1.764 | -.506 |
| $T_1 + B_{10°}$ | 0 | -1.113 | +.115 |
| | 5 | -1.172 | +.077 |
| | 10 | -1.358 | -.116 |
| | 15 | -1.682 | -.425 |
| $T_1 + F_{5°}$ | 0 | -1.806 | -.548 |
| | 5 | -1.666 | -.410 |
| | 10 | -1.655 | -.399 |
| | 15 | -1.920 | -.660 |
| $T_1 + F_{10°}$ | 0 | -1.946 | -.686 |
| | 5 | -1.805 | -.547 |
| | 10 | -1.629 | -.373 |
| | 15 | -1.952 | -.691 |

TABLE 9

Base Pressure Coefficients for $T_2$ Series of Configurations for Smoke Tunnel Test

| Configuration | Angle of Attack (Degrees) | $P_{bg}$ (lb/ft$^2$) | $C'_{pb}$ |
|---|---|---|---|
| $T_2$ | 0 | -1.665 | -.408 |
| | 5 | -1.598 | -.343 |
| | 10 | -1.535 | -.281 |
| | 15 | -1.743 | -.486 |
| $T_{2R}$ | 0 | -1.730 | -.473 |
| | 5 | -1.578 | -.323 |
| | 10 | -1.645 | -.389 |
| | 15 | -1.880 | -.620 |
| $T_2 + F_{5°}$ | 0 | -1.840 | -.581 |
| | 5 | -1.790 | -.532 |
| | 10 | -1.670 | -.413 |
| | 15 | -1.795 | -.537 |
| $T_2 + F_{10°}$ | 0 | -2.050 | -.798 |
| | 5 | -1.980 | -.718 |
| | 10 | -1.745 | -.488 |
| | 15 | -1.895 | -.635 |
| $T_2 + B_{5°}$ | 0 | -1.525 | -.271 |
| | 5 | -1.490 | -.236 |
| | 10 | -1.470 | -.217 |
| | 15 | -1.750 | -.493 |
| $T_2 + B_{10°}$ | 0 | -1.318 | -.067 |
| | 5 | -1.321 | -.070 |
| | 10 | -1.372 | -.120 |
| | 15 | -1.568 | -.313 |

TABLE 10

Base Pressure Coefficients for $T_3$ Series of Configurations for Smoke Tunnel Test

| Configuration | Angle of Attack (Degrees) | $P_{b_g}$ (lb/ft$^2$) | $C'_{pb}$ |
|---|---|---|---|
| $T_3$ | 0 | -1.830 | -.571 |
| | 5 | -1.815 | -.556 |
| | 10 | -1.750 | -.492 |
| | 15 | -1.700 | -.443 |
| $T_3 + B_{5°}$ | 0 | -1.675 | -.419 |
| | 5 | -1.650 | -.394 |
| | 10 | -1.610 | -.355 |
| | 15 | -1.645 | -.389 |
| $T_3 + B_{10°}$ | 0 | -1.483 | -.229 |
| | 5 | -1.478 | -.225 |
| | 10 | -1.534 | -.280 |
| | 15 | -1.624 | -.368 |
| $T_3 + 1/2\ B_{10°}$ | 0 | -1.560 | -.306 |
| | 5 | -1.588 | -.333 |
| | 10 | -1.525 | -.271 |
| | 15 | -1.493 | -.239 |
| $T_3 + F_{10°}$ | 0 | -2.130 | -.866 |
| | 5 | -2.110 | -.847 |
| | 10 | -2.015 | -.753 |
| | 15 | -1.785 | -.527 |
| $T_3 + 1/2\ F_{10°}$ | 0 | -2.000 | -.739 |
| | 5 | -1.900 | -.640 |
| | 10 | -1.763 | -.505 |
| | 15 | -1.770 | -.512 |

TABLE 11
2-D Configurations
(Convair Tests)
Average Base Pressures

| Run | Configuration | q | Avg. Base Pressure $\alpha = 0$ | $\alpha = 3$ | $\alpha = 6$ |
|---|---|---|---|---|---|
| 2* | $T_{10}$ | 60 | -.81465 | -.80504 | -.80526 |
| 3* | $T_{10}$ | 30 | -.79695 | -.77259 | -.75329 |
| 5 | $T_{10}$ | 60 | -.80981 | -.79609 | -.79339 |
| 6 | $T_{10}$ | 30 | -.76839 | -.77885 | -.75801 |
| 7 | $T_{10}+P$ | 15 | -.44628 | | |
| 7 | $T_{10}+P$ | 30 | -.45163 | | |
| 7 | $T_{10}+P$ | 45 | -.42149 | | |
| 7 | $T_{10}+P$ | 60 | -.4374 | | |
| 9 | $T_8+F_{10}+P$ | 60 | -.53598 | | |
| 9 | $T_8+F_{10}+P$ | 30 | -.57199 | | |
| 10 | $T_8+F_{10}$ | 60 | -.99236 | -.97204 | -.94929 |
| 11 | $T_{12}+B_{10}+P$ | 60 | -.33162 | | |
| 11 | $T_{12}+B_{10}+P$ | 30 | -.33294 | | |
| 13 | $T_{12}+B_{10}$ | 60 | -.63833 | -.60587 | -.58788 |
| 14 | $T_{12}+B_{10}$ | 30 | -.55122 | -.55250 | -.55250 |
| 15 | $T_{12}$ | 60 | -.81488 | -.82467 | -.80561 |
| 16 | $T_{12}$ | 30 | -.84950 | -.84081 | -.81711 |

* Runs 2 and 3 do not have transition grit.

TABLE 12
3-D Configurations
Average Base Pressures
(Corrected for Tares)
(Cal Tech Tests)

| Run | Configuration | q | Average Base Pressure α = 0 | α = 5 | α = 10 |
|---|---|---|---|---|---|
| CT 1 | $M_1$ | 30 | -.15149 | -.18685 | -.23737 |
| 2 | $M_1$ | 45 | -.16046 | -.18663 | -.2346 |
| 3 | $M_1+B_{10}$ | 45 | +.02802 | +.001401 | -.03799 |
| 4 | $M_1+B_{10}$ | 30 | +.03144 | +.000238 | -.04876 |
| 5 | $W_3$ | 45 | -.46919 | -.46863 | |
| 6 | $W_3$ | 30 | -.46658 | -.48719 | |
| 9 | $W_3+1/2M_2$ | 45 | -.28234 | -.29310 | |
| 10 | $W_3+1/2M_2$ | 30 | -.28484 | -.29113 | |
| 11 | $W_3+S_{30}$ | 45 | -.59690 | -.62249 | |
| 12 | $W_3+S_{30}$ | 30 | -.64110 | -.64153 | |
| 13 | $W_3+S_{45}$ | 45 | -.60846 | | |
| 14 | $W_3+S_{45}$ | 30 | -.60882 | | |
| 17 | $W_4$ | 45 | -.45678 | -.48823 | |
| 18 | $W_4$ | 30 | -.44993 | -.47334 | |
| 19 | $W_4+U_{10}$ | 45 | -.31957 | -.37312 | |
| 20 | $W_4+U_{10}$ | 30 | -.31381 | -.37429 | |
| 21 | $W_4+U_5$ | 45 | -.37416 | -.38928 | |
| 22 | $W_4+U_5$ | 30 | -.37046 | -.38110 | |

| Run | Configuration | q | Average base pressure $\alpha = 0$ | $\alpha = 5$ | $\alpha = 10$ |
|---|---|---|---|---|---|
| CT 23 | $M_1+A_1$ | 45 | -.24974 | -.26180 | |
| 24 | $M_1+A_1$ | 30 | -.27222 | -.24870 | |
| 25 | $M_1+1/2A_1$ | 45 | -.20351 | -.21980 | -.26184 |
| 26 | $M_1+1/2A_1$ | 30 | -.22262 | -.22628 | -.25971 |
| 27 | $M_1+A_2$ | 30 | -.31583 | -.31885 | -.31513 |
| 28 | $M_1+A_2$ | 45 | -.33103 | -.32458 | -.32155 |
| 29 | $M_1+1/2A_2$ | 45 | -.26184 | -.25307 | -.26794 |
| 30 | $M_1+1/2A_2$ | 30 | -.26910 | -.26122 | -.27192 |
| 31 | $M_1+R$ | 30 | -.14482 | -.15966 | -.21490 |
| 32 | $M_1+R$ | 45 | -.14624 | -.16599 | -.22482 |
| 33 | $M_1+F_{10}$ | 45 | -.3000 | -.29783 | |
| 34 | $M_1+F_{10}$ | 30 | -.29866 | -.29524 | |

Security Classification

## DOCUMENT CONTROL DATA - R&D

*(Security classification of title, body of abstract and indexing annotation must be entered when the overall report is classified)*

**1. ORIGINATING ACTIVITY (Corporate author)**
GD/Convair
General Dynamics Corporation

**2a. REPORT SECURITY CLASSIFICATION**
Unclassified

**2b. GROUP**

**3. REPORT TITLE**
Development of Subsonic Base Pressure Prediction Methods - Volume II

**4. DESCRIPTIVE NOTES (Type of report and inclusive dates)**
Final Report

**5. AUTHOR(S) (Last name, first name, initial)**
Butsko, J.E., Carter, W.V., Herman, W.

| 6. REPORT DATE | 7a. TOTAL NO. OF PAGES | 7b. NO. OF REFS |
|---|---|---|
| September 1965 | 122 | 3 |

**8a. CONTRACT OR GRANT NO.**
AF 33(615)-1615

**b. PROJECT NO.**
1366

**c.** Task
136613

**d.**

**9a. ORIGINATOR'S REPORT NUMBER(S)**
AFFDL-TR-65-157 - Vol. II

**9b. OTHER REPORT NO(S) (Any other numbers that may be assigned this report)**

**10. AVAILABILITY/LIMITATION NOTICES**
Qualified users may obtain copies of this report from DDC. Foreign announcement and dissemination of this report is not authorized. [redacted]

**11. SUPPLEMENTARY NOTES**

**12. SPONSORING MILITARY ACTIVITY**
AF Flight Dynamics Laboratory
Research and Technology Division
Air Force Systems Command
WPAFB, Ohio 45433

**13. ABSTRACT**

Volume II contains the results of the wind tunnel test conducted under CAF 33(615)-1615.

The methods and scope of the experimental investigation are presented, as well as, the tabulated, plotted and photographic data obtained.

DD FORM 1 JAN 64 1473

Unclassified
Security Classification

| 14. KEY WORDS | LINK A | | LINK B | | LINK C | |
|---|---|---|---|---|---|---|
| | ROLE | WT | ROLE | WT | ROLE | WT |
| | | | | | | |

## INSTRUCTIONS

1. ORIGINATING ACTIVITY: Enter the name and address of the contractor, subcontractor, grantee, Department of Defense activity or other organization *(corporate author)* issuing the report.

2*a*. REPORT SECURITY CLASSIFICATION: Enter the overall security classification of the report. Indicate whether "Restricted Data" is included. Marking is to be in accordance with appropriate security regulations.

2*b*. GROUP: Automatic downgrading is specified in DoD Directive 5200.10 and Armed Forces Industrial Manual. Enter the group number. Also, when applicable, show that optional markings have been used for Group 3 and Group 4 as authorized.

3. REPORT TITLE: Enter the complete report title in all capital letters. Titles in all cases should be unclassified. If a meaningful title cannot be selected without classification, show title classification in all capitals in parenthesis immediately following the title.

4. DESCRIPTIVE NOTES: If appropriate, enter the type of report, e.g., interim, progress, summary, annual, or final. Give the inclusive dates when a specific reporting period is covered.

5. AUTHOR(S): Enter the name(s) of author(s) as shown on or in the report. Enter last name, first name, middle initial. If military, show rank and branch of service. The name of the principal author is an absolute minimum requirement.

6. REPORT DATE: Enter the date of the report as day, month, year; or month, year. If more than one date appears on the report, use date of publication.

7*a*. TOTAL NUMBER OF PAGES: The total page count should follow normal pagination procedures, i.e., enter the number of pages containing information.

7*b*. NUMBER OF REFERENCES: Enter the total number of references cited in the report.

8*a*. CONTRACT OR GRANT NUMBER: If appropriate, enter the applicable number of the contract or grant under which the report was written.

8*b*, 8*c*, & 8*d*. PROJECT NUMBER: Enter the appropriate military department identification, such as project number, subproject number, system numbers, task number, etc.

9*a*. ORIGINATOR'S REPORT NUMBER(S): Enter the official report number by which the document will be identified and controlled by the originating activity. This number must be unique to this report.

9*b*. OTHER REPORT NUMBER(S): If the report has been assigned any other report numbers *(either by the originator or by the sponsor)*, also enter this number(s).

10. AVAILABILITY/LIMITATION NOTICES: Enter any limitations on further dissemination of the report, other than those imposed by security classification, using standard statements such as:

(1) "Qualified requesters may obtain copies of this report from DDC."

(2) "Foreign announcement and dissemination of this report by DDC is not authorized."

(3) "U. S. Government agencies may obtain copies of this report directly from DDC. Other qualified DDC users shall request through ________________."

(4) "U. S. military agencies may obtain copies of this report directly from DDC. Other qualified users shall request through ________________."

(5) "All distribution of this report is controlled. Qualified DDC users shall request through ________________."

If the report has been furnished to the Office of Technical Services, Department of Commerce, for sale to the public, indicate this fact and enter the price, if known.

11. SUPPLEMENTARY NOTES: Use for additional explanatory notes.

12. SPONSORING MILITARY ACTIVITY: Enter the name of the departmental project office or laboratory sponsoring *(paying for)* the research and development. Include address.

13. ABSTRACT: Enter an abstract giving a brief and factual summary of the document indicative of the report, even though it may also appear elsewhere in the body of the technical report. If additional space is required, a continuation sheet shall be attached.

It is highly desirable that the abstract of classified reports be unclassified. Each paragraph of the abstract shall end with an indication of the military security classification of the information in the paragraph, represented as *(TS)*, *(S)*, *(C)*, or *(U)*.

There is no limitation on the length of the abstract. However, the suggested length is from 150 to 225 words.

14. KEY WORDS: Key words are technically meaningful terms or short phrases that characterize a report and may be used as index entries for cataloging the report. Key words must be selected so that no security classification is required. Identifiers, such as equipment model designation, trade name, military project code name, geographic location, may be used as key words but will be followed by an indication of technical context. The assignment of links, rules, and weights is optional.